

**PROCESS TOMOGRAPHY Ltd.**  
**ELECTRICAL CAPACITANCE TOMOGRAPHY SYSTEM**  
**TYPE PTL300E**

**OPERATING MANUAL**

**Issue 7**

**September 2010**

**VOLUME 4. APPLICATION NOTES**

ECT32v2 Software Version 2.38  
Firmware version 1.47  
System hardware .DLL DAM200E\_2\_27

---

**PROCESS TOMOGRAPHY LTD**  
**86 Water Lane, Wilmslow, Cheshire. SK9 5BB United Kingdom.**  
**Phone/Fax 01625-549021**  
(From outside UK +44-1625-549021)  
email: [enquiries@tomography.com](mailto:enquiries@tomography.com) Web site: [www.tomography.com](http://www.tomography.com)

---

# **PTL300E OPERATION MANUAL**

## **VOLUME 4 PTL APPLICATION NOTES**

AN1. Generation of ECT images from capacitance measurements

AN2. Calculation of volume ratio for ECT sensors

AN3. Engineering design rules for ECT sensors

AN4. An iterative method for improving ECT images

AN10. Linearising ECT sensors

## **PTL APPLICATION NOTE 1**

## **PTL APPLICATION NOTE AN1**

### **GENERATION OF ECT IMAGES FROM CAPACITANCE MEASUREMENTS**

**Issue 3**

**March 2001**

#### **SUMMARY**

This note describes how the permittivity distribution of the material inside an ECT sensor is obtained from measurements of the capacitances between pairs of electrodes placed around the perimeter of the sensor using the Linear-Back-Projection method.

---

#### **PROCESS TOMOGRAPHY LTD**

**86 Water Lane, Wilmslow, Cheshire. SK9 5BB United Kingdom.**

**Phone/Fax 01625-549021**

**(From outside UK +44-1625-549021)**

**email: [ptl@tomography.com](mailto:ptl@tomography.com) Web site: [www.tomography.com](http://www.tomography.com)**

---

Registered in England No. 2908507. Registered Office 15, Croft Road, Wilmslow, Cheshire. SK9 6JJ United Kingdom.

# GENERATION OF ECT IMAGES FROM CAPACITANCE MEASUREMENTS

## 1. INTRODUCTION

An ECT system provides a means for determining the distribution of a mixture of two dielectric (insulating) materials inside a vessel. It does this by measuring the capacitances between combinations of pairs of electrodes (**electrode-pairs**) placed around the perimeter of the sensor. The sensor cross-section can be of any shape, but most work to-date has concentrated on sensors having a circular cross-section.

For practical reasons, the number of electrodes placed around the sensor perimeter rarely exceeds 16 and values of 6,8 or 12 are more common. The maximum number of independent electrode-pair capacitance measurements is given by the equation:

$$M = E.(E - 1)/2 \quad (1.1)$$

where E is the number of electrodes. For a 12-electrode sensor, there will be 66 independent electrode-pair capacitances.

The permittivity distribution can be defined in any convenient form. A common format, uses a square grid of  $32 \times 32 = 1024$  pixels to represent the sensor cross-section.

An ECT system attempts to compute the permittivity distribution from the electrode pair capacitance measurements. With a  $32 \times 32$  grid, the task can be seen to be to calculate the values of 1024 pixel elements from 66 capacitance measurements. It is mathematically impossible to carry out this calculation accurately as there is insufficient information available due to the limited number of electrode-pair capacitance measurements. The task therefore reduces to finding the best possible approximate solution to the problem. In the following sections we will attempt to explain how this is achieved in a practical ECT system.

The techniques used to solve this problem evolved over an extended period of time during the original research into ECT at UMIST and elsewhere. However, very little information appears to have been published about this aspect of the research work. What follows was uncovered by reading the original ECT papers and UMIST PhD theses, together with extensive discussions of the problem with some of the original and current UMIST researchers.

The UMIST researchers made several successive refinements during their quest to find a practical method which would allow reasonably accurate images to be constructed from the electrode-pair capacitance measurements. As the image construction concept is not particularly easy to understand, we will explain the technique by following the steps taken by the original researchers to arrive at the method which is in current use. We will do this by considering initially a very simple (and artificial) sensor model. Once the principles have been explained, we will move onto more realistic sensor models.

## 1.2 A NOTE ON THE FORMAT OF THE TEXT

In what follows, we have tried to keep the explanation as simple as possible. At the same time, we want to lead the reader to the final solution adopted. We have tried to do this by indicating some sections in square brackets [ ]. These sections can be ignored on a first reading of the text. However, they will need to be read and understood ultimately to allow the reader to follow the mathematics introduced later.

## 2. SIMPLE SQUARE SENSOR MODEL

An ECT sensor is normally used to measure the permittivity distribution of a mixture of two dielectric materials. For simplicity in what follows, we shall assume that the lower permittivity material is air (ie the sensor is empty).

It is convenient to work in normalised units for both the permittivities and electrode-pair capacitances. Using this system, we define the normalised permittivity of the lower permittivity material to be represented by the value zero and the normalised permittivity of the higher permittivity material to be represented by the value 1.

We shall start by considering a very simple square capacitance sensor having 12 electrodes, with 3 electrodes located along each side of the square. The cross-section inside the sensor is represented by a grid of  $3 \times 3 = 9$  pixels, labelled A to I, as shown in figure 1.

For simplicity, we shall assume that the electric field lines run only parallel to the sides of the square as shown in figure 2. This is a gross simplification of what happens in reality, but is a useful starting point in our attempt to explain how an ECT sensor works. We will show later how the principle can be extended for use with more realistic electric field distributions.

The capacitance between any pair of electrodes will only be affected by a pixel inside this sensor if the pixel intercepts the electric field lines between these electrodes. It follows that, for this simple sensor model, only those electrodes which are opposite each other on opposing sides of the sensor will be affected by changes in the permittivity of the pixels inside the sensor.

For this simple sensor model, we therefore need to consider only the capacitances between 6 electrode-pair combinations, namely:

1 - 9, 2 - 8, 3 - 7, 4 - 12, 5 - 11, and 6 - 10

We designate these capacitances as  $C_{1-9}$  etc. where  $C_{1-9}$  means the capacitance between electrodes 1 and 9 etc.

The capacitances measured between these electrode-pairs are also normalised in a similar manner to those of the permittivity values. When the sensor contains the lower permittivity material, we define the value of the normalised capacitances measured between the electrode pairs to be zero and to be 1 when the sensor is filled with the higher permittivity material.

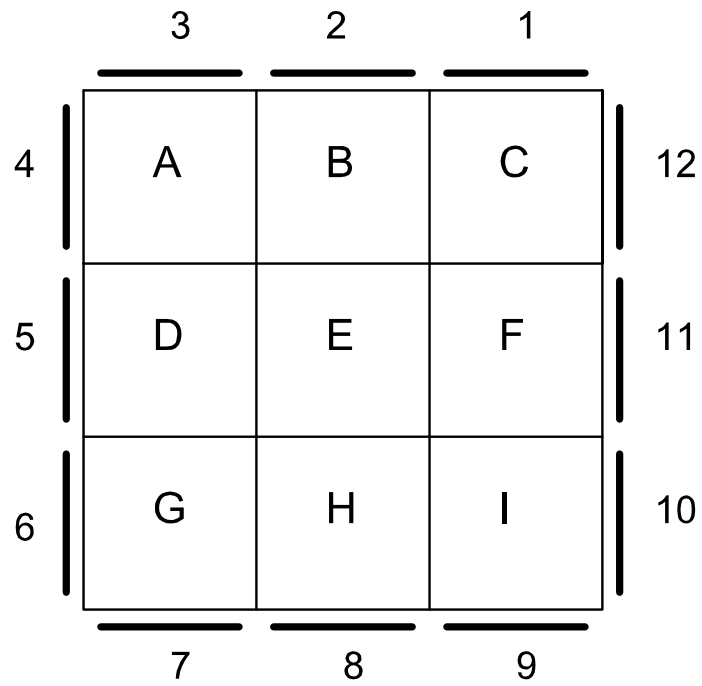


**Figure 1. 12 - electrode square ECT sensor**

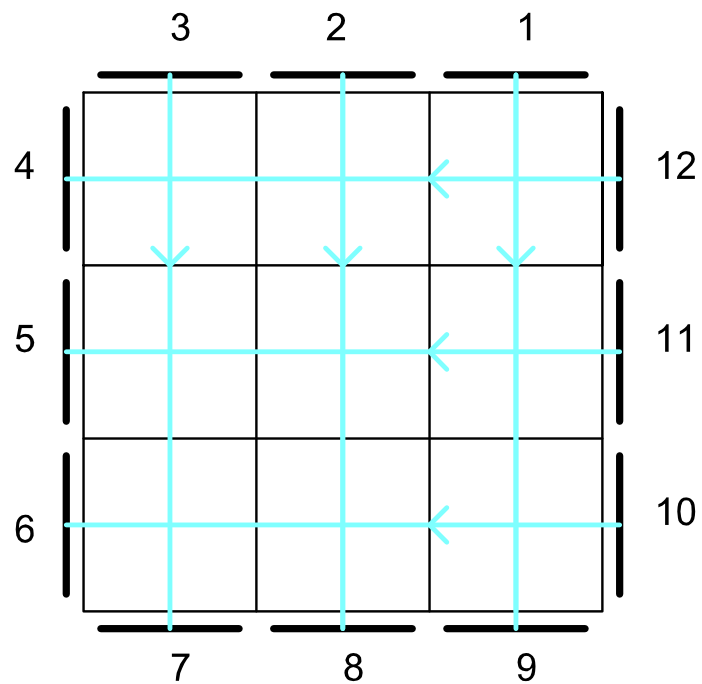


**Figure 2. Simplified Electric field distribution**

### 3. THE SENSITIVITY MAP OF THE SENSOR

We are going to consider how the capacitances measured between the electrode pairs of an empty sensor are affected when a dielectric probe, consisting of a square dielectric rod whose cross-section is the same size as one pixel, is located at each of the 9 pixel locations in turn.

By our previous definition, the normalised capacitances measured between any two pairs of electrodes will be zero when the sensor is empty.

We will first consider what happens when the dielectric probe is located at Pixel E in the otherwise empty sensor. This situation is represented in figure 3, where the red colour indicates that the centre pixel E is occupied by material having the higher value of permittivity (the dielectric bar) and the dark blue colour indicates that the remaining pixels are occupied by lower permittivity material (air).

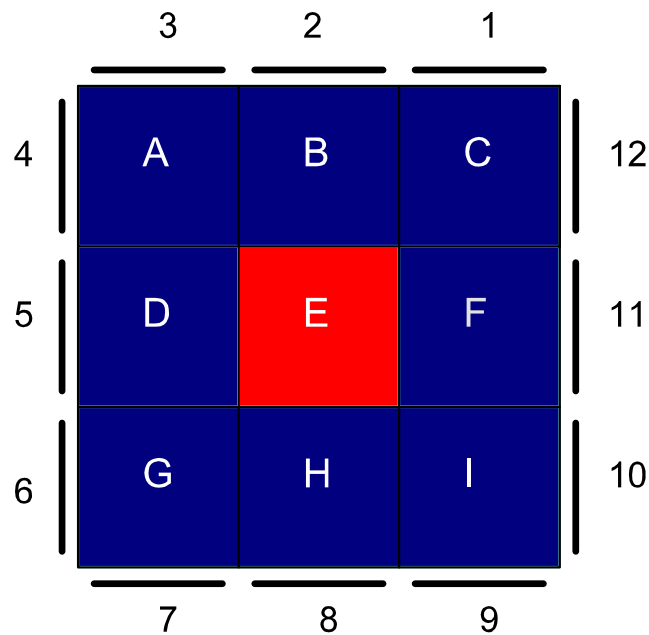


**Figure 3. Pixel E containing high-permittivity material**

In our simple sensor model, we have assumed that the electric field lines are parallel to the sides of the sensor, and it follows that the dielectric probe will only affect the capacitance measured between electrodes whose electric field lines interact with the cross section of the probe. Hence, in this case, the only electrode pairs whose capacitance will be affected will be electrode pairs 2-8 and 5-11.

If the probe is now moved to pixel B, the electrode pairs whose capacitance is changed will be electrodes 2-8 and 4-12. The same arguments can be used to determine which electrode pairs will be affected when the probe is placed in any of the other 7 pixels.



By locating the permittivity probe at each pixel location in turn, we can construct a 3 X 3 element matrix, for each electrode pair combination. These are known as sensitivity matrices, and show, for each electrode-pair, how the permittivity probe will affect the capacitance between the electrodes for each pixel location.

In the case of a 3 X 3 pixel grid, the sensitivity matrix for each electrode-pair consists of a set of 9 sensitivity coefficients corresponding to each of the pixels inside the sensor. The sensitivity matrix can be written as follows:

$$\begin{matrix} S_A & S_B & S_C \\ S_D & S_E & S_F \\ S_G & S_H & S_I \end{matrix}$$

where  $S_A$ ,  $S_B$  etc. are the sensitivity coefficients for pixels A,B etc.

We will now further simplify the situation by representing the sensitivity coefficients in binary format. That is, if the probe affects the electrode pair capacitance at a particular pixel location, we signify this by entering the value 1 in the sensitivity matrix for this pixel location. Similarly, if there is no effect, we illustrate this by writing 0 in the pixel location.

This is best illustrated by some examples.

Consider the electrode pair combination  $S_{2-8}$ . Bearing in mind our previous (highly simplified) assumption about the paths of the electric field lines inside the sensor, the sensitivity matrix for this electrode pair can be written down by inspection as follows:

$$S_{2-8} \quad \begin{matrix} 0 & 1 & 0 \\ 0 & 1 & 0 \\ 0 & 1 & 0 \end{matrix}$$

Similarly, the matrix for the electrode pair 5-11 can be written:

$$S_{5-11} \quad \begin{matrix} 0 & 0 & 0 \\ 1 & 1 & 1 \\ 0 & 0 & 0 \end{matrix}$$

All of the other sensitivity matrices can be written down in a similar manner.

Note that, for this sensor model, only 4 other electrode combinations will have matrices containing non-zero sensitivity coefficients (for electrode pairs 3 -7, 4 -12, 5 -11 and 6 - 10). All of the matrices for the remaining electrode pair combinations will contain only zeroes. This is because we have assumed that there is no capacitive coupling between any other electrode combinations, which in turn, follows from the simple electric field paths which we have assumed for this sensor.

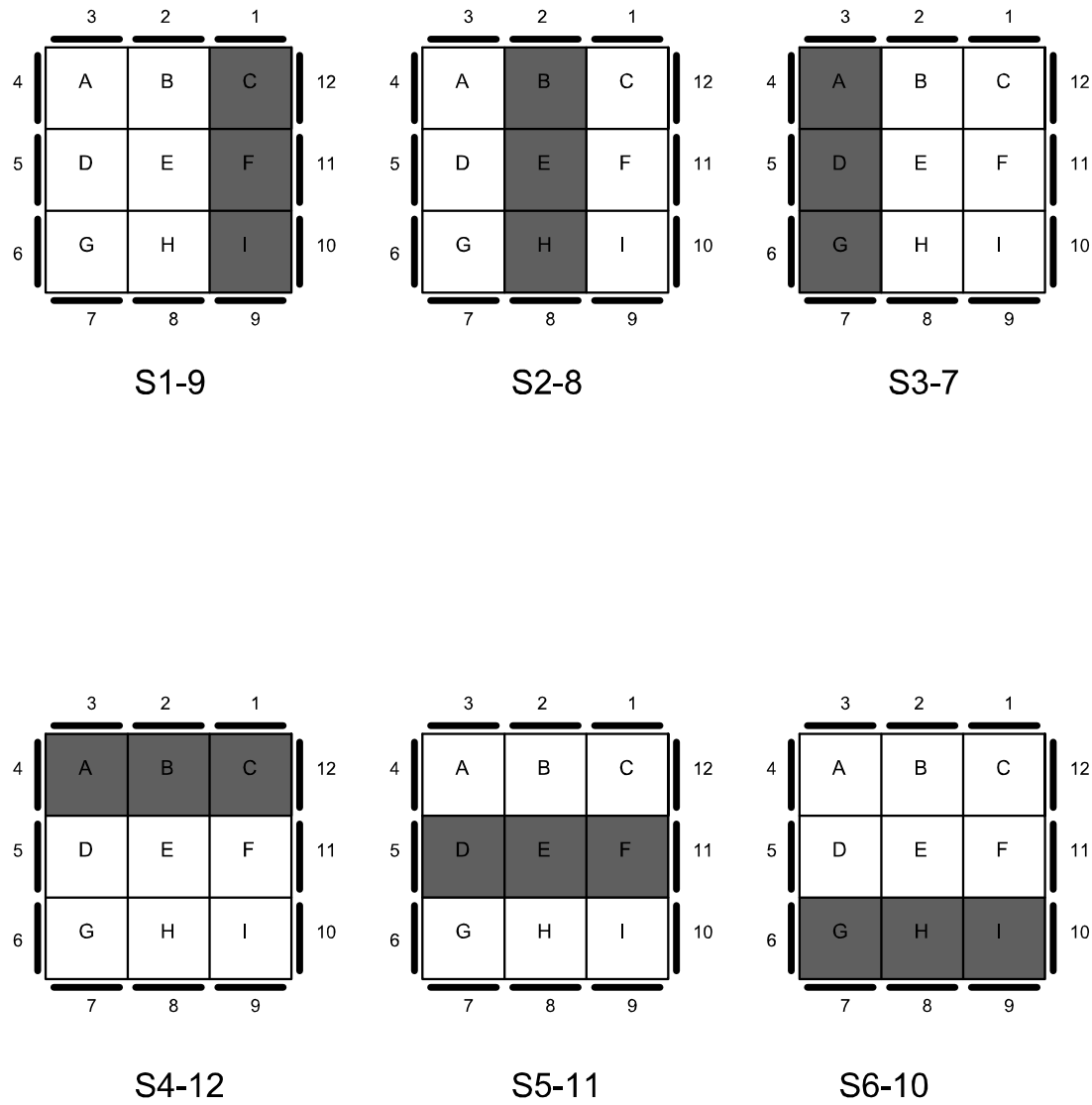


Figure 4. Simplified binary sensitivity maps for square ECT sensor

The six sensitivity matrices which contain non-zero sensitivity coefficients are shown in diagrammatic form in figure 4. The white pixels represent sensitivity coefficients with zero coefficients and the dark pixels represent sensitivity coefficients with the value 1.

To summarise, each electrode-pair combination will have an associated sensitivity matrix containing N elements, where N is the number of pixels. The elements in the sensitivity matrix for each electrode pair indicate whether a change in the permittivity of a single pixel inside the sensor will affect the capacitance measured between the electrodes of this pair. In our first, very simple sensor model, if the capacitance changes when the permittivity of a particular pixel is increased or decreased, the pixel sensitivity coefficient for that pixel is assigned the value 1. If there is no change to the electrode-pair capacitance, then the pixel sensitivity coefficient is set to zero.

## 4. THE FORWARD PROBLEM

The next question to consider is how the electrode-pair capacitances change when an arbitrary permittivity distribution exists inside the sensor.

We will assume that the sensor is filled with a mixture of the lower and upper permittivity materials. This will give rise to a set of normalised capacitance values for the set of electrode pairs and we will assume that these normalised capacitances will have values somewhere within the range 0 to 1.

The first task is to determine how to calculate the inter-electrode capacitances from the values of the normalised permittivities of the pixels for any distribution of permittivity inside the sensor. This is known as the **Forward problem**.

The method which is adopted to solve the **Forward problem** is based on the Electrical Network **Superposition Theorem**. Expressing this theorem in a form which is relevant to the forward problem, the Superposition Theorem states that, in a linear electrical network, the combined effect of a large number of stimuli can be found by adding up the effects which result when each stimulus acts individually.

In our case the **stimuli** are the **permittivity values** of the individual **pixels** inside the sensor and the **effects** are the **inter-electrode capacitances** measured between the **electrode-pairs**.

We can now apply this theorem to find the capacitances between the electrode pairs when the sensor is filled with the higher permittivity material as follows:

For each electrode-pair, we measure the set of elemental normalised capacitances between the electrodes when each pixel in turn (the probe pixel) contains the higher permittivity material, while all of the remaining pixels contain the lower permittivity material. For our simple square sensor with 9 pixels, there will obviously be 9 elemental capacitances to measure for each location of the probe pixel.

To find the capacitance between these two electrodes when the sensor is completely filled with the higher permittivity material, the Superposition theorem states that we should simply add up all of these 9 elemental capacitances.

For our simple sensor model, we know that for any particular electrode-pair, only some of the pixels inside the sensor will change the capacitance between this pair of electrodes and this information is contained in the sensitivity matrix. For the simple binary sensitivity matrix which we have discussed so far, the matrix tells us which pixels influence the capacitance between a given pair of electrodes and which pixels have no effect on this capacitance.

Applying the **Superposition theorem**, the capacitance  $C_m$  between any pair of electrodes can therefore be written in the following general form:

$$C_m = P_m.(S_A.K_A + S_B.K_B + S_C.K_C + ..... S_I.K_I) \quad (4.1)$$

Where:

$m$  represents the electrode pair combinations (1-9, 2-8 etc.) and  $C_m$  is the (normalised) inter-electrode capacitance for the  $m$ th electrode-pair.

$S_A$ ,  $S_B$ , etc are the sensitivity coefficients of each individual pixel in the grid for the  $m$ th electrode pair.

$K_A$ ,  $K_B$  etc. are the values of (normalised) permittivity of the material in each pixel.

$P_m$  is a constant included to ensure that the normalising remains valid, whose value can be determined as described below.

Now consider specifically the capacitance between electrodes 2 and 8 when the sensor is full of the higher permittivity material. In this situation, the normalised permittivity of each pixel ( $K_A$ ,  $K_B$  etc.) will, by definition, have the value 1.

In the case of the square sensor, we have already shown that the sensitivity coefficients  $S_B$ ,  $S_E$  and  $S_H$  have the value 1 while all of the remaining sensitivity coefficients for this electrode combination are zero.

In this case, equation 4.1 becomes

$$C_{2-8} = P_{2-8}.(1.1 + 1.1 + 1.1) = 3.P_{2-8} \quad (4.2)$$

However, we also know that, by definition, the normalised electrode-pair capacitances for all electrode pairs have the value 1 when the sensor is full of the higher permittivity material. It follows that the value of the normalising constant  $P_{2-8}$  for electrode-pair 2-8 must have the value  $1/3$ .

We can calculate the value of  $P_m$  for all of the other electrode pair combinations in a similar manner. For the simple sensor model which we are currently using, it is clear that all values of  $P_m$  have the value  $1/3$ . However, this simple result will not generally hold for more complex field distributions.

For any other values of pixel permittivity, we can find the electrode-pair capacitances by substituting the known values of normalised permittivity into equation 4.1 as follows:

eg for electrode-pair 2-8

$$C_{2-8} = (1/3).(1.K_B + 1.K_E + 1.K_H) \quad (4.3)$$

For example, if the normalised pixel permittivities  $S_B$ ,  $S_E$  and  $S_H$  are reduced to values of 0.5, then the capacitance  $C_{2-8}$  calculated from equation 4.3 will have the value:

$$C_{2-8} = (1/3).(0.5 + 0.5 + 0.5) = 0.5 \quad (4.4)$$

As a second example, let us assume that the normalised pixels have different values e.g. let  $K_B = 1$ ,  $K_E = 0.5$  and  $K_H = 0.3$ .

In this case,  $C_{2-8}$  will have the normalised capacitance given by:

$$C_{2-8} = (1/3).(1 + 0.5 + 0.3) = 0.6. \quad (4.5)$$

So far, we have based our model on the use of binary sensitivity coefficients, in the interests of simplicity. However, as will be shown later, if the true values of the sensitivity coefficients can be found (either by calculation or by measurement), these can be used instead of the crude binary coefficients which we have so-far assumed.

It turns out that by using these more accurate sensitivity coefficients, the solution to the forward problem can be found with reasonable accuracy. However, we will stay with the binary sensitivity coefficients for the present for reasons which will become clear in the following sections.

## [5. THE GENERAL SOLUTION OF THE FORWARD PROBLEM

Using equation 4.1, we can use the general expression for  $C_m$  to find, for example, the value of  $C_{2-8}$  as follows:

$$C_{2-8} = P_{2-8} \cdot (S_A \cdot K_A + S_B \cdot K_B + S_C \cdot K_C + S_D \cdot K_D + S_E \cdot K_E + S_F \cdot K_F + S_G \cdot K_G + S_H \cdot K_H + S_I \cdot K_I) \quad (5.1)$$

There will of course be similar equations for the other electrode pairs. For example,

$$C_{1-9} = P_{1-9} \cdot (S_A \cdot K_A + S_B \cdot K_B + S_C \cdot K_C + S_D \cdot K_D + S_E \cdot K_E + S_F \cdot K_F + S_G \cdot K_G + S_H \cdot K_H + S_I \cdot K_I) \quad (5.2)$$

The complete set of relationships for all electrode pairs can be written concisely in matrix form as follows:

$$C = S \cdot K \quad (5.3)$$

where :

**C** is an **M x 1** matrix containing the normalised electrode-pair capacitances  $C_m$  (in the nominal range 0 to 1).

**M** is the number of unique electrode-pair combinations (eg 66 for a 12-electrode sensor)

Each  $m$  value corresponds to an electrode - pair combination. For example,  $m=1$  might be defined to be the pair 1-9,  $m = 2$  to be the pair 2-8 etc.

**K** is an **N x 1** matrix containing the normalised pixel permittivities (in the nominal range 0 to 1)

**N** is the number of pixels representing the sensor cross-section (eg 1024 for a 32 x 32 grid)

**S** is an **M x N** matrix containing the set of sensitivity matrices for each electrode-pair. The matrix **S** is commonly referred to as the **sensitivity map** of the sensor.

Note that in this equation, the matrix **S** incorporates the normalising constants **P** mentioned previously. That is, the sensitivity coefficients are now normalised as well as the vales of **C** and **K**.

This matrix equation defines the general solution to the **forward problem**. ]

## 6. THE INVERSE PROBLEM

As we have seen, once the set of sensitivity matrices (the sensitivity map) for the sensor has been found, it is a relatively straightforward process to calculate what the electrode-pair capacitances will be for a given permittivity distribution inside the sensor.

However, in an ECT system we normally want to be able to determine the **permittivity distribution inside the sensor** from knowledge of the **capacitances between the pairs of electrodes** which surround the sensor, ie the **inverse** of the problem which we have just outlined.

The question which therefore needs to be answered is, given a set of (measured) normalised electrode-pair capacitances, what are the values of normalised permittivity of each of the pixels inside the sensor which have given rise to this set of electrode-pair capacitances? This is known as the **inverse problem**.

We will seek to find a solution to the **inverse problem** using the sensitivity matrices which we have derived above. The method which we shall use is called **Linear Back-Projection (LBP)**.

The basis of the method is to consider each electrode-pair capacitance in turn and to consider which pixels inside the sensor have contributed to the change in the normalised capacitance from the zero values when the sensor is empty.

We do this by referring to the binary **sensitivity matrix** for each **unique electrode-pair**. Consider electrode-pair **2-8** for example. We know from the previous sections that only pixels B, E and H can have contributed to any change in the capacitance  $C_{2-8}$ . However, **we have no means of knowing how much of the change in capacitance to attribute to each pixel**.

Faced with this problem, the LBP method makes the pragmatic assumption that, for a specific electrode-pair, all of the pixels with non-zero sensitivity coefficients contribute equally to the capacitance change for each specific electrode pair and that they do this by changing their permittivity values by identical amounts. It further assumes that these incremental changes in the permittivities of the pixels which contributed to this capacitance change are proportional to the change in the electrode-pair capacitance. That is:

$$\Delta K_B = \Delta K_E = \Delta K_H = Q_n \cdot C_{2-8} \quad (6.1)$$

where  $\Delta K_B$  is the elemental change in the normalised permittivity of pixel B etc.,  $C_{2-8}$  is the normalised capacitance measured between electrode pairs 2 and 8 and  $Q_n$  is another scaling constant which is required to ensure that the normalising remains valid.

This situation is represented in figure 5 for electrode-pair  $C_{2-8}$ , which shows, in light-blue, the pixels which are assumed to have contributed to the capacitance between this pair of electrodes. Figure 6 similarly shows the pixels which contribute to the capacitance between electrodes 5 and 11.

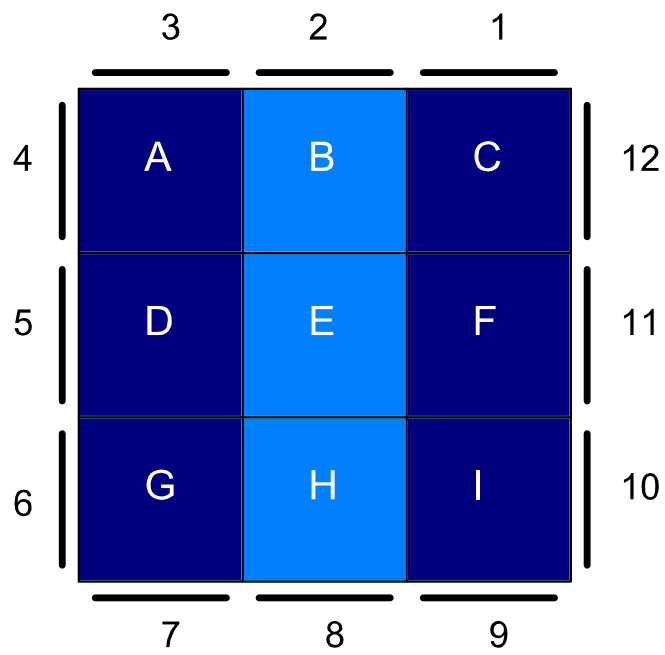


**Figure 5. Elemental pixel values due to C2-8**

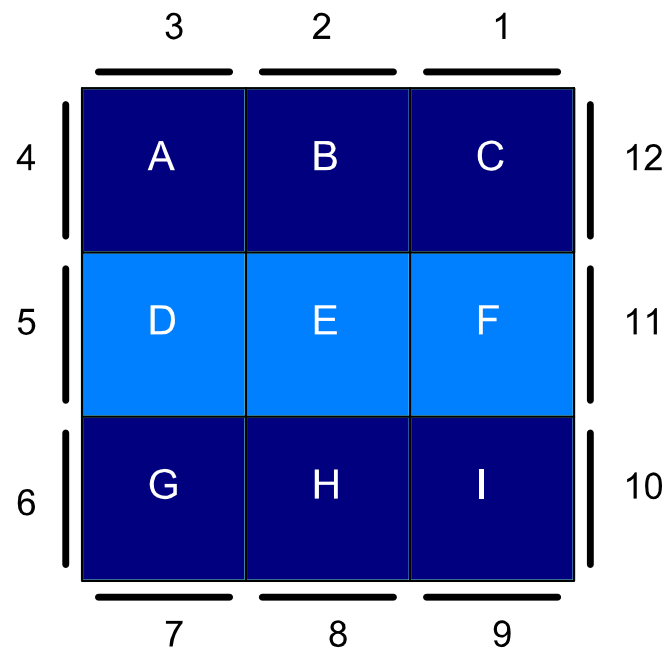


**Figure 6. Elemental pixel values due to C5-11**



[Equation 6.1 is a special case of the more general expression which needs to be written if we make no assumptions about the values of the sensitivity coefficients for each pixel. This general expression can be written as:

$$\Delta K_n = Q_n \cdot S_{nm} \cdot C_m \quad (6.2)$$

where:

$\Delta K_n$  is the elemental change in permittivity of pixel n due to the capacitance  $C_m$  of electrode-pair m

$Q_n$  is a normalising constant

$S_{mn}$  is the sensitivity coefficient which corresponds to the nth pixel and the mth electrode-pair capacitance.]

The next assumption is that this process can be applied for each electrode-pair in turn and that the overall value of pixel permittivity for each individual pixel can again be found by applying the **Superposition theorem**.

Hence we obtain the pixel permittivity by summing the elemental values of permittivity obtained from the equations for each electrode pair.

For our simple square sensor, this can be expressed as follows, using pixel B as an example.

$$K_B = \Delta K_{B(1-9)} + \Delta K_{B(2-8)} + \Delta K_{B(3-7)} + \Delta K_{B(4-12)} + \Delta K_{B(5-11)} + \Delta K_{B(6-10)} \quad (6.3)$$

Where  $\Delta K_{B(1-9)}$  means the elemental change in permittivity of pixel B due to the capacitance change of electrode-pair 1-9 etc. Using equation 6.1 or 6.2 we obtain:

$$\begin{aligned} K_B = & Q_B \cdot (S_{B(1-9)} \cdot C_{(1-9)} + S_{B(2-8)} \cdot C_{(2-8)} + S_{B(3-7)} \cdot C_{(3-7)} + S_{B(4-12)} \cdot C_{(4-12)} + S_{B(5-11)} \cdot C_{(5-11)} \\ & + S_{B(6-10)} \cdot C_{(6-10)}) \end{aligned} \quad (6.4)$$

where  $S_{B(1-9)}$  is the sensitivity coefficient of pixel B for electrode-pair 1-9,  $C_{(1-9)}$  is the normalised capacitance between electrode pair 1-9 etc. and  $Q_B$  is a normalising constant for the permittivity of pixel B.

By inspection of figures 1 and 2, pixel B will only affect the capacitance between electrode-pairs 2-8 and 4-12.

Hence  $S_{B(2-8)} = 1$  and  $S_{B(4-12)} = 1$ , while all of the other values of  $S_B$  are zero, giving:

$$K_B = Q_B \cdot (1 + 1) = 2 \cdot Q_B \quad (6.5)$$

We know that when all of the electrode-pair capacitances are 1, the normalised capacitances also have the value 1.

Substituting these conditions in equation 6.5 we obtain:

$$1 = Q_B \cdot (2) \quad (6.6)$$

and hence the value of  $Q_B = 1/2$ .

Similar expressions can be written for each of the other pixels.

For example, the permittivity of pixel A is given by:

$$K_A = \Delta K_{A(1-9)} + \Delta K_{A(2-8)} + \Delta K_{A(3-7)} + \Delta K_{A(4-12)} + \Delta K_{A(5-11)} + \Delta K_{A(6-10)} \quad (6.7)$$

$$= Q_A \cdot (S_{A(1-9)} \cdot C_{(1-9)} + S_{A(2-8)} \cdot C_{(2-8)} + S_{A(3-7)} \cdot C_{(3-7)} + S_{A(4-12)} \cdot C_{(4-12)} + S_{A(5-11)} \cdot C_{(5-11)} + S_{A(6-10)} \cdot C_{(6-10)}) \quad (6.8)$$

By similar reasoning, it is clear that the value of  $Q_A$  is also  $1/2$ . It turns out that the values of all of the normalising constants for the simple square sensor are also  $1/2$ .

[In general terms, the permittivity of an individual pixel is given by:

$$K_n = \sum_{m=1}^M Q_n \cdot S_{nm} \cdot C_m \quad (6.9)$$

where

$K_n$  is the permittivity of pixel n

$C_m$  are the set of normalised capacitance measurements for the M electrode pairs.

$Q_n$  are the set of normalising constants for the pixel n.

$S_{nm}$  are the set of sensitivity coefficients for pixel n and the M sets of electrode-pairs.

This can be written in matrix format as follows:

$$K = S^T \cdot C \quad (6.10)$$

where

**K** is an **N x 1** matrix containing the normalised permittivities of each of the **N** pixels.

**S<sup>T</sup>** is the normalised transpose sensitivity map (formed by interchanging the rows and columns of the sensitivity map matrix **S**)

**C** is an **M x 1** matrix containing the **M** normalised electrode-pair capacitances.

Equation 6.10 is the general equation which is used in the LBP algorithm to solve the **inverse problem** and hence to calculate the **pixel permittivity distribution**.]

## 7. A SIMPLE EXAMPLE OF LINEAR BACK-PROJECTION

Having explained the principle of **Linear Back-Projection**, we will now consider a simple example.

Let's assume that the sensor contains a dielectric bar of square cross-section and normalised permittivity 1, which occupies pixel E in the centre of the sensor, as shown in figure 3. All of the other pixels will be assumed to contain material of normalised permittivity zero.

We have represented this situation in figure 3 using the colour scale which is used widely to display permittivity images in ECT systems. In this system, the upper value of normalised permittivity (1) is shown in red and the lower value (0) is shown in dark-blue. Intermediate permittivity values are shown on a scale which extends from blue through green to red.

We know from the sensitivity matrices, that pixel E will only affect the capacitance between electrode-pairs 2-8 and 5-11.

Using our knowledge of the sensitivity coefficients and the values of pixel permittivities, we can first calculate what the values of  $C_{2-8}$  and  $C_{5-11}$  will be using equation 4.1 as follows:

$$C_{2-8} = (1/3). (1.1) = 1/3 \quad (7.1)$$

similarly

$$C_{5-11} = (1/3).(1.1) = 1/3 \quad (7.2)$$

We can now apply the equation of back-projection (6.10) to re-calculate the value of the pixels from the electrode-pair capacitances.

Taking pixel A as an example, and bearing in mind that the only non-zero electrode-pair capacitances generated by the “dielectric bar” in pixel E are  $C_{(2-8)}$  and  $C_{(5-11)}$ , we can calculate the value of pixel A as follows:

$$K_A = (1/2). (S_{A(2-8)} . C_{(2-8)} + S_{A(5-11)} . C_{(5-11)}). \quad 7.3)$$

However, both  $S_{A(2-8)}$  and  $S_{A(5-11)}$  are zero for these two electrode-pair combinations.

Hence the value of  $K_A$  calculated using the LBP method is zero, which is correct, as the only pixel occupied by an object of non-zero permittivity is pixel E.

Using the obvious symmetry properties of the sensor, it is clear that similar results will be obtained for pixels C, G and I, and hence  $K_C$ ,  $K_G$  and  $K_I$  will all have zero values.

This is a promising start, as we know from figure 3 that the actual pixel permittivities for pixels A, C, G and D are zero.

We will now repeat this process for pixel B.

$$K_B = (1/2) \cdot (S_{B(2-8)} \cdot C_{(2-8)} + S_{B(5-11)} \cdot C_{(5-11)}). \quad (7.4)$$

In this case,  $S_{B(2-8)}$  has the value 1 while  $S_{A(5-11)}$  is zero for these two electrode-pair combinations.

Hence the value of  $K_B$  calculated by the LBP method is  $(1/2) \cdot (1/3) = 1/6$ .

Again, using the symmetry properties of the sensor, it is clear that the values of pixels D, F and H will be identical to that of pixel B, ie  $K_D$ ,  $K_F$  and  $K_H$  will all have the value  $1/6$ .

By inspecting figure 3, we know that these values should be zero. However, in this case, the LBP algorithm has assigned pixels B, D, F and H a finite positive value of  $1/6$ .

We will now complete the process by calculating the value of pixel E.

$$K_E = (1/2) \cdot (S_{E(2-8)} \cdot C_{(2-8)} + S_{E(5-11)} \cdot C_{(5-11)}) \quad (7.5)$$

In this case, both  $S_{B(2-8)}$  and  $S_{A(5-11)}$  have the value 1 for these two electrode-pair combinations.

Hence the value of  $K_E$  calculated by the LBP method is  $(1/2) \cdot ((1/3) + (1/3)) = 1/3$ .

Referring back to figure 3, we know that the value of  $K_E$  should be 1. The LBP algorithm has therefore produced a value for pixel E which is significantly lower than its known value.

The results for the calculated pixel permittivities (in matrix format) can be summarised as follows:

$$\begin{matrix} 0 & 1/6 & 0 \\ 1/6 & 1/3 & 1/6 \\ 0 & 1/6 & 0 \end{matrix}$$

These results are represented in figure 7, which represents pixel values of 0 as dark blue,  $1/6$  as light blue and  $1/3$  as green.

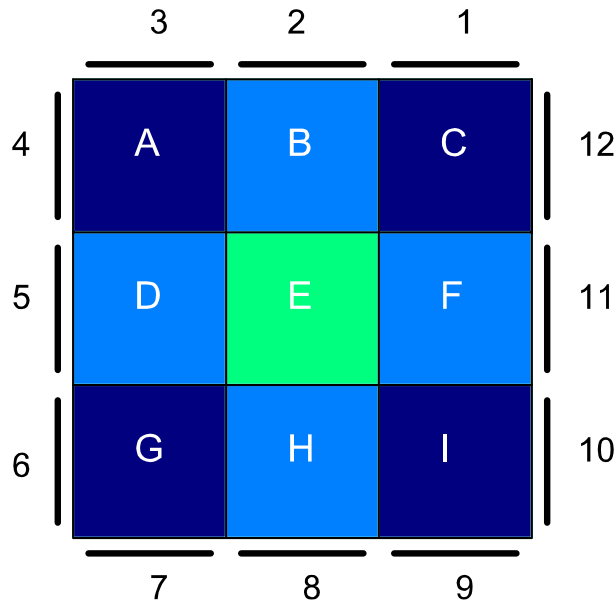


**Figure 7. Composite pixel values from sums of elemental values**

However, we know that the correct answer is the following matrix:

0	0	0
0	1	0
0	0	0

And this situation is shown in figure 3 on the same colour scale.

We have attempted to indicate how this permittivity distribution has occurred by showing the elemental pixel permittivities which result from the only two non-zero capacitance pair measurements  $C_{2-8}$  and  $C_{5-11}$  in figures 5 and 6.

Figure 5 shows the elemental pixel permittivities which result from the  $C_{2-8}$  capacitance and figure 6 shows the elemental pixel permittivities which result from the  $C_{5-11}$  capacitance. In these figures, the dark blue pixels have zero values and the light blue squares have normalised permittivities of  $1/6$  as calculated above.

When we add up these two permittivity distributions, we obtain figure 7, where the green pixel (E) has the value  $1/3$ .

By comparing the known permittivity distribution (figure 3) with the results calculated using the LBP method, (figure 7), it is clear that what has happened is that the LBP algorithm has spread out, or blurred the original probe pixel over a much larger area than that occupied by the original pixel probe.

## **7.1 INHERENT CHARACTERISTICS AND ERRORS OF THE LBP METHOD**

By comparing the LBP solution (figure 7) with the correct answer (figure 3), we can now identify some of the main characteristics of the LBP algorithm:

1. The calculated value of the probe pixel is 1/3 of its known value. In general, the LBP algorithm will always under-estimate areas of high permittivity.
2. Some of the pixels which should have zero values have had finite values assigned to them. In general, the LBP algorithm will over-estimate areas of low permittivity.
3. The sum of the calculated pixel permittivities equals that of the original single probe pixel. In general, the average permittivity of all of the pixels calculated by the LBP algorithm will approximately equal that of the sensor when it contains the test object. The LBP algorithm is therefore useful for calculating the average voidages or volume ratios of the sensor contents.

In practice, the use of a very simple sensor model and binary sensitivity coefficients have aggravated the deficiencies of the LBP algorithm and this is therefore a rather extreme example. However, the results obtained here illustrate the principle and also the main failings of the LBP algorithm.

## **8. EXTENSION TO CIRCULAR SENSORS**

Until now, we have considered a simple and rather artificial square sensor with a limited number of pixels and very restricted electric field lines. We will now show how the method can be extended to a circular sensor containing a much larger number of pixels and where we will not make any unrealistic assumptions about the electric field lines and inter-electrode coupling. For the case of the circular sensor, we will assume that there is capacitive coupling between all pairs of electrodes.

### **8.1 8-ELECTRODE CIRCULAR SENSOR**

Consider the 8-electrode circular sensor shown in figure 8. The sensor is shown superimposed on a grid of 32 X 32 square pixels.

The approximate binary sensitivity maps of the sensor can be deduced by considering the paths of the Electric field lines between the electrode pairs. For example, the binary sensitivity map for pairs 1-2 is shown in figure 9(a). The black pixels indicate that the pixel will influence the capacitance between that electrode pair and the white pixels indicate that the pixel will have no influence on the capacitance between those pairs.

The binary sensitivity maps for electrodes pairs 1-3, 1-4 and 1-5 are shown in figures 9(b) to 9(d). It is obvious that the sensitivity maps for any other electrode-pair combination will be identical to one of these four basic maps (although rotated around the sensor), because of the symmetry properties of the sensor.

## 8.2 APPLICATION OF LINEAR BACK-PROJECTION

The principle of back-projection for circular sensors remains the same as that outlined in sections 6 and 7 for the simple square sensor. For each inter-electrode capacitance measurement, using the simple binary sensitivity maps, we assume that all pixels which have a non-zero sensitivity coefficient contribute equally to the measured change in capacitance between the electrode pairs.

Hence, for each electrode pair measurement, we allocate each pixel which has a non-zero sensitivity coefficient an elemental value which is proportional to the measured change in the normalised capacitance between these electrodes. We then add up the elemental values for the pixel for all of the electrode-pair capacitance measurements to obtain the value of the pixel permittivity.

The final step is to normalise this procedure so that all of the pixels have the value 1 when the normalised inter-electrode pair capacitances are all 1 and have the value 0 when all of the normalised inter-electrode pair capacitances are zero.

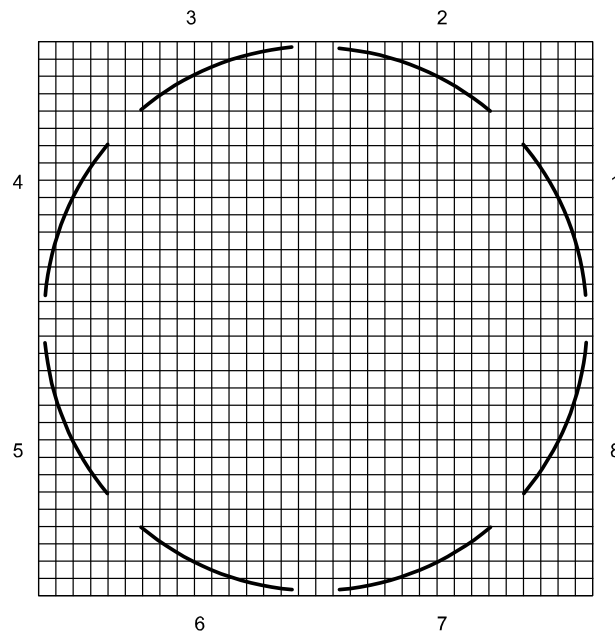
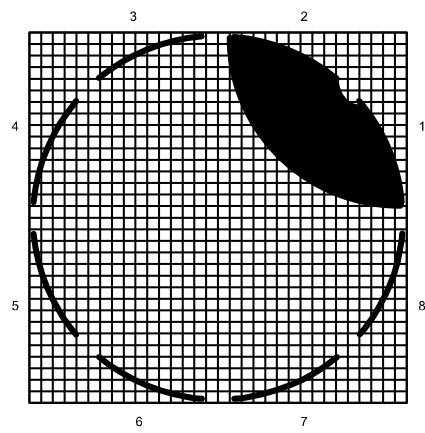
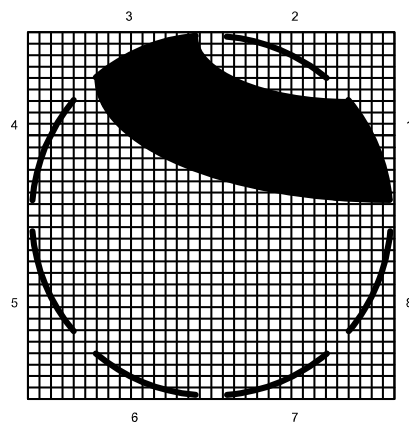


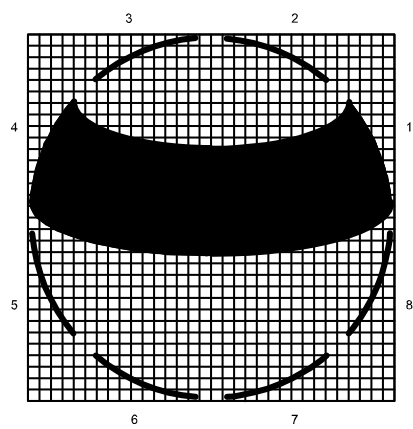
**Figure 8. 8 - electrode circular sensor and 32 X 32 pixel grid**



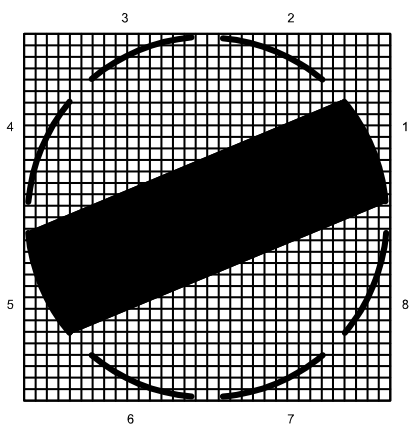
(a) S12



(b) S13



(c) S14



(d) S15

**Figure 9. Binary sensitivity maps for 8 - electrode sensor**



### 8.3 THE USE OF REAL SENSITIVITY MAPS

The LBP method can be easily extended for the more practical case where the sensitivity coefficients are not simply binary, but have values which lie within the nominal range 0 to 1. In this case, the elemental pixel values are found by multiplying the sensitivity coefficients by the normalised capacitance measurements using equations 6.9 and 6.10.

Some typical sensitivity matrices for an 8-electrode circular ECT sensor are shown in figure 10.

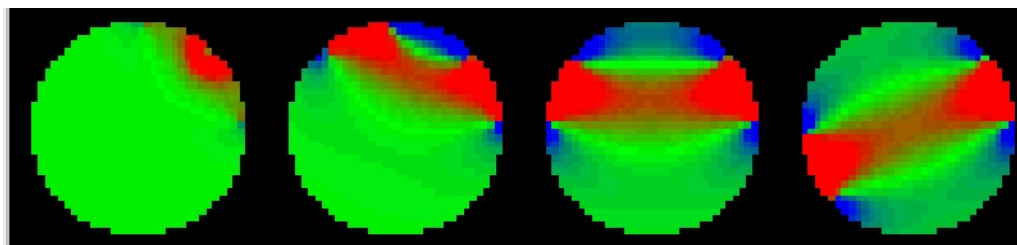


**Figure 10. Primary sensitivity maps for an 8-electrode sensor.**

We can therefore apply equation 6.10 directly to obtain the permittivity values of each pixel from the set of capacitance measurements.

### 8.3 CHARACTERISTIC RESULTS

From the description of the LBP method given in section 8.2 and previously, it is clear that images produced by this method will always be approximate. The method spreads the true image over the whole of the sensor area and consequently produces very blurred images. Moreover, because the image has been spread out over the sensor area, the magnitude of the pixels will always be less than the true values. However, the sum of all of the image pixels will approximate to the true value .

A typical image for a circular tube, containing the same material used to calibrate the sensor is shown in figure 11. The actual tube diameter was 40mm and the sensor internal diameter was 100mm. This corresponds to a nominal voidage of 16%. The LBP algorithm gave an overall voidage of between 12 and 16%, depending on the sensor model which was used\*. The effects of image blurring are clearly visible. The correct image would be a filled red circle of diameter 40% of that of the sensor, where red corresponds to a normalised permittivity of 1. The central area of the actual image produced by back-projection has a much lower value of permittivity, around 0.5 and displayed as green in figure 11.

It is possible to improve this image using simple iterative techniques. One method for doing this is described in PTL application note AN4 (An iterative method for improving ECT images). An example of the improvement in image quality which can be obtained using this method is shown in figure 12 for the same measurement data as shown in figure 11. The image of the rod is now of the correct size and magnitude.

\* See PTL Application note AN2, Calculation of Volume ratio for ECT sensors.

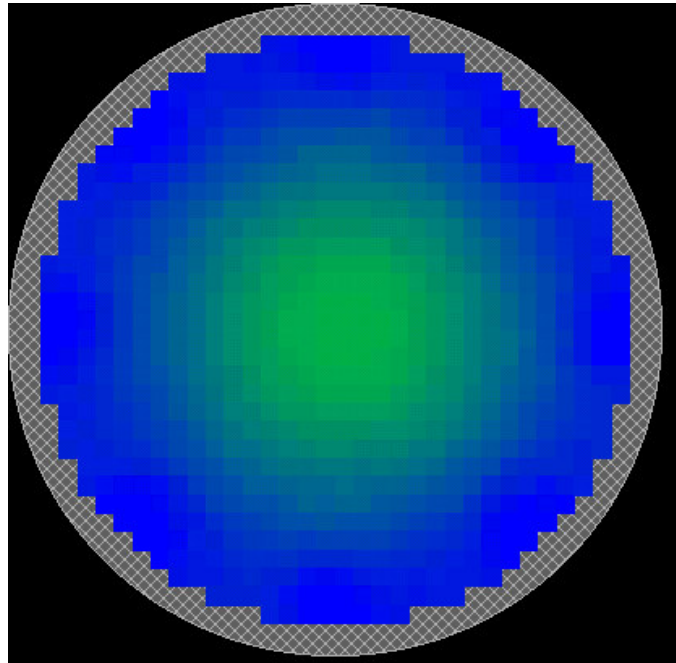


Figure 11. LBP image of circular rod

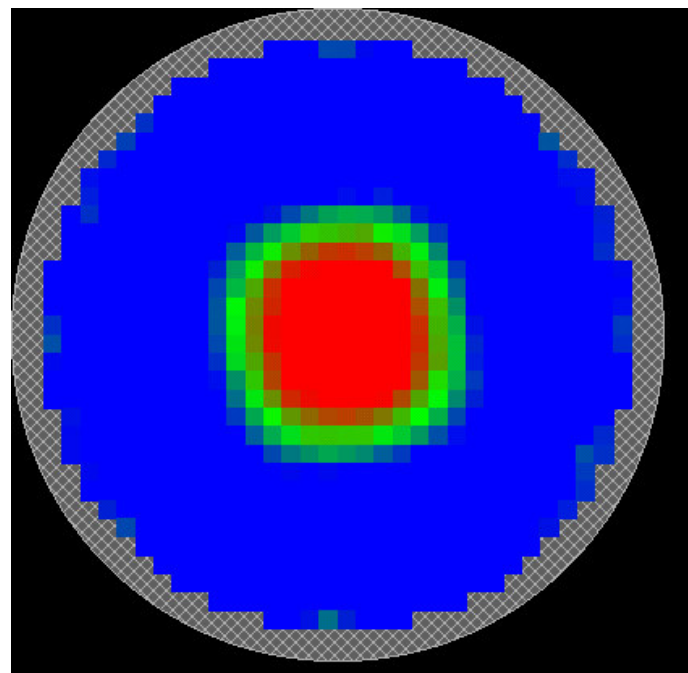


Figure 12. Same image after 50 iterations

## **PTL APPLICATION NOTE 2**

## **PTL APPLICATION NOTE AN2**

### **CALCULATION OF VOLUME RATIO FOR ECT SENSORS**

Issue 5

November 2005

#### **SUMMARY**

This note explains how the overall volume ratio (voidage), of a mixture of two dielectric materials inside an ECT sensor, and also the distribution of this voidage across the sensor, is calculated. The overall voidage can be obtained either from the measurements of the normalised capacitances between the sensor electrodes or from the permittivity distribution of the mixture, derived from these measurements. The voidage distribution is obtained from the permittivity distribution.

There are a number of possible methods which can be used to calculate the voidage and the choice of the optimum method depends on the electrical model used to describe the physical distribution of the two materials inside the sensor. For some applications, such as liquid or dense-phase mixtures, a simple parallel capacitance model can be used to obtain the voidage distribution directly from the permittivity distribution of the mixture. However, in other applications, such as fluidised beds with high levels of fluidisation, the use of a model based on capacitances in series produces better accuracy and sensitivity. A further model which combines the parallel and series models and which was developed by Maxwell in the 19th century is a useful compromise in many practical applications.

---

#### **PROCESS TOMOGRAPHY LTD**

**86 Water Lane, Wilmslow, Cheshire. SK9 5BB United Kingdom.**

**Phone/Fax 01625-549021**

(From outside UK +44-1625-549021)

email: [enquiries@tomography.com](mailto:enquiries@tomography.com) Web site: [www.tomography.com](http://www.tomography.com)

---

Registered in England No. 2908507. Registered Office 15, Croft Road, Wilmslow, Cheshire. SK9 6JJ United Kingdom.

## 1. INTRODUCTION

ECT systems can be used to obtain **images of the distribution of permittivity** inside ECT sensors for **any arbitrary mixture of different dielectric materials**.

However, an important application of ECT is viewing and measuring the spatial distribution of a **mixture of two different dielectric materials (a two-phase mixture)**. For a **two-phase mixture**, ECT can be used to measure the **spatial distribution** of the **composite permittivity** of the two materials inside the sensor. From this permittivity distribution, it is possible to obtain the distribution of the **relative concentration (volume ratio)** of the two components over the cross-section of the vessel.

A typical ECT permittivity image format uses a **square grid of 32 x 32 pixels** to display the distribution of the **normalised composite permittivity of each pixel**. For a circular sensor, 812 pixels are used to approximate the cross-section of the sensor. The **values of each pixel** represent the **normalised value of the effective permittivity of that pixel**. In the case of a **mixture of two dielectric materials**, these **permittivity values** are related to the fraction of the higher permittivity material present (the **volume ratio** (or **voidage**)) **at that pixel location**.

The **overall volume ratio**, which defines the **ratio of the two materials present, averaged over the volume of the sensor**, can also be obtained. The **overall volume ratio** of the materials inside the sensor at any moment in time is defined to be **the percentage of the volume of the sensor occupied by the higher permittivity material**. The volume of the sensor is the product of the cross-sectional area of the sensor and the length of the sensor measurement electrodes.

In all of the following we shall be referring to the **relative permittivity** (or **dielectric constant**) of materials. The **relative permittivity** of a material is its **absolute permittivity** divided by the **permittivity of free space** (or air). Hence the relative permittivity of air is 1 and typical values for other materials in solid or liquid format are polystyrene (2.5), glass (6.0) and mineral oil (2.3).

We have also used three different terms to describe the same concept, as they are all in common use. These are **volume ratio**, **voidage** and **concentration**, which we define to be the fraction of the higher permittivity material present in the mixture. These terms are interchangeable in the following test.

## 2. EFFECT OF CALIBRATION PROCEDURE ON VOIDAGE CALCULATION

### 2.1 ECT SYSTEM CALIBRATION PROCEDURE

In the normal method of operation, an ECT system is calibrated by filling the sensor with the **two reference materials in turn** and by measuring the **resultant inter-electrode capacitance values** at these **two extreme values of relative permittivity**.

This situation is shown diagrammatically in figure 1, which illustrates how the measured inter-electrode capacitances change between the higher and lower values of calibration for two materials of relative permittivity  $K_L$  and  $K_H$ . For simplicity, it has been assumed that the variation is linear, although, as will be seen later, this may not always be a valid assumption.

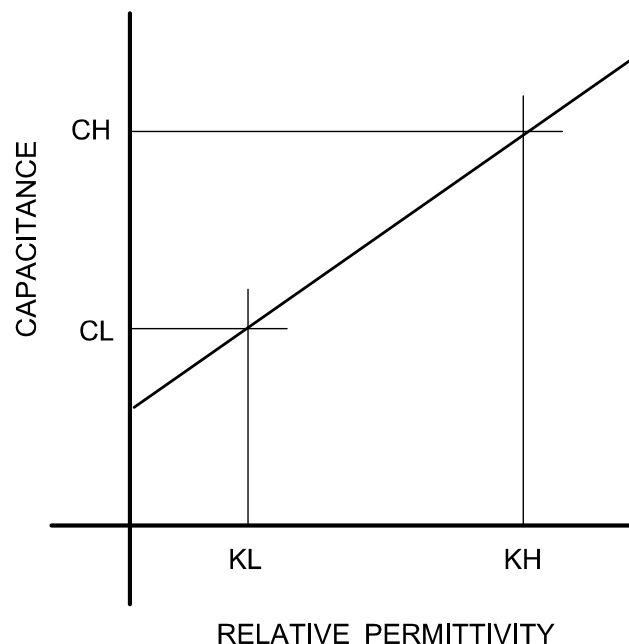


Figure 1. Relationship between the measured inter-electrode capacitances and the permittivity of the material inside the sensor.

This method of calibration defines the **two end points** of the **measurement range** for most types of ECT measurement.

## 2.2 ABSOLUTE AND RELATIVE VOIDAGES

All **voidage** values obtained from the ECT system are based on the assumption that the **voidage is 100%** when the sensor is full of the **higher permittivity material** and is **zero** when the sensor is filled with the **lower permittivity material**. Consequently, the **voidage values obtained from an ECT system are Relative Voidages**.

If the two materials used for calibration are **liquids**, then the **voidages** obtained from the ECT system will correspond nominally to the actual **absolute voidages**.

However, in many cases, one of the reference materials (the lower permittivity material) will be **air**. Air has a dielectric constant (relative permittivity) of 1, which is, by definition, the lowest possible value of dielectric constant which can exist for any real material. If the **second reference material** is in **granular or powder form**, the **upper calibration point** will be formed by a **mixture of air and the granular material**.

This will result in a **lower permittivity** for the **upper calibration point** than would be obtained by simply assuming the relative permittivity of the dielectric material in its solid form. For example for a mixture of glass beads and air, the measured permittivity of the mixture is around 3, whereas the permittivity of solid glass is approximately 6.

In this case, the **absolute voidage** for both the individual pixels and the sensor as a whole is obtained by multiplying the indicated **relative voidage** by the **actual voidage** at the upper calibration point.

For example, if the indicated **relative voidage** of a pixel is **p** and the **absolute voidage** when the sensor is full of the higher permittivity material is **f**, then **the absolute voidage of the pixel, VR**, will be given by:

$$VR = p.f \quad (2.2.1)$$

It should be noted that the permittivity or volume ratio distribution can only be obtained from the inter-electrode capacitance measurements if:

1. There are no more than 2 materials present inside the sensor.
2. The sensor has been correctly calibrated using these two materials.

### 3. NORMALISATION OF MEASUREMENT PARAMETERS

In PTL ECT systems, use is made of **normalised parameters** to represent **the inter-electrode capacitance measurements** and also the displayed values of **pixel permittivity**. The most important advantages of normalisation are:

1. It eliminates the need for the user to know the dielectric constants of the individual materials inside the sensor.
2. The widely different ranges of capacitance measurements between different combinations of electrodes are reduced to a single measurement range from 0 to 1.
3. The effect of measurement errors inside the DAM200 unit (including cross-coupling between measurement channels) is reduced.
4. ECT system calibration and operation are greatly simplified.

There are also some disadvantages to the use of normalised parameters. However, at present, the advantages of normalisation out-weigh the disadvantages and allow the ECT system to be operated in a much simpler way than would be possible if absolute values were used.

In the data capture process, the measured values of inter-electrode capacitances for the ECT sensor for each image frame and the pixel permittivity values derived from them, are normalised to lie between the values 0 and 1, where 0 corresponds to the values measured at the lower permittivity calibration point and 1 corresponds to the values measured at the upper permittivity calibration point. This is carried out using the reference data in the calibration file which is generated during the calibration process.

The following sections describe in detail how these capacitance measurements and pixel permittivities are normalised and used to calculate the volume ratio of the materials inside the ECT sensor.



### 3.1 NORMALISATION OF INTER-ELECTRODE CAPACITANCES

The inter-electrode capacitances measured at the lower calibration point ( $C_L$ ) are assigned values of 0 while the inter-electrode capacitances measured at the higher calibration point ( $C_H$ ) are assigned values of 1. This relationship is shown in graphical format below.

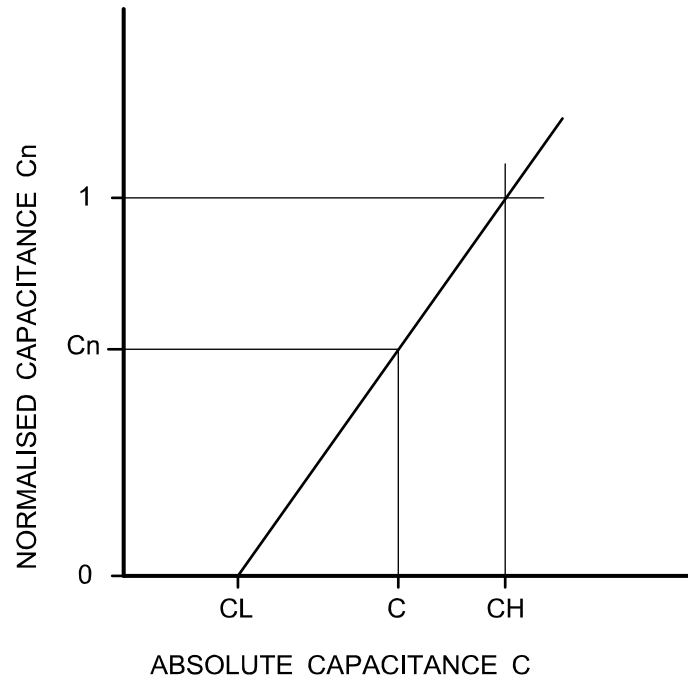


Figure 2. Normalisation of measured capacitance values

This relationship is defined by the equation:

$$C_n = (C - C_L) / (C_H - C_L) \quad (3.1.1)$$

where  $C_n$  is the set of normalised inter-electrode capacitances and  $C$  is the set of absolute capacitances measured with the sensor containing a material of arbitrary permittivity,  $C_H$  is the set of capacitances measured at the higher permittivity calibration point and  $C_L$  is the set of capacitances measured at the lower permittivity calibration point.

### 3.2 NORMALISATION OF PIXEL PERMITTIVITY VALUES

The permittivity values are normalised in a similar manner to the inter-electrode capacitances.

The permittivity values for each pixel in the ECT image for the lower permittivity calibration point ( $K_L$ ) are assigned values of 0, while the pixel permittivities in the image at the higher calibration point ( $K_H$ ) are assigned values of 1. This relationship is shown in graphical format below.

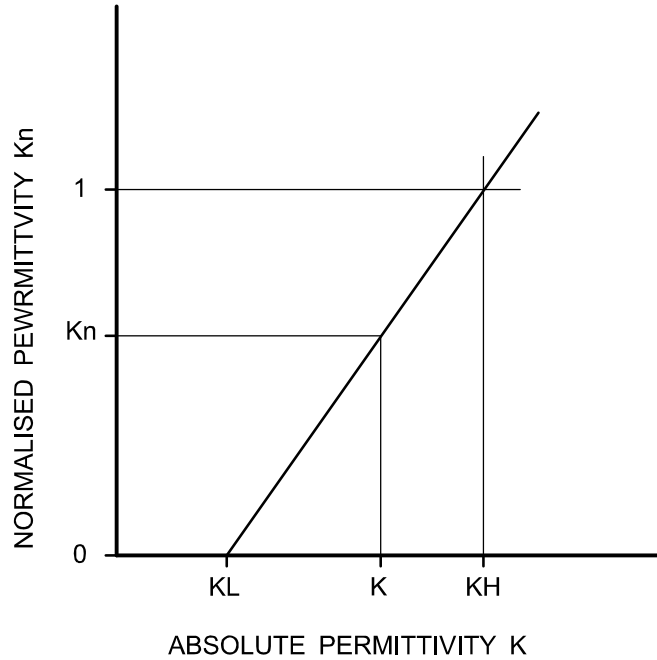


Figure 3. Normalisation of pixel permittivity values

This relationship is defined by the equation:

$$K_n = (K - K_L) / (K_H - K_L) \quad (3.2.1)$$

where  $K_n$  is the set of normalised permittivities (pixel values) when the sensor is filled with a material of permittivity  $K$ ,  $K_H$  is the effective permittivity of the material used to calibrate the sensor at the higher permittivity calibration point and  $K_L$  is the permittivity of the material used to calibrate the sensor at the lower permittivity calibration point.

### 3.3 RELATIONSHIP BETWEEN NORMALISED CAPACITANCES AND PIXEL PERMITTIVITIES

The ECT system constructs images from the normalised capacitances using Linear Back-Projection. For an ideal ECT sensor with internal electrodes and containing a dielectric material of uniform permittivity, there will be a linear relationship between the normalised inter-electrode capacitances and the resulting normalised pixel permittivity values. For example, if the sensor contains a uniform material of normalised permittivity  $K_n = P$ , the normalised inter-electrode capacitances will all have the value  $P$  and this will result in an image where each pixel also has the value  $P$ .

#### 4. CALCULATION OF RELATIVE VOIDAGE FROM ECT MEASUREMENTS

The **overall voidage** of the contents of the ECT sensor can be calculated from either the **normalised pixel values** in the reconstructed **ECT image** or from the **normalised capacitance measurements** directly. The choice is left as an option for the user to determine the method which gives results closest to the actual overall voidage. In general, the use of the pixel permittivities tends to give the most accurate results.

In the case of calculation from **image pixels**, the voidage is calculated by summing the values of the individual pixels in the ECT image for the required image frame and dividing this figure by the sum of these pixel values when the sensor is full of the higher permittivity material.

Putting this in mathematical terms,

$$VR = (1/M) \sum_{i=1}^M (P(i) / P_k) \quad (4.1)$$

where VR is the voidage, M is the total number of pixels, P(i) is the value of the ith pixel, and P<sub>k</sub> is the value of the ith pixel when the sensor is filled with the higher permittivity material (nominally 1).

In the case of calculation from the **normalised inter-electrode capacitances**, the voidage is obtained by summing all of the normalised capacitance values for one image frame and dividing these by the sum of the normalised capacitances when the sensor is filled with the higher permittivity material.

Again, putting this in mathematical terms,

$$VR = (1/N) \sum_{n=1}^N (C_n / C_k) \quad (4.2)$$

where N is the total number of electrode-pair measurements, C<sub>n</sub> are the individual electrode-pair normalised capacitances and C<sub>k</sub> are the electrode pair capacitances with the sensor full of the higher permittivity material (nominally 1).

In both of these cases, the voidage is calculated either directly or indirectly from the measurements of normalised capacitance and it is therefore necessary to consider how these capacitances or the pixel permittivity values derived from them, will be affected by the distribution of the two dielectric materials inside the ECT sensor.

This is necessary to determine whether these measurements will give an accurate assessment of the voidage. The sensor is calibrated accurately at the extreme ends of the measuring range and the voidage will be correct at these two points. However, at all points in between these two calibration points, the measured values of inter-electrode capacitances or pixel values will depend on the distribution of the dielectric materials inside the sensor.

In the next few sections we will explore how the combination of two dielectric materials determines the effective permittivity of the mixture. This is an important question as the answer will affect the accuracy of the volume ratio calculation.

## **5. EFFECTIVE PERMITTIVITY OF A MIXTURE OF TWO DIELECTRIC MATERIALS**

We are going to consider the case where we have a mixture of the two dielectric materials with which the sensor was calibrated inside the ECT sensor. Assume that these materials are uniformly mixed so that the mixture contains a fraction  $X$  of the higher permittivity material and hence  $(1 - X)$  of the lower permittivity material, ie the proportions of the two materials are constant everywhere. In this situation, we would expect the ECT image to display a uniform permittivity distribution with some constant value of effective permittivity  $K_E$ . However, we need to know how the effective permittivity  $K_E$  relates to the fraction or concentration ( $X$ ) of the higher permittivity material present in the mixture ( $X$  is also commonly referred to as the volume ratio or voidage).

The answer to this question depends on the model chosen to represent the fluid mixture. Further information about the basis of these models is given in Appendix 1.

## 5.1 THE PARALLEL CAPACITANCE MODEL

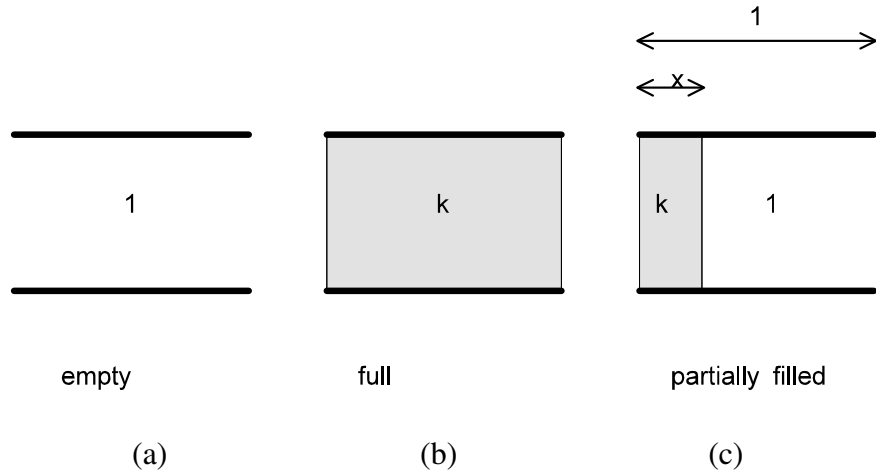


Figure 5.1 Capacitance cell containing vertically-stratified material

The simplest case assumes that the effective permittivity of the mixture can be obtained simply by summing the effects of the two components. This is known as the parallel capacitance model and corresponds to the case where there are effectively continuous bands of each dielectric material between the electrodes of the sensor as shown in figure 5.1.

In this case, the effective permittivity of the mixture  $K_E$  is given by:

$$K_E = X.K_H + (1 - X).K_L \quad (5.1.1)$$

Normalising this using equation (3.2.1), we obtain:

$$K_{EN} = (X.K_H + (1 - X).K_L - K_L) / (K_H - K_L) \quad (5.1.2)$$

giving:

$$K_{EN} = (X.K_H + K_L - X.K_L - K_L) / (K_H - K_L) \quad (5.1.3)$$

which simplifies to:

$$K_{EN} = X \quad (5.1.4)$$

So if we assume that the effective permittivities of the two materials can be found by adding their individual permittivities weighted by their relative concentrations, then the pixel values in the ECT image will correspond to the relative concentration (volume ratio)  $X$  of the higher permittivity material directly. Hence the implicit assumption made in equation 4.1, that the volume ratio distribution can be obtained directly from the permittivity distribution is correct.

The parallel capacitance model tends to be valid for densely packed materials, such as liquids, or powdered/granular materials in dense-phase processes.

More detailed information about the parallel capacitance model is given in Appendix 1.1.

## 5.2 THE SERIES CAPACITANCE MODEL

An alternative model is required for the situation where the higher permittivity material is present in dilute quantities in the mixture. This situation occurs, for example, in lean-phase fluidised beds or pneumatic conveying applications.

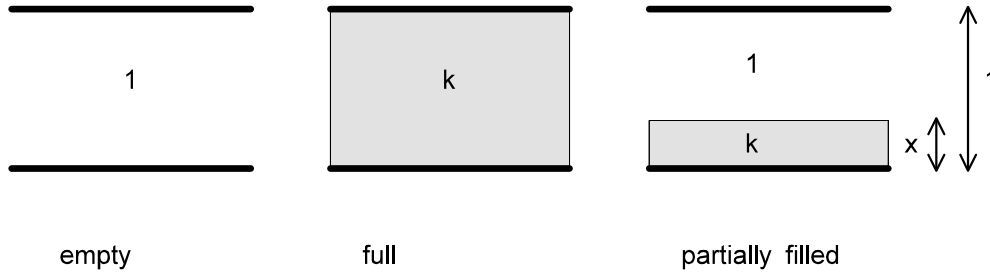


Figure 5.2. Capacitance cell containing horizontally-stratified material

The model which fits this situation is the series capacitance model, where we assume that the effective permittivity of a mixture of two materials can be found by assuming that the two materials act as two capacitors connected in series. (This model applies where neither material exists as continuous bands between the sensor electrodes). The first capacitor consists of a unit cell containing the higher permittivity material and the second capacitor consists of a similar cell containing the lower permittivity material. The cell capacitances are weighted by their permittivity values and concentrations, so that the effective permittivity of the mixture ( $K_E$ ) is obtained using the reciprocal law for two capacitors in series, ie:

$$1/C = 1/C_L + 1/C_H \quad (5.2.1)$$

These capacitances are proportional to the permittivity and inversely proportional to the concentration (see Appendix 1.2). Hence:

$$1 / K_E = (1 - X) / K_L + (X / K_H) \quad (5.2.2)$$

which simplifies to:

$$K_E = K_L \cdot K_H / (K_H + X \cdot (K_L - K_H)) \quad (5.2.3)$$

We can now calculate the normalised permittivity  $K_{EN}$  using equation 3.2.1.

$$K_{EN} = (K_L \cdot K_H / (K_H + X \cdot (K_L - K_H)) - K_L) / (K_H - K_L) \quad (5.2.4)$$

which simplifies to:  $K_{EN} = K_L \cdot X / ((K_H \cdot (1 - X) + K_L \cdot X)) \quad (5.2.5)$

It is a simple task to invert this equation to obtain the volume ratio  $X$  as a function of the normalised pixel permittivity values  $K_{EN}$ :

$$X = K_{EN} \cdot K_H / [K_L + K_{EN} \cdot (K_H - K_L)] \quad (5.2.6)$$

It is clear from this equation, that volume ratio  $X$  is no longer equal to the values of normalised pixel permittivities  $K_{en}$  and equation 4.1 is no longer valid.

### 5.3 CORRECTION OF PIXEL PERMITTIVITY VALUES

Equation 5.2.6 shows that to obtain the correct values of volume ratio when applying the series capacitance model, the pixel values obtained by linear back-projection must be modified by multiplying them by a correction factor CF where:

$$CF = K_H / (K_L + K_{en}(K_H - K_L)) \quad (5.3.1)$$

This correction factor requires knowledge of the higher and lower permittivity values used for calibration, (or their ratio  $K=K_H/K_L$ ). Figure 4, which plots this correction factor for several values of  $K_H/K_L$ , shows how the indicated voidage must be modified to give the correct voidage when the series model is used.

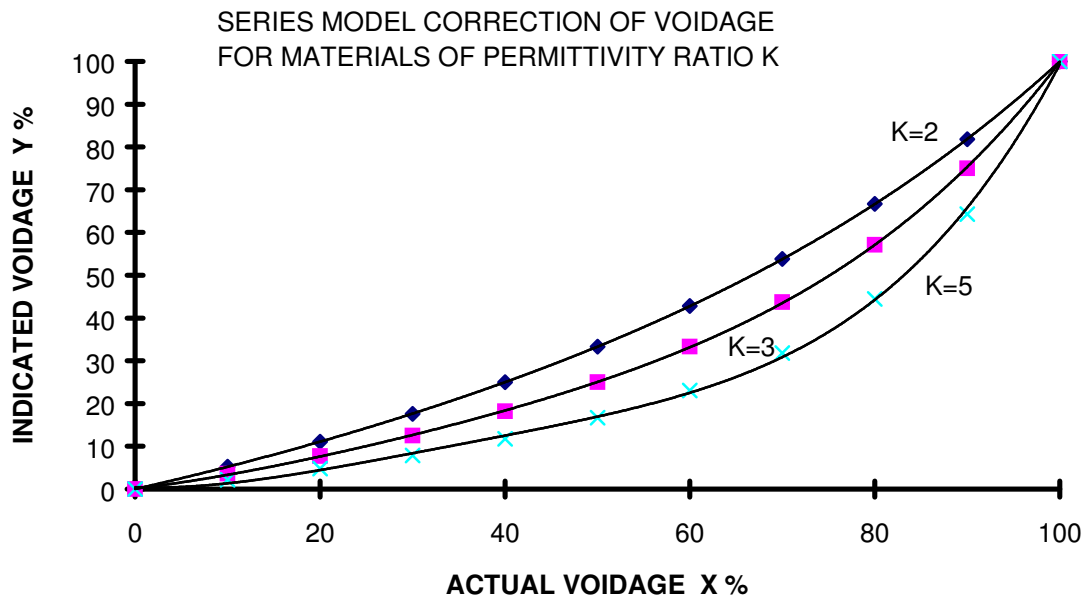


Figure 4. Correction of pixel permittivity values using the series model.

As the pixel permittivity values are obtained via a linear summation process from the normalised inter-electrode capacitance values, it is convenient, in practice, to apply this correction factor to the measured capacitances rather than to the pixel values directly. This has the added advantage that the average volume ratio of the ECT sensor contents, which can be calculated either from the pixel values or from the measured capacitances, is automatically corrected for both options.

Note that equation 5.2.6 can be re-written to give the concentration X in terms of the ratio of the high and low material permittivities (K) as follows:

$$X = K_{EN} \cdot K / [1 + K_{EN} \cdot (K - 1)] \quad (5.3.4)$$

where  $K = K_H/K_L$

## 6. OTHER PERMITTIVITY MODELS

There are a number of other models which can be used to calculate the relationship between the voidage and the effective permittivity of the material inside the sensor.

### 6.1 Maxwell Model

Details of this model are given in Appendix 2.

This yields a slightly different correction factor which, in practice is applicable to mixtures of two materials where both the parallel and series model apply in different regions of the mixture.

$$X = K_{EN} \cdot (2 + K) / [3 + K_{EN} \cdot (K - 1)] \quad (6.1.1)$$

where  $K = K_H / K_L$

### 6.2 Yang/Szuster Model

A variation on the series model, which does not rely on knowing the ratio of the permittivities of the materials used at calibration, has been developed independently by Dr W. Yang of UMIST in the UK and K. Szuster in Poland. This method effectively deduces the permittivity ratio from the calibration data.

The method is described in reference 1.

The correction factor which results from this model is given in equation 6.2.1.

$$X = K_{EN} \cdot (C_H / C_m) \quad (6.2.1)$$

where:

$C_H$  is the absolute value of the capacitance measured during calibration for the higher permittivity material.

$C_m$  is the absolute value of the measured capacitance.

## 7. REFERENCE

"An improved Normalisation Approach for Electrical Capacitance Tomography.", Yang, W.Q. and Byars, M., 1st World Congress on Industrial Process Tomography, Buxton, UK, 14-17 April 1999.



## APPENDIX 1

### A1 CAPACITANCE MODELS FOR DISTRIBUTIONS OF DIELECTRIC MATERIALS

Any mixture of two materials can be represented by sets of elemental capacitors containing one or other of the dielectrics. These elemental capacitors can be envisaged as being interconnected either in parallel with each other (in which case the total capacitance will be the sum of the elemental capacitors) or in series with each other (in which case the reciprocal rule must be used to obtain the total capacitance). We can simplify these two situations to the case of a simple horizontal parallel plate capacitor containing two dielectric materials which may be distributed either horizontally or vertically as described in the following sections.

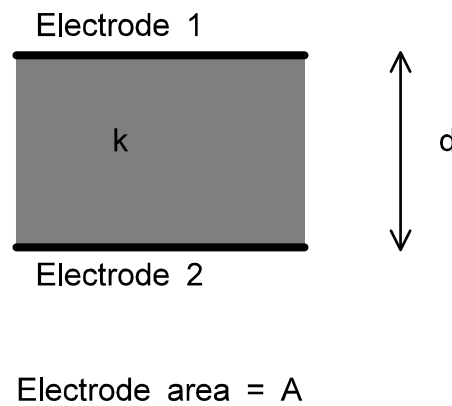


Figure A1.1. Parallel plate capacitance cell

Consider the case of the simple parallel plate capacitance cell shown in figure A1.1. The capacitance of this cell is given by the equation :

$$C = \epsilon_0 \cdot \epsilon_r \cdot A / d \quad (\text{A1.1})$$

where  $\epsilon_0$  is the permittivity of free space,  $\epsilon_r$  is the dielectric constant of the material inside the cell, A is the area of the capacitance plates and d is the spacing between the plates.

We are going to consider how the capacitance of this type of cell changes when it is filled with varying quantities of dielectric material. As the cross sectional area, the permittivity of free space and the plate spacing d will remain constant throughout, we can arbitrarily set

A.  $\epsilon_0/d = 1$  and calculate a set of relative capacitance values  $C_r$ .

In this case, equation (A1.1) simplifies to:

$$C_r = \epsilon_r \quad (\text{A1.2})$$

## A1.1 CASE 1. VERTICAL DIVISION OF MATERIALS

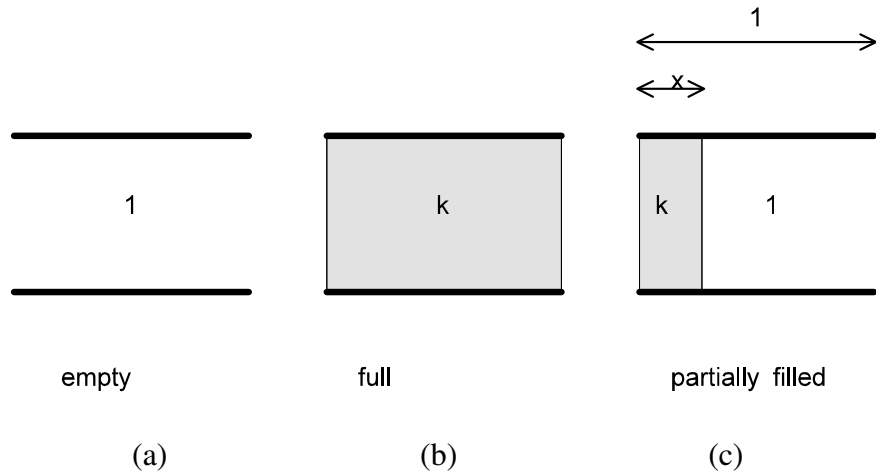


Figure A1.1.1 Capacitance cell containing vertically-stratified material

The first case to consider is that shown in the figure A1.1.1, where the cell is shown (a) empty (containing air), (b) filled with a dielectric material of relative permittivity  $k$  and (c) partially filled, with a vertical division between the dielectric material and air.

When the cell is filled with air (a),  $\epsilon_r = 1$  and equation (6.2) becomes:

$$C_{\text{air}} = 1 \quad (\text{A1.1.1})$$

When the cell is filled with dielectric material of dielectric constant  $k$  (b), the capacitance becomes:

$$C_k = k \quad (\text{A1.1.2})$$

When the cell is partially filled with dielectric material of dielectric constant  $k$  (c), the cell becomes two capacitors  $C_{\text{air}}$  and  $C_k$  in parallel, where the values of  $C_{\text{air}}$  and  $C_k$  depend on the proportion of the cell width occupied by each component.

The capacitance of parallel capacitors is simply the sum of the two individual capacitors. Hence the capacitance for the case of 2c is given by:

$$C_r = C_{\text{air}} + C_k \quad (\text{A1.1.3})$$

or 
$$C_r = 1.(1-X) + k.X \quad (\text{A1.1.4})$$

giving 
$$C_r = X.(k - 1) + 1 \quad (\text{A11.5})$$

In this case, the capacitance of the cell will simply increase in proportion to the width of the cell occupied by the dielectric material. Hence the **cell capacitance will increase linearly as the proportion of higher dielectric material in the cell increases** and this capacitance **will accurately represent the cell voidage**.

This model for the relationship between permittivity and capacitance is referred to as the **parallel capacitance model**.

## A1.2. CASE 2. HORIZONTAL DIVISION OF MATERIALS

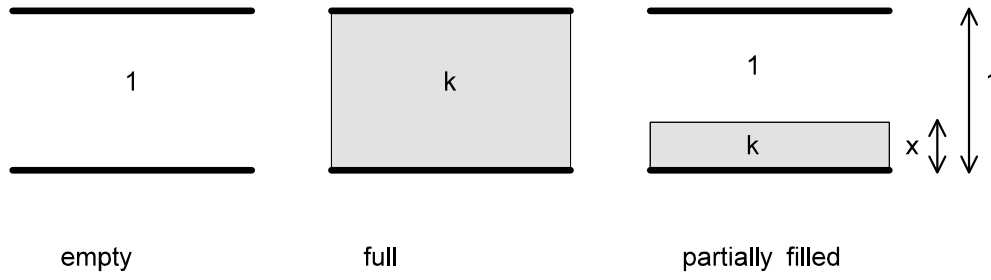


Figure A1.2.1 Capacitance cell containing horizontally-stratified material

The second case to consider is that shown in figure 5, where the cell is shown (a) empty (containing air), (b) filled with a dielectric material of relative permittivity  $k$  and (c) partially filled with a horizontal division between the dielectric material and air.

When the cell is filled with air (a),  $\epsilon_r = 1$  and equation (6.2) becomes:

$$C_{\text{air}} = 1 \quad (\text{A1.2.1})$$

When the cell is filled with dielectric material of dielectric constant  $k$  (b), the capacitance becomes:

$$C_k = k \quad (\text{A1.2.2})$$

When the cell is partially filled with dielectric material of dielectric constant  $k$  (c), the cell becomes two capacitors  $C_{\text{air}}$  and  $C_k$  in series, where the values of  $C_{\text{air}}$  and  $C_k$  depend on the proportion of the cell height occupied by each component.

Unlike the situation for capacitors connected in parallel, the capacitance of capacitors connected in series is not simply the sum of the two individual capacitors but is obtained by adding up their reciprocals. Hence the capacitance for the case of 2c is given by:

$$1/C_r = 1/C_{\text{air}} + 1/C_k \quad (\text{A1.2.3})$$

Now  $C_{\text{air}} = 1/(1 - X) \quad (\text{A1.2.4})$

and  $C_k = k/X \quad (\text{A1.2.5})$

Hence  $1/C_r = (1 - X) + X/k \quad (\text{A1.2.6})$

Giving  $C_r = k/(k(1 - X) + X) \quad (\text{A1.2.7})$

In this case, **the capacitance of the cell increases in a non-linear manner as the proportion of the cell occupied by the dielectric material increases. Moreover, the rate of increase depends on the dielectric constant of the material.**

This model for the relationship between permittivity and capacitance is referred to as the series **capacitance model**. In many cases (such as fluidised beds), the series capacitance model is a more realistic accurate representation of the physical model than the parallel capacitance model.

## APPENDIX 2

### MAXWELL PERMITTIVITY MODEL

This model is based on the work of Maxwell in the 19th Century. Maxwell showed that, for a homogeneous mixture containing small spheres of equal diameter of a higher permittivity material  $\epsilon_2$  distributed within a lower permittivity material  $\epsilon_1$ , the effective permittivity of the material is given by:

$$\epsilon_m = \epsilon_1 \cdot \frac{2 \cdot \epsilon_1 + \epsilon_2 - 2 \cdot X \cdot (\epsilon_1 - \epsilon_2)}{2 \cdot \epsilon_1 + \epsilon_2 + X \cdot (\epsilon_1 - \epsilon_2)} \quad (\text{A2.1})$$

As the measured capacitances will be proportional to the effective permittivity  $\epsilon_m$ , we can re-write equation A2.1 as follows:

$$C = \frac{2 + K - 2 \cdot X \cdot (1 - K)}{2 + K + X \cdot (1 - K)} \quad (\text{A2.2})$$

where  $K = \epsilon_2 / \epsilon_1$

We can now repeat the process outlined in Appendix 1 and section 5 to calculate the effective normalised permittivity  $K_{EN}$  (which is equal to the normalised capacitance  $C_n$ ), in terms of the voidage  $X$ , which yields:

$$K_{EN} = 3 \cdot X / [2 + k + X \cdot (1 - K)] \quad (\text{A2.3})$$

As before, we can invert this equation to obtain the actual voidage  $x$  in terms of the pixel permittivity  $K_{en}$  as follows:

$$X = K_{EN} \cdot (2 + K) / [3 + K_{EN} \cdot (K - 1)] \quad (\text{A2.4})$$

This yields an alternative correction factor for the measured inter-electrode capacitances.

## **PTL APPLICATION NOTE 3**

**PTL APPLICATION NOTE AN3**  
**ENGINEERING DESIGN RULES FOR ECT SENSORS**

Issue 4

March 2001

**ABSTRACT**

This Application Note explains how the design of a capacitance sensor for use with an Electrical Capacitance Tomography (ECT) system influences the performance of the system. A set of engineering rules are developed which allows successful working ECT sensors to be designed for use with specific materials.

---

**PROCESS TOMOGRAPHY LTD**

**86 Water Lane, Wilmslow, Cheshire. SK9 5BB United Kingdom.**

**Phone/Fax 01625-549021**

(From outside UK +44-1625-549021)

email: [ptl@tomography.com](mailto:ptl@tomography.com) Web site: [www.tomography.com](http://www.tomography.com)

---

Registered in England No. 2908507. Registered Office 15, Croft Road, Wilmslow, Cheshire. SK9 6JJ United Kingdom.

## 1. INTRODUCTION

Electrical Capacitance Tomography is a technique for obtaining information about the contents of vessels, based on measuring variations in the dielectric properties of the material inside the vessel. The basic idea is to fit a number conducting plates (electrodes) around the periphery of the vessel and to measure the capacitance variations which occur between combinations of electrodes when a dielectric material is introduced inside the vessel.

An important step in planning a successful ECT application is the design of the capacitance sensor unit, as this will normally be unique for each new application. This note explains how the various design parameters of ECT sensors interact and affect the overall sensor performance, and develops a set of design rules which allow an effective ECT sensor to be constructed for a specific application. The Application Note concentrates on the design of sensors for use with vessels having circular cross sections (although many of the comments apply to vessels of any cross section).

The design of ECT sensors is closely linked to the capabilities of the capacitance measuring equipment to be used with the sensor. An ideal capacitance measuring system will have a very low noise level, a wide dynamic measurement range, high immunity to stray capacitance to earth and be able to carry out measurements at high speed. The information given in this paper is largely based on the capabilities of the PTL DAM200 Data Acquisition Module which can measure capacitance in the range 0.1 to 2000 fF with an rms noise level around 0.07 fF.

The sequence of electrode excitation is fixed in the DAM200 unit and only one electrode can be a SOURCE electrode, excited at a potential above that of earth, at any one time. The remaining electrodes are set to be DETECTOR electrodes and are maintained at virtual earth potential. This is not the only possible mode of operation of an ECT system but is the one on which most experience has been gained to-date and this note will therefore be restricted to a discussion of sensors suitable for use with single electrode excitation ECT systems of this type.

## 2. OVERVIEW OF SENSORS FOR ECT SYSTEMS

### *2.1 Sensors with external electrodes*

Capacitance sensors for use with vessels of circular cross-section are normally customised modules which are individually designed for each specific application and can take one of two basic forms. The simplest arrangement from a constructional viewpoint consists of a non-conducting section of pipe surrounded by an array of equally-spaced capacitance electrodes with an overall outer earthed screen as shown in figure 1(a). A simple sensor of this type is shown in figure 2. This arrangement has the advantage that contact with and possible contamination of the electrodes by the fluid inside the pipe is avoided and the measurement is therefore non-invasive. However, sensors with electrodes on the outside of the vessel wall can exhibit considerable non-linearity in their response to dielectric materials introduced inside the sensor. This effect is caused by the presence of the sensor wall, which introduces an additional (and unhelpful) series coupling capacitance into the measurement of the inter-electrode capacitances.

### *2.2 Sensors with internal electrodes*

An alternative arrangement is to fit the electrodes inside the vessel as shown in figure 1(b). In the case of a metal-walled vessel, this requires the use of some form of insulated liner supporting the electrodes, which then is placed inside the vessel. Although it is more difficult to design and construct this type of sensor from a mechanical viewpoint, sensors with electrodes inside the vessel do not suffer from the non-linearity problems exhibited by sensors with external electrodes and if the highest accuracy is required, this type of sensor should be used in preference to a unit with external electrodes.

### *2.3 Screening arrangements*

For both types of sensor, the inter-electrode capacitances are typically fractions of a picoFarad and an earthed screen must be placed around the electrodes to eliminate the effects of extraneous signals and variations in the stray capacitance to earth, which would otherwise predominate and corrupt the measurements. ECT sensors must have a high level of mechanical stability, as any small movement between electrodes will change the values of inter-electrode capacitances. The electrodes are connected to the capacitance measuring system by individual coaxial connecting leads.

The capacitance measuring system normally imposes an upper limit on the allowable capacitance between each sensor electrode and earth. In the case of the PTL DAM200 unit, this value is 200 pF and this figure includes the capacitance of the coaxial connecting leads (typically 100pF/metre) as well as the capacitance between each measurement electrode and the external sensor screen.



## *2.4 Guard electrodes*

If the sensor electrodes are short compared with the diameter of the sensor, extra axial guard electrodes will normally be required at each end of the measuring electrodes. The purpose of the guard electrodes is to maintain a parallel electric field pattern across the sensor in the region of the measuring electrodes, by preventing the electric field lines from spreading axially at the ends of the measuring electrodes. This improves both the axial resolution and the sensitivity of the sensor. The guard electrodes are connected to guard driving circuitry in the capacitance measuring unit. Earthed axial electrode tracks may also be needed between adjacent measuring electrodes to reduce the standing capacitance between adjacent electrodes to a value low enough to avoid overloading or saturating the capacitance measuring system. These earthed tracks can also be extended radially out to the earthed outer screen to further reduce the adjacent electrode capacitances.

## *2.5 Number of electrodes*

The choice of the number of electrodes around the circumference of the sensor is a tradeoff between axial and radial resolution, sensitivity and image capture rate. Existing PTL ECT systems can be used with sensors having 6, 8, or 12 electrodes. The electrodes normally occupy most of the circumference of the sensor and as the measurement sensitivity depends on the surface area of the sensor electrodes, the same sensitivity can be achieved with either a small number of short electrodes or a larger number of longer electrodes. If the number of electrodes is increased, the radial resolution will be improved, while a reduction in the length of electrodes will give better axial resolution. As measurements are made between each electrode and every other electrode, there are  $N(N-1)/2$  possible unique capacitance measurements per image for a system with  $N$  measuring electrodes (corresponding to 66 individual measurements for a 12 electrode sensor). It follows that more measurements will be required to collect data for each image as the number of electrodes is increased, and hence the speed of data capture will be reduced as the number of electrodes is increased.

## *2.6 Electrode Numbering Convention*

By convention, electrodes are numbered anticlockwise, starting in the first quadrant above the horizontal. So for a 12 electrode system, electrode 1 lies in the sector from 0 to 30 degrees, electrode 2 in the sector from 30 to 60 degrees and so on as shown in figure 1.

## *2.7 Typical Inter-Electrode Capacitance Values*

The values of measured inter-electrode capacitances for a typical 12-electrode sensor containing air are shown in figure 3. These figures were measured using a 50 cm diameter sensor having relatively long external measurement electrodes (10 cm). The sensor did not contain driven guard electrodes. Although there are 66 possible unique values of inter-electrode capacitance, these reduce to a set of 6 generic capacitances (C1-2, C1-3, .....C1-6) as long as the sensor is symmetrical and is either empty or is filled with a uniform material. Note that C1-2 means the capacitance measured between electrode 1 and electrode 2 etc..

From the results shown in figure 3, it can be seen that there is a wide range of values for the inter-electrode capacitances, ranging from a high figure of 500fF for adjacent electrodes to a low value of 10fF between opposite electrodes. These values were measured with the sensor containing air and will normally increase if any other dielectric material is introduced into the sensor.

Note that an asymmetrical capacitance distribution has occurred because the sensor measured used a pcb foil construction (see section 2.8) with the join between electrodes 1 and 12. Small errors in the inter-electrode gap cause large errors in inter-electrode capacitance values and it is therefore preferable to locate the join along the centre of an electrode for this reason.

This wide range of standing capacitances causes problems for the capacitance measuring unit, which will normally have an upper and lower limit for the range of measurable capacitances ( $C_{max}$  and  $C_{min}$ ). In the case of the PTL DAM200 unit, the upper measurement limit  $C_{max}$  is 2000fF and the lower limit  $C_{min}$  is approximately 0.1fF.

The value of the standing capacitance between adjacent electrodes can be reduced either by simply increasing the spacing between the electrodes (at the expense of reducing the capacitance between all electrodes per unit length) or by the combined effects of an earthed axial screening track placed between the electrodes and the presence of an external circumferential earthed screen. Experience has shown that for typical sensors, with an earthed axial screening track and an outer screen located approximately 0.5cm from the electrodes, the capacitance between adjacent electrodes is approximately halved compared with the value in the absence of the screens. However, this produces little effect on the capacitance between non-adjacent electrodes.

Typical capacitances for a 12 electrode sensor with suitable driven guard electrodes (see design rules 4.4 and 4.5) are approximately 100fF per cm of electrode length ( $K1$ ) between adjacent electrodes and 1 fF/cm ( $K2$ ) between opposite electrodes. For an 8 electrode sensor, the capacitance per unit length between adjacent electrodes is similar to that for 12 electrode sensors, ie around 100fF/cm, however, the capacitance per unit length for opposite electrodes increases to around 2 fF/cm.

## *2.8 Electrode fabrication*

A typical electrode arrangement for a single plane 8 electrode sensor with driven guard electrodes is shown in figure 4. The electrodes are fabricated using photolithography techniques from flexible copper-coated plastic laminate which is etched with the required electrode pattern and then wrapped around the outside of the pipe or vessel. Figure 4 shows a negative image of an unrolled electrode laminate. The white areas are copper foil and the black lines represent insulating gaps between the electrodes. The 8 measurement electrodes are in the centre of the sensor and driven guard electrodes are located at each end of the measurement electrodes. Axial conducting strips separate the sets of electrodes and are connected to earthed areas at each end of the sensor.

The laminate is attached to the outside of an insulating pipe with the copper foil on the outside and connections are soldered to the measurement electrodes and guard electrodes using coaxial connecting leads. The two sets of guard electrodes must be interconnected using lengths of insulated wire which pass over each measurement electrode. Further detailed information about sensor fabrication is given in Appendix 1.

## *2.9 Lengths of Measurement and Guard Electrodes*

The image produced by an ECT system is derived from the capacitances measured between the sensor electrodes. As these capacitances are proportional to the surface area of the electrodes, the measurement electrodes must have a finite length  $L_m$ . The image is therefore derived from capacitance measurements averaged over the length of the electrodes and it follows that an ECT system can not produce images with very high axial resolution because of the need to have electrodes of finite length.

In an ideal ECT sensor, the electric field lines will be normal to the sensor axis. However, if electrodes are used which are short compared with the diameter of the sensor, the field lines will spread out at the ends of the measurement electrodes. This will have two consequences:

1. The capacitance measured between electrodes will be reduced and hence the measurement sensitivity will also be reduced.
2. The axial resolution of the sensor will be degraded because of the axial spreading of the field lines at the end of the sensor.

This problem can be virtually eliminated by the use of driven guard electrodes at each end of the measuring electrodes as described previously. Experiments have been carried out to establish the required length for guard electrodes  $L_g$ . Figure 5 shows how the length of guard electrodes increases the capacitance measured between two electrodes of length 1cm in an 8 electrode sensor of diameter 15 cm, with driven guard electrodes of equal length  $L_g$  at each end of the measurement electrodes. It can be seen from figure 5 that when  $L_g$  equals the sensor radius, the capacitance measured between opposite electrodes is approximately 60% of the maximum possible value (which can only be realised with infinitely long guard electrodes).

## *2.10 Electrostatic charge precautions*

As ECT sensors often contain dielectric materials which are in motion, there is a high probability of electrostatic charge accumulating on the measuring electrodes, resulting in the development of high voltages between the electrodes and earth. These voltages could easily damage the sensitive electronic circuitry in the capacitance measuring unit and precautions must be taken to prevent excessive voltages from becoming established on individual electrodes. This is done in practice by connecting discharge resistors (of value 100K - 10M Ohm) between each individual measuring and guard electrode and earth. The discharge resistors must be integrated into the sensor itself (not the capacitance measuring unit).

## *2.11 Sensor Calibration*

The standard method currently in use for calibrating ECT systems and sensors is to measure the inter-electrode capacitances when the sensor is filled with dielectric materials having permittivities at the extreme ends of the measurement range of interest. Hence the sensor will first be filled with a material having a low dielectric constant, emptied, and then refilled with a second material having a higher dielectric constant. These sets of inter-electrode capacitances are then normalised to values of 0 at the lower permittivity calibration point and 1 at the higher permittivity calibration point. From these capacitance measurements, images are constructed in which the image pixels have nominal values between 0 (corresponding to the lower permittivity material) and 1 (corresponding to the higher permittivity material).

## *2.12 Sources Of Image Distortion*

ECT is a so-called soft-field measuring technique. The object space is interrogated by electric field lines, which can be envisaged as curved lines running between the measuring electrodes. If a uniform dielectric material is introduced inside an ECT sensor with internal electrodes, so that the material completely fills the sensor, then the pattern formed by the electric field lines inside the sensor will be the same, irrespective of the permittivity of the dielectric material. However, if the space inside the sensor is only partially filled by dielectric, or if the dielectric material is non-uniform, the pattern of the electric field lines will be changed by the material inside the sensor. The effect will be to distort any image obtained from the measurements of the inter-electrode capacitances. This is analogous to the distortion of an optical image by an imperfect lens. Further image distortion is introduced by sensors which contain electrodes located outside the vessel wall. As the objective of an ECT system is to obtain an image based on variations in the permittivity of the material inside the sensor, allowance must be made for this distortion in the image reconstruction algorithm if an accurate image is to be obtained.

### 3. SENSOR PERFORMANCE

#### *3.1 Sensitivity to permittivity perturbations*

The sensitivity of an ECT sensor to small changes in permittivity inside the sensor varies with the radial position of the perturbation and is also a function of the size of the perturbation and the magnitude of its permittivity change. Circular ECT sensors have maximum sensitivity near the sensor wall and minimum sensitivity at the centre of the sensor.

#### *3.2 Axial and Orthogonal Resolution.*

Provided that adequate driven guard electrodes are used, the axial resolution achievable with a given sensor will be approximately equal to the axial length of the measuring electrodes.

It is more difficult to define the orthogonal resolution (ie the resolution across a diameter) because the sensitivity of the sensor to a minor perturbation in permittivity varies along the diameter as described in the previous section. As a rule of thumb, the orthogonal resolution will be approximately equal to  $D/N$  where  $D$  is the diameter of the vessel and  $N$  is the number of measurement electrodes placed around the circumference of the sensor.

## 4. SENSOR DESIGN RULES

### *4.1 Internal or external electrodes*

If the vessel wall is metallic, internal electrodes must be used. If the vessel wall is made of an insulating material, the electrodes can be placed either inside or outside the vessel wall. A sensor with internal electrodes will normally have superior electrical performance to one with internal electrodes, but the design and construction of sensors with internal electrodes is considerably more complex than that for sensors with external electrodes.

### *4.2 Number of electrodes.*

The maximum number of electrodes (12) should be used wherever possible, provided that sufficient measuring sensitivity and axial resolution can be achieved. For the best axial resolution, a small number of short measurement electrodes should be used. The axial resolution will be approximately equal to the length of the measurement electrodes. For the best resolution across the image plane, a large number of longer measurement electrodes should be chosen. The orthogonal resolution will be approximately  $D/N$  where  $D$  is the sensor diameter and  $N$  is the number of measuring electrodes.

### *4.3 Maximum and minimum inter-electrode capacitance values..*

For a sensor to be able to image materials having permittivities in the range from a lower value of  $E1$  to an upper value of  $E2$ , with a measurement system which can measure capacitance over a range from  $Cmin$  to  $Cmax$ , the sensor should be designed so that:

- The capacitance measured between **adjacent** electrodes, with the sensor containing the **lower permittivity material** ( $E1$ ), must be less than  **$Cmax.(E1/E2)$** . This is necessary to allow the capacitance when the sensor is full of the higher permittivity material ( $E2$ ) to be less than the maximum measurable value  $Cmax$ .
- The capacitance measured between **opposite** electrodes with the sensor containing **the lower permittivity material** must not be less than  **$K.Cmin$** , where  $K$  is a constant (typically 50) This ensures that a relatively noise-free measurement of the opposite electrode capacitance can be made.

These capacitance values can be translated into equivalent electrode lengths using the typical figures for capacitance per unit length for adjacent and opposite electrodes ( $K1$  and  $K2$ ) given in section 2.7.

### *4.4 Total electrode length*

The total electrode length  $Lt$  (including the measurement and driven guard electrodes, but excluding the earthed end regions) should normally be at least equal to the diameter of the vessel to be imaged as discussed in section 2.9. A larger value for  $Lt$  will further increase the sensitivity of the sensor.

#### *4.5 Lengths of measurement and guard electrodes*

The minimum usable length of measuring electrodes is  $L_{min} = C_{min}/K_2$  and the maximum length  $L_{max}$  is  $C_{max}/K_1$ , where  $C_{min}$  and  $C_{max}$  and the values for  $K_1$  and  $K_2$  are those given in section 2.7. This will define the range of possible lengths for the measurement electrodes. The final choice will need to be made on the basis of the required axial resolution and measurement sensitivity.

Once the length of the measurement electrodes has been chosen, the length of the guard electrodes can be evaluated using the following equation:

$$L_t = L_m + 2.L_g .$$

where  $L_t$  is the total electrode length (section 4.4),  $L_m$  is the length of the measurement electrodes and  $L_g$  is the length of the driven guard electrodes.

#### *4.6 Screening arrangements*

The measuring electrodes must be completely surrounded by an earthed, metal screen and the measuring and guard electrodes must be connected to the measuring unit by screened coaxial connecting leads. For the PTL DAM200 unit, the maximum capacitance between any measuring electrode and the earthed screen should not exceed 200 pF. It should be noted that this figure includes the capacitance of the coaxial connecting leads (100pF per metre length).

#### *4.7 Connecting leads*

The measurement and guard electrodes must be connected to the capacitance measuring unit by screened coaxial cables (recommended type RG174), terminated in SMB coaxial connectors. The maximum length of connecting lead should not exceed 1.5 metres. The inner conductor of each coaxial cable should be connected to the pcb electrode and the outer braid of the cable must be connected to an earthed area of the pcb laminate.

#### *4.8 Electrostatic precautions*

Each measurement and guard electrode must be connected to an earthed area on the sensor laminate by an individual discharge resistor. Suitable values of resistor are 1Mohm, 0.25 Watts.

## 5. PRACTICAL VALUES

From experience gained to-date with the PTL300 ECT system, we suggest the following minimum lengths should be used for measurement and guard electrodes:

No of electrodes	Minimum length of measurement electrodes cm	Total electrode length including guard electrodes cm
6	2.5	D
8	3.5	D
12	5	D

where **D** is the diameter of the sensor. Improved sensitivity will occur by increasing either the length of the measurement or guard electrodes or both of these.



## **APPENDIX 1**

### **SENSOR FABRICATION**

#### **A1.1 FLEXIBLE COPPER-COATED LAMINATE**

One flexible laminate material which has been used successfully by PTL to fabricate sensors is GTS77012ED copper polyimide (Kapton) laminate. This material is available in rolls of 610mm width and consists of a 50 micron film of plastic coated with a 35 micron layer of copper. The material can be soldered without damage at a temperature of 300 degrees centigrade.

The UK supplier is:  
GTS Flexible Ltd.,  
41 Rassau Industrial Estate,  
Ebbw Vale,  
Gwent.  
NP3 5SD,  
UK.

Phone 01495 307060, Fax 01495 306333.

The electrode pattern is produced using standard printed circuit board design techniques. The electrode pattern must be drawn using a suitable CAD package and plotted by a photoplotting bureau to produce an accurate artwork suitable for pcb manufacture.

#### **A1.2 EXTERNAL SCREEN**

This can take a number of forms.

If a metallic tube of a convenient size is available, then this can be used directly.

If a plastic tube is available, it can be used by lining it either internally or externally with a conducting material. For experimental work, self-adhesive copper tape is suitable.

The screen can also be formed from a flexible copper sheet wrapped around the sensor and held in place with cable ties.

In all cases, the external screen must be connected electrically to the earthed region of the sensor foil using a short length of flexible connecting lead.

#### **A1.3 GUARD ELECTRODE INTERCONNECTION**

The driven guard electrodes at the ends of the measurement electrodes must be interconnected by short lengths of insulated wire, connected to each driven guard electrode. The coaxial connecting leads for the guard electrodes then only need to be connected to one electrode of each pair of guard electrodes.

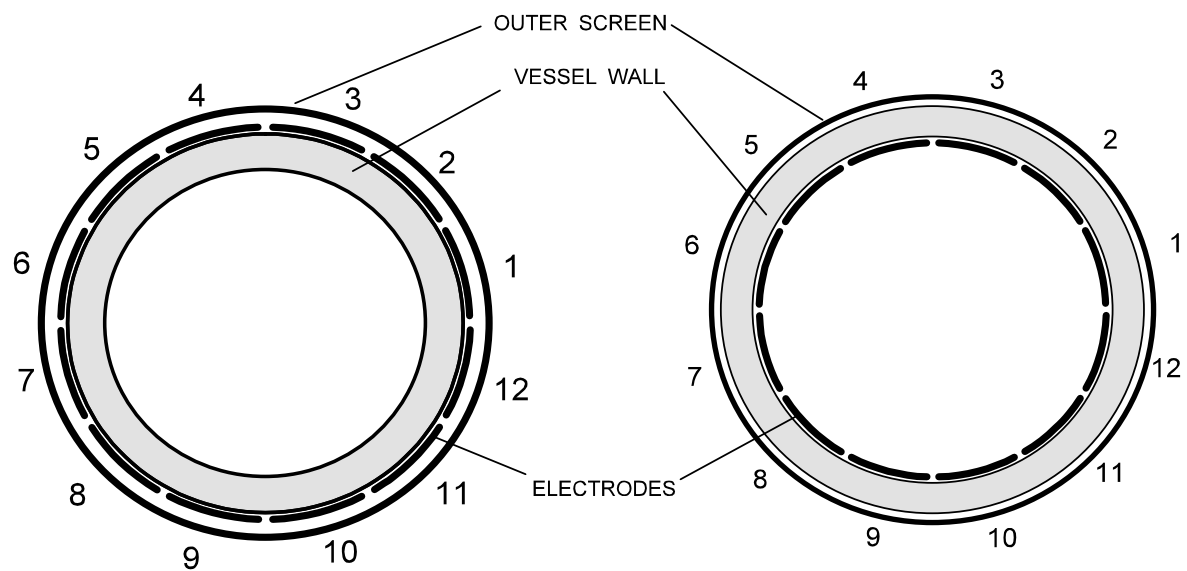


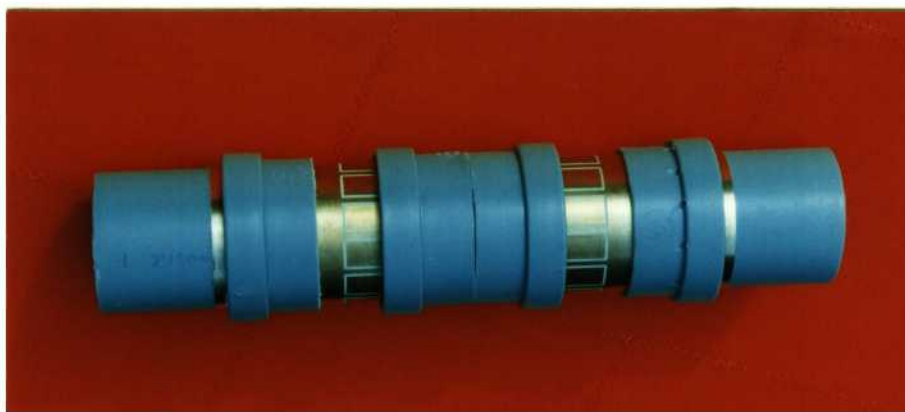
FIGURE 1(a) EXTERNAL ELECTRODES

FIGURE 1(b) INTERNAL ELECTRODES

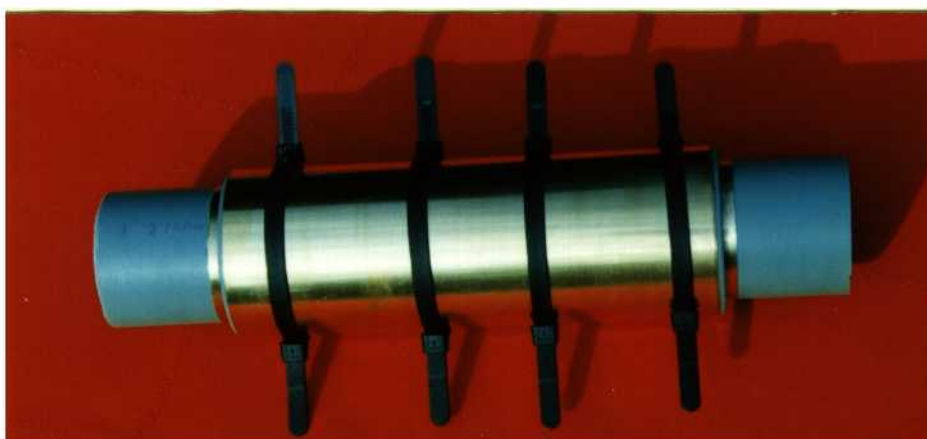
FIGURE 1. CROSS SECTIONS OF SENSORS WITH INTERNAL AND EXTERNAL ELECTRODES



Pipe with sensor electrodes



Addition of radial spacers



Addition of outer screen

**Figure 2 Views showing construction of Demonstration ECT sensor**

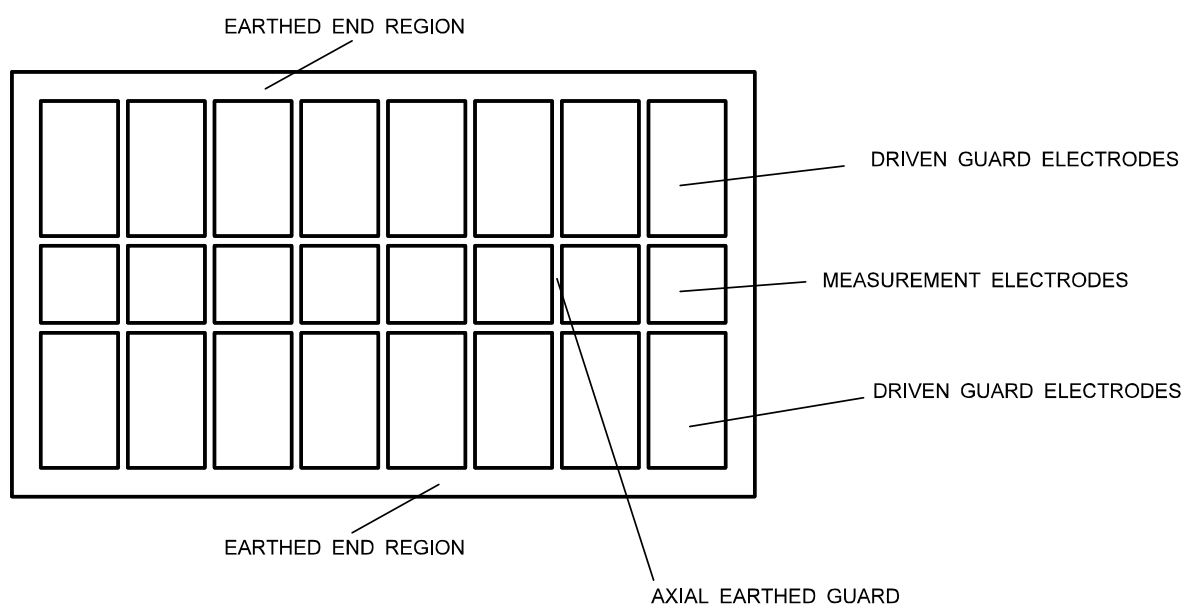
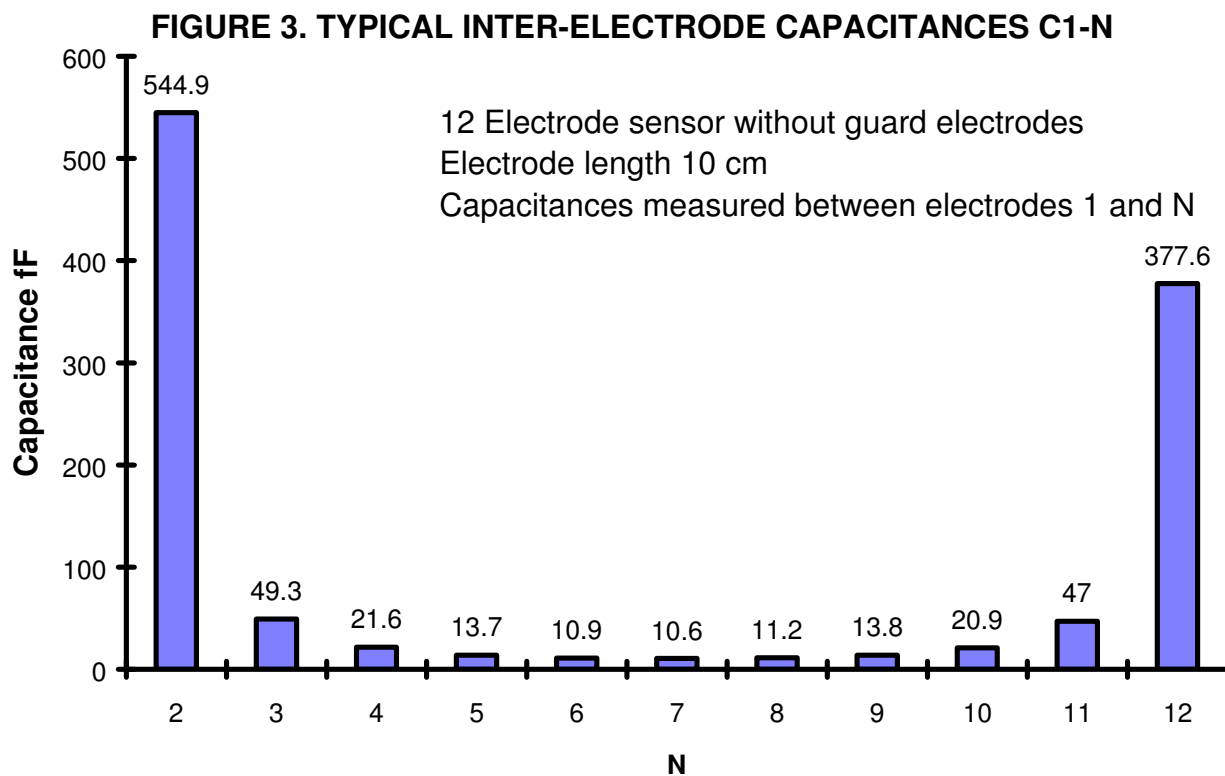
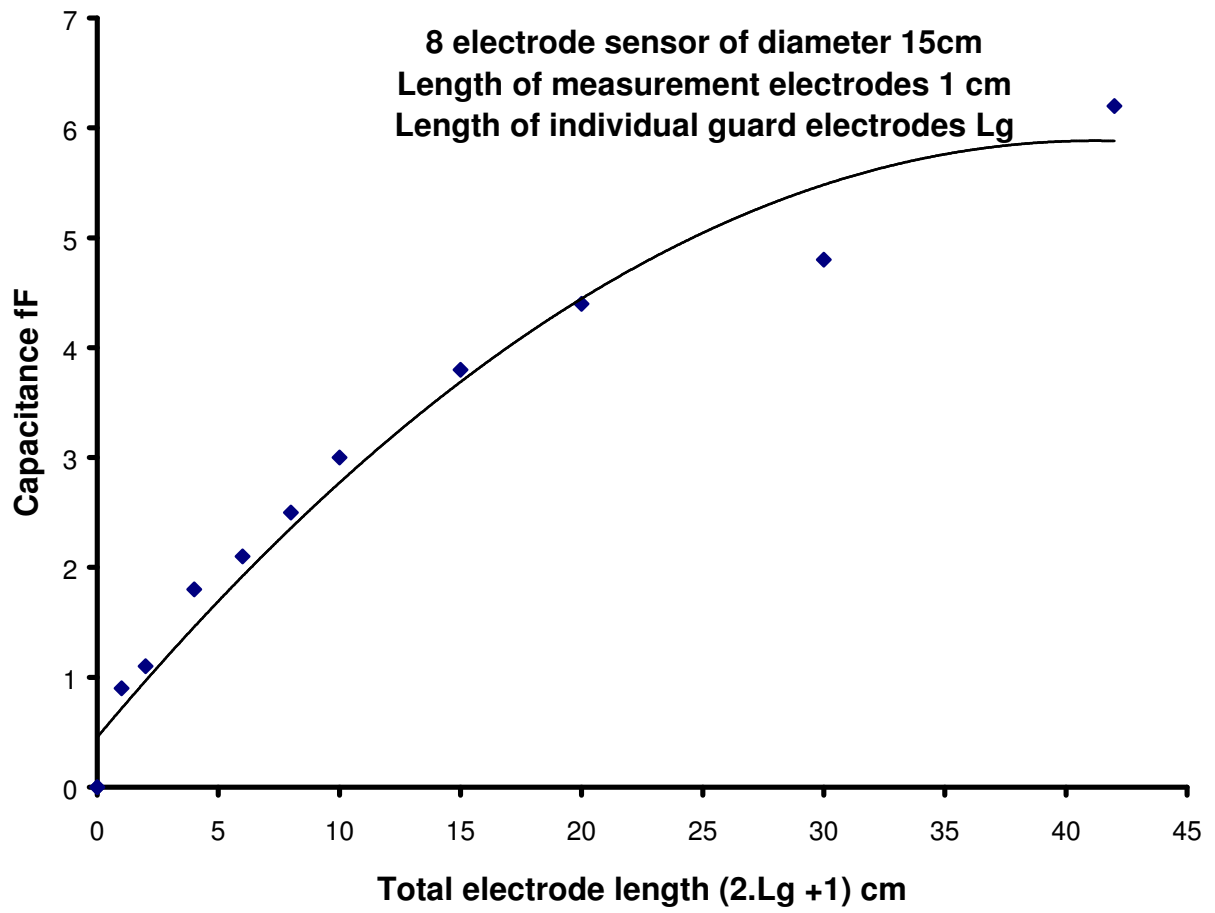


**FIGURE 4. ELECTRODE FOIL ARRANGEMENT**

**Figure 5. Variation of capacitance between opposite electrodes with electrode length**



## **PTL APPLICATION NOTE 4**

# **PROCESS TOMOGRAPHY Ltd.**

## **APPLICATION NOTE AN4**

### **AN ITERATIVE METHOD FOR IMPROVING ECT IMAGES**

Issue 2

April 1999

#### **SUMMARY**

The method normally used to obtain ECT images from capacitance measurements is the **Linear Back-Projection (LBP)** algorithm, which produces relatively low-accuracy images. This note describes a method for improving the accuracy of LBP images using a simple **iterative image computation method**. This information is provided by Process Tomography Ltd. to encourage users of ECT systems to experiment with this technique. There are many possible ways in which this method can be developed and improved and we welcome feedback from customers with suggestions for how this technique can be further optimised.

---

#### **PROCESS TOMOGRAPHY LTD**

**86 Water Lane, Wilmslow, Cheshire. SK9 5BB United Kingdom.**

**Phone/Fax 01625-549021**

(From outside UK +44-1625-549021)

email: [ptl@tomography.com](mailto:ptl@tomography.com) website: [www.tomography.com](http://www.tomography.com)

---

Registered in England No. 2908507. Registered Office 15, Croft Road, Wilmslow, Cheshire. SK9 6JJ United Kingdom.

## ACKNOWLEDGMENT

The work reported here was assisted by knowledge of the work of several other researchers. We would therefore like to acknowledge contributions from the following people:

1. Dr J. Salkeld of UMIST. Description of iterative method for ECT image reconstruction in PhD thesis, 1991.
2. Dr W.Q. Yang of UMIST. Patent application and publication and demonstration of an iterative algorithm using a forward field solving technique, 1997.
3. John Pendleton of John Pendleton Associates. Development of Matlab software algorithm for ECT image reconstruction, 1998.



# AN ITERATIVE METHOD FOR IMPROVING ECT IMAGES

## 1. THE LBP ALGORITHM

Before considering how the iterative algorithm works, it is necessary to understand the principle of the simple linear back-projection (LBP) algorithm. In an ECT system, images are constructed of the cross-sectional distribution of dielectric material inside an ECT sensor from values of capacitance measured between combinations of electrodes located around the periphery of the sensor. In PTL ECT systems, the ECT image is normally based on a grid of 32 x 32 square pixels.

The method used to derive the values of each pixel in the image from the capacitance measurements is the so-called **Linear Back-Projection (LBP)** algorithm, which was originally developed for use in X-ray tomography systems. In this algorithm, it is assumed that the relationship between the measured values of inter-electrode capacitance  $\mathbf{c}$  and the permittivity  $\mathbf{k}$  of each pixel can be written in matrix form as follows:

$$\mathbf{C} = \mathbf{S} \cdot \mathbf{K} \quad (1)$$

where  $\mathbf{C}$  is a column vector containing the set of  $\mathbf{m}$  normalised inter-electrode capacitance measurements  $\mathbf{c}$  for one image frame,  $\mathbf{K}$  is a column vector containing the set of  $\mathbf{n}$  normalised pixel permittivities  $\mathbf{k}$  and  $\mathbf{S}$  is a normalised  $\mathbf{m} \times \mathbf{n}$  matrix known as the sensitivity matrix (or map). All of the values in these matrices and column vectors are normalised to lie within the nominal range 0 to 1.

The value of  $\mathbf{m}$  (the number of possible unique inter-electrode capacitance measurements) is **28** for an 8-electrode sensor or **66** for a 12-electrode sensor. The value of  $\mathbf{n}$  will be **1024** for a 32 x 32 pixel grid.

An ECT system is normally used to image a combination of two materials having different permittivities. The ECT system is calibrated at a lower point when full of the lower permittivity material and then at a higher point when full of the higher permittivity material.

The sensitivity matrix  $\mathbf{S}$  is the normalised set of inter-electrode capacitance measurements obtained when all of the pixels except one are occupied by the lower permittivity material and the remaining pixel (which we will refer to as the probe pixel) is occupied by the higher permittivity material. The elements in the matrix  $\mathbf{S}$  will be referred to as capacitance coefficients. The sensitivity matrix will consist of  $\mathbf{m}$  (eg 66) sets of capacitance coefficients, each set containing 1024 capacitance coefficients corresponding to each individual pixel location. Note that the values of the coefficients for pixel locations outside the sensor boundary will be zero.

Equation 1 shows that for any arbitrary permittivity distribution inside the sensor, the individual inter-electrode capacitances are obtained by adding up the effects of each individual probe pixel, weighted by its actual permittivity,  $k$ . That is, by summing the combined effects of the 812 pixels inside the circle (out of the 1024 total number of pixels) on the measured inter-electrode capacitances, when each of these pixels is a probe pixel in turn, but weighted by its actual permittivity, rather than that used to derive the sensitivity matrix pixel (the higher calibration permittivity).

If each probe pixel contains the higher permittivity material, then the effect of adding up the inter-electrode capacitances which occur for each probe pixel location should give values of capacitances which equal those measured when the sensor is full of the higher permittivity material (the values measured at the upper calibration point). However, in practice, because of field distortion, this will only be approximately true and this is the first of several possible sources of error in the LBP algorithm. Clearly, if the probe pixels contain dielectric material of lower permittivity than that of the higher permittivity material, then the resultant inter-electrode capacitances will have lower values than those measured at the higher calibration point.

Equation 1 relates the measured capacitances to the permittivity distribution inside the sensor. However, the object of an ECT system is to derive the permittivity distribution from the measured inter-electrode capacitances. In principle, this can be done by simply inverting equation 1. That is:

$$\mathbf{K} = \mathbf{S}^{-1} \cdot \mathbf{C} \quad (2)$$

where  $\mathbf{S}^{-1}$  is the inverse matrix of  $\mathbf{S}$ .

Unfortunately, it is only possible to obtain the inverse of a matrix if it is square, that is, one where  $\mathbf{m} = \mathbf{n}$ . As this is not the case for ECT systems, it is not possible to invert the sensitivity matrix and hence some other method must be found to generate the permittivity distribution from the capacitance measurements.

The method used in the LBP algorithm is based on the assumption, already stated, that the measured inter-electrode capacitances are equal to the sum of the capacitances for that particular electrode combination caused by each pixel location inside the sensor acting individually, using the actual normalised permittivity for each pixel location in turn. This process is known as **forward projection**

Conversely, the image pixel values are obtained by assuming that the inverse relationship is true, namely that the permittivity of each individual pixel can be obtained by some relationship of the form:

$$\mathbf{K} = \mathbf{Q} \cdot \mathbf{C} \quad (3)$$

where  $\mathbf{Q}$  is a matrix to be defined. This technique is known as **back projection**.

Now as  $\mathbf{K}$  is an  $\mathbf{n} \times \mathbf{1}$  matrix and  $\mathbf{C}$  is an  $\mathbf{m} \times \mathbf{1}$  matrix, it is clear that  $\mathbf{Q}$  must be an  $\mathbf{n} \times \mathbf{m}$  matrix if equation 3 is to be valid. The matrix which is chosen for  $\mathbf{Q}$  in the LBP algorithm is the transpose sensitivity matrix  $\mathbf{S}^T$  (formed by interchanging the rows and columns of  $\mathbf{S}$ ), which has the required dimensional form ( $\mathbf{n} \times \mathbf{m}$ )

Hence equation 3 becomes:

$$\mathbf{K} = \mathbf{S}^T \cdot \mathbf{C} \quad (4)$$

The transpose sensitivity matrix  $\mathbf{S}^T$  can be considered to be the matrix of normalised permittivity coefficients which, when multiplied by the matrix of inter-electrode capacitance measurements  $\mathbf{C}$ , yields the required matrix of permittivity pixels  $\mathbf{K}$ . The transpose sensitivity matrix  $\mathbf{S}^T$  will consist of  $\mathbf{n}$  (1024) sets of permittivity coefficients, each set containing  $\mathbf{m}$  (eg 66) permittivity coefficients corresponding to each individual inter-electrode capacitance measurement. Note that the values of the coefficients for pixel locations outside the sensor boundary will again be zero.

Equation 4 is the basis of the LBP algorithm and is used to calculate the required pixel permittivity distribution.

The LBP algorithm is simple and fast. However, the images produced by this algorithm are blurred because, unlike the case of X-rays, where a single ray path between source and detector will pass through only one set of pixels, the electric field between two capacitance electrodes spreads out and intercepts many pixels. The effect of this is to give a spurious and unwanted level of background permittivity to each pixel. This can be removed by some form of filtering or thresholding if required. In the standard PTL PCECT operating software, no thresholding or filtering is used at present.

## 2. AN ITERATIVE METHOD FOR IMPROVING IMAGE QUALITY

The iterative image reconstruction method is based on the use of equations 1 and 4. The idea is to use these two equations alternately to correct the sets of capacitance and pixel values in turn and hence produce a more accurate image from the capacitance measurements. The details are as follows:

1. Measure a set of (66) normalised capacitances  $C_1$  for one image frame.
2. Correct the set of measured capacitances  $C_1$  using the series model correction formula (or some other correction formula, see Appendix 1).
3. Calculate the set of (1024) pixel permittivities  $K_1$  corresponding to  $C_1$  using equation (4) ie.

$$K_1 = S^T \cdot C_1 \quad (5)$$

Note that the matrix  $S^T$  must be normalised as follows: As  $K_1$  is a set of 1024 pixels and  $C_1$  is a set of (eg 66) capacitance readings, then  $S^T$  must be normalised by dividing each of the elements (permittivity coefficients) in  $S^T$  which contribute to each specific pixel value in  $K_1$  by the sum of all of the values of permittivity coefficients in  $S^T$  which contribute to the specific pixel location (a sum of eg 66 permittivity coefficients).

4. Truncate the individual pixel values  $k$  so that they lie within the range  $0 < k < 1$  and save and display the image.
5. Use these new values of permittivity to back-calculate a new set of inter-electrode capacitances  $C_2$  using equation (1) ie:

$$C_2 = S \cdot K_1 \quad (6)$$

Note that in this case, the matrix  $S$  must be normalised as follows: As  $C_2$  is a set of eg 66 inter-electrode capacitance measurements and  $K_1$  is a set of 1024 pixel values, then  $S$  must be normalised by dividing each of the elements (capacitance coefficients) in  $S$  which contribute to each specific inter-electrode capacitance measurement by the sum of all of the capacitance coefficients in  $S$  which contribute to this capacitance measurement (a sum of 1024 capacitance coefficients).

6. Calculate a set of error capacitances  $\Delta C$  where:

$$\Delta C = (C_2 - C_1) \quad (7)$$

7. Truncate  $\Delta C$  to limit the maximum values of  $\Delta C$  so that they lie within the range  $(-0.05 < \Delta C < 0.05)$  or some other pre-defined limits. This is necessary to prevent the feedback loop from becoming unstable.

8. Multiply  $\Delta C$  by a gain factor (typically 2) which is determined by empirical means.

9. Use equation (4) and the error capacitances  $\Delta C$  to calculate a set of error pixel values  $\Delta K$ . ie:

$$\Delta K = S^T \cdot \Delta C \quad (8)$$

10. Use the set of error pixels to generate a new set of pixel values  $K_2$  where:

$$K_2 = (K_1 - \Delta K) \quad (9)$$

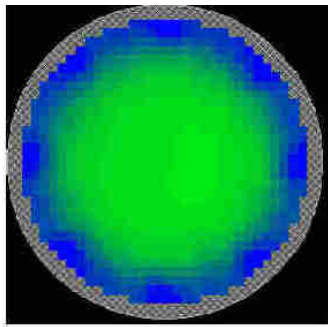
11. Truncate these pixel values to lie within the range  $0 < k < 1$  and save and display the image.

12. Repeat steps 5 to 11 using the new set of  $K$  values  $K_2$  (instead of  $K_1$ ) in equation (5). In equation 7, generate the error capacitances by subtracting the **original** measured capacitances from the current set.

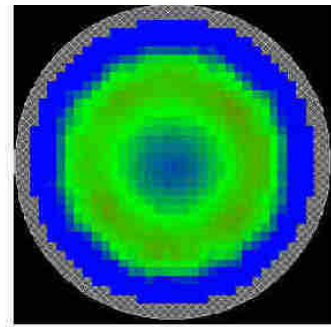
11. Repeat step 12 as many times as necessary to obtain an accurate image.

A simple Matlab program for implementing this procedure is described in Appendix 2.

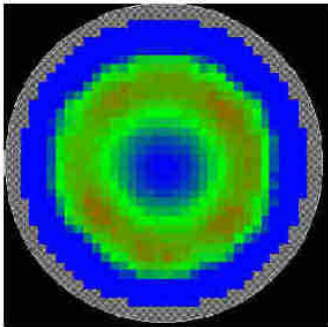
An illustration of the image improvement which can be obtained is shown in the following figure, which was obtained using the program described in Appendix 2. The image data is for a 60mm OD plexiglass tube with 5mm walls, placed approximately centrally inside an 8 electrode ECT sensor having an internal diameter of 100mm. The figure shows the improvements in the image as the number of iterations is steadily increased.



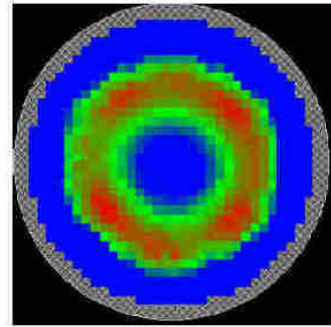
LBP IMAGE



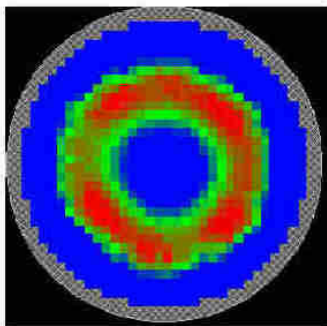
10 ITERATIONS



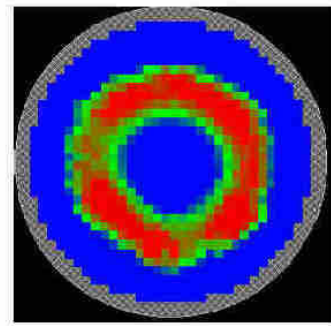
20 ITERATIONS



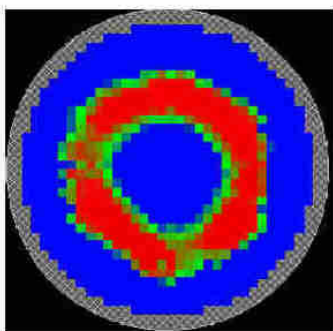
50 ITERATIONS



100 ITERATIONS



200 ITERATIONS



500 ITERATIONS

TUBE IMAGE SHOWING IMPROVEMENTS WITH INCREASING NUMBER OF ITERATIONS

## APPENDIX 1

### 1. CORRECTION OF MEASURED CAPACITANCES FOR SERIES MODEL

If the measured values of normalised capacitance are **C<sub>n</sub>**, then a new set of normalised capacitances **C<sub>n(new)</sub>** should be calculated where **C<sub>n(new)</sub>** are given by:

$$\mathbf{C_{n(new)} = R \cdot C_n / (1 + C_n.(R - 1))}$$

where **R** is the ratio of the permittivities (>1) of the two materials used for calibration.

### 2. CORRECTION OF MEASURED CAPACITANCES FOR MAXWELL MODEL

If the measured values of normalised capacitance are **C<sub>n</sub>**, then a new set of normalised capacitances **C<sub>n(new)</sub>** should be calculated where **C<sub>n(new)</sub>** are given by:

$$\mathbf{C_{n(new)} = C_n.(2 + R)/(3 + C_n.(R - 1))}$$

where **R** is the ratio of the permittivities (>1) of the two materials used for calibration.

## APPENDIX 2

### MATLAB PROGRAM FOR CALCULATING ITERATIVE ECT IMAGES

#### PROGRAM NOTES

The listing for the demonstration Matlab program (**ITERBP.M**) is given in the following pages. The program listing is a standard **Matlab M file** which can be run using **Matlab version 4** or later.

**To run the program**, copy all of the files on the demonstration disk to the **Matlab** directory. Then insert a blank floppy disk in the a: drive, start Matlab and type **ITERBP** in the Matlab screen. The program will run and two image files will be copied to the floppy disk.

The data file used in the demonstration program (8tube.ncp) was obtained using a perspex tube of OD 60 mm and wall thickness 5mm, inside an 8-element sensor of internal diameter 100mm. The sensor had been calibrated with air and polypropylene beads.

#### FURTHER INFORMATION

The following data files must be available in the directory which contains the Matlab program files: (The actual data files and parameter settings used in the demonstration program are shown in *italics*.)

1. The program M file: (*iterbp.m*)
2. The colour scheme for the plot files: (*ptl.m*)
3. The Threshold function program: (*thresh.m*)
4. The appropriate sensitivity map for the sensor: (*e8\_bin.p32*)
5. The normalised capacitance file for the image frame to be constructed: (*8tube.ncp*)

Note that the normalised capacitance file must include only the capacitance values. The first figure in the .ncp file obtained from the standard PTL PCECT software, which is the frame number, must be deleted from the file using a text editor.

All of these files (together with an extra file for 12 electrode sensitivity map) are included on the demonstration program disk. These files should be copied to the Matlab directory.

The program can be easily modified to process other data files by changing the capacitance file name in the program listing and by changing the input parameters (see below) and sensitivity map file name as appropriate.



## INPUT PARAMETERS

In addition to the data files, the following input parameters must be defined on the first page of the program listing: (default values in demo program in italics).

Number of electrodes: (*Electrodes = 8*)

Permittivity ratio: (*PermRatio = 2*)

Feedback gain: (*gain = 2*)

Number of iterations: (*ITER = 50*)

Threshold parameter: (*Thresh = 1*)

Pixel Resolution: (*Resolution = 32*)

Note that the number of electrodes and pixel resolution must be compatible with the sensitivity map and measured capacitance data file.

The capacitance model to be used should be enabled by commenting out the program line referring to the unwanted model using a % character at the start of the line. In the listing here, the series model is used.

The program generates two image files image1.img and image2.img which can be saved to a floppy disk. These files can then be viewed using the PTL IMGCON utility. Image1.img is the simple LBP image and image2.img is the iterated image.

This program was developed by John Pendleton and Malcolm Byars.

## DEMONSTRATION MATLAB PROGRAM ITERBP.M

```
%*****
% Iterative backprojection with thresholding.
% MB/JDP 5/98.
%*****

clear;
clc;
format;

%*****
% Input Parameters *****
%*****

Electrodes = 8;
PermRatio = 2
gain = 2
ITER = 50
Thresh = 1
Resolution = 32;

n=Resolution^2;
PR = PermRatio;
NE = Electrodes;
Meas = NE * (NE -1)/2
m=Meas;

K = zeros(m,n);
M = zeros(1,m);
N = zeros(1,n);
R1 = zeros(1,n);
R2 = zeros(1,m);
C2 = zeros(1,m);

%*****
% load sensitivity map.*****
%*****
fid = fopen('e8_bin.p32');
for i = 1:m
    S(i,1:1024) = fread(fid,n,'float');
end
fclose (fid);
```

```

%*****
% load normalised capacitance file.*****
%*****
fid = fopen('8tube.ncp');
CMeas = fscanf (fid,'%f',[Meas]);
fclose (fid);

%*****
% Correct measured capacitances according to **
% series or Maxwell model*****
%*****

for i = 1:m

%*****
% Series Model.*****
%*****

        C(i,1) = (PermRatio*CMeas(i))/(1+CMeas(i)*(PermRatio-1));

%*****
% Maxwell Model *****
%*****

%      C(i,1) = CMeas(i)*(2 + PR)/(3 + CMeas(i)*(PR - 1));

end

C1 = C;

%*****
% derive normalisation matrix for S by summing maps *
% avoiding devision by zero *****
%*****

'Normalising Matrix Denominators'

for i = 1:m
    N(1,:) = N(1,:) + S(i,:);
end

for j = 1:n
    if N(j) ~= 0
        R1(j) = 1 / N(j);
    end
end
end

```

```
%*****
% derive normalisation matrix for ST by summing maps *
% avoiding devison by zero *****
%*****
```

$ST = S'$ ;

```
for i = 1:n
    M(1,:) = M(1,:) + ST(i,:);
end
```

```
for j = 1:m
    if M(j) ~= 0
        R2(j) = 1 / M(j);
    end
end
```

```
%*****
% Normalise sensitivity map S *****
%*****
```

'Normalising Sensitivity Maps'

```
for i = 1:m
    SN(i,:) = S(i,:) .* R1(1,:);
end
```

```
%*****
% Normalise sensitivity map ST *****
%*****
```

```
for i = 1:n
    SNT(i,:) = ST(i,:) .* R2(1,:);
end
```

```
%*****
% Backproject *****
%*****
```

'Backprojecting'

$K = SN' * C1$ ;

```

%*****
% Threshold *****
%*****

K = thresh(K,0,Thresh);

K1 = K;

%*****
% Calculate volume ratio for original image ***
%*****

vr0 = 0;
for iv=1:n
vr0 = vr0 + K(iv);
end
vr0 = vr0/1024

%*****
% Start iteration loop *****
%*****

for L = 1:ITER

C2 = SNT'* K1;

DC = (C2 - C1);

    capsum = 0;
    for i = 1:m;
    capsum = capsum + (DC(i))^2;
    end
    caperror = sqrt(capsum)/m

DC = gain * thresh(DC,-0.05,0.05);

DK = SN' * DC;

K2 = (K1 - DK);

%*****
% Threshold *****
%*****

K2 = thresh(K2,0,Thresh);

K1 = K2;

```

```

%*****
% Calculate volume ratio for each iteration ***
%*****

vrf = 0;
for iv=1:n
    vrf = vrf + K2(iv);
end
vrf = vrf/1024

end

%*****
% End of iteration loop *****
%*****

%*****
% Construct image as an 32 by 32 array *****
%*****

I1 = reshape(K,Resolution,Resolution);
I2 = reshape(K2,Resolution,Resolution);

%*****
% Adjust image array so that it spans color ***
% map and set values outside void space to 1 **
% (1 maps to black, > 1 to colour in palette) *
%*****

for x = 1:Resolution
    for y = 1:Resolution
        if N(x+(y-1)*Resolution) > 0
            I1(x,y)=2+62*I1(x,y);
        else
            I1(x,y)=1;
        end
    end
end
end

```

```

%*****
% Adjust image array so that it spans color ***
% map and set values outside void space to 1 **
% (1 maps to black, > 1 to colour in palette) *
%*****

for x = 1:Resolution
    for y = 1:Resolution
        if N(x+(y-1)*Resolution) > 0
            I2(x,y)=2+62*I2(x,y);
        else
            I2(x,y)=1;
        end
    end
end

%*****
% Display original image in 2-D *****
%*****

figure
colormap(plt);
image(I1);

% Ensure 1:1 aspect ratio,
% set height and width to be ave of current settings.
Win = get(gcf,'Position');
WinW = Win(3);WinH = Win(4);
Win(3)= (WinW + WinH)/2;
Win(4)= (WinW + WinH)/2;
set(gcf,'Position',Win)

'press a key'
pause

%*****
% Display iterated image in 2-D *****
%*****

figure
colormap(plt);
image(I2);

% Ensure 1:1 aspect ratio,
% set height and width to be ave of current settings.
Win = get(gcf,'Position');
WinW = Win(3);WinH = Win(4);
Win(3)= (WinW + WinH)/2;
Win(4)= (WinW + WinH)/2;
set(gcf,'Position',Win)

```

```

'press a key'
pause

%*****
% Display original image in 3-D *****
%*****

frame1 = reshape(K,Resolution,Resolution);

figure
colormap(ptl);
surf(frame1)

% Ensure 1:1 aspect ratio,
% set height and width to be ave of current settings.
Win = get(gcf,'Position');
WinW = Win(3);WinH = Win(4);
Win(3)= (WinW + WinH)/2;
Win(4)= (WinW + WinH)/2;
set(gcf,'Position',Win)

'press a key'
pause

%*****
% Display iterated image in 3-D *****
%*****

frame2 = reshape(K2,Resolution,Resolution);

figure
colormap(ptl);
surf(frame2);

% Ensure 1:1 aspect ratio,
% set height and width to be ave of current settings.
Win = get(gcf,'Position');
WinW = Win(3);WinH = Win(4);
Win(3)= (WinW + WinH)/2;
Win(4)= (WinW + WinH)/2;
set(gcf,'Position',Win)

'press a key'
pause

```



```

%*****
% Write original and iterated images to files *
%*****

'Writing original image to file'

fid = fopen('a:image1.img','w')
for x = 1 : Resolution;
for y = 1 : Resolution;
fprintf(fid,'%4.2ft',frame1(x,y));
end
fprintf(fid,'\r\n');
end
fclose(fid);

'Writing iterated image to file'

fid = fopen('a:image2.img','w')
for x = 1 : Resolution;
for y = 1 : Resolution;
fprintf(fid,'%4.2ft',frame2(x,y));
end
fprintf(fid,'\r\n');
end
fclose(fid);

%*****

```

## PTL APPLICATION NOTE 10

## **PTL APPLICATION NOTE AN10**

### **LINEARISING ECT SENSORS**

**NOVEMBER 2005**

#### **SUMMARY**

In ECT systems, the primary objective is often the measurement of the concentration of one component in a 2-phase mixture of dielectric materials. The concentration is derived from the permittivity distribution inside the ECT sensor, which, in turn, is calculated from the measured normalised inter-electrode capacitances. An ideal ECT sensor would allow the concentration to be calculated directly from the measured capacitances. However, all practical ECT sensors are non-linear and this non-linearity will cause errors in the concentration results if this simple approach is adopted. Consequently, linearisation of the ECT sensor characteristics is usually necessary if accurate concentration results are to be obtained from the capacitance measurements.

There are two primary causes of non-linearity in ECT sensors. The first is the relationship between the permittivity of the material inside the sensor and the measured inter-electrode capacitances and the second is the relationship between the concentration and the permittivity of the mixture. Both of these relationships can be linearised by applying corrections to the measured normalised capacitance values in an appropriate manner.

The sensor capacitance/permittivity characteristics can be linearised by first measuring the sensor inter-electrode-pair capacitances with the sensor filled with a range of materials having different but known permittivities. This data is then used to generate a sensor capacitance/permittivity file, which contains data for each individual capacitance-pair measurement. The resulting capacitance/permittivity curves are used to modify the measured normalised capacitances, which are then used to generate the pixel permittivity values via a linear matrix transform.

The calculated pixel permittivities must then be further modified so that they correspond to concentration rather than permittivity. This correction can be carried out by applying a suitable concentration/permittivity model (eg the Maxwell model) to the calculated pixel permittivity values. In practice, this correction is applied directly to the measured capacitances before the pixel permittivities are calculated, rather than to the pixel permittivities.

This application note explains the theoretical background and practical implementation of these linearisation processes.

---

**PROCESS TOMOGRAPHY LTD**

**86 Water Lane, Wilmslow, Cheshire. SK9 5BB United Kingdom.**

**Phone/Fax 01625-549021**

(From outside UK +44-1625-549021)

email: [enquiries@tomography.com](mailto:enquiries@tomography.com) Web site: [www.tomography.com](http://www.tomography.com)

## **CONTENTS**

1. Overview
2. Sensor capacitance/permittivity characteristics
  - 2.1 ECT Sensor C/K characteristics
  - 2.2 Measurement of sensor C/K characteristics
  - 2.3 Correction for sensor C/K characteristics
  - 2.4 Practical Implementation of the sensor C/K correction.
3. Sensor concentration/effective permittivity characteristics
  - 3.1 The Parallel capacitance model
  - 3.2 The Series capacitance model
  - 3.3 The Maxwell model
  - 3.4 Concentration model characteristics
4. Correcting the pixel concentration using the Series and Maxwell models
  - 4.1 Normalisation of measured parameters
  - 4.2 Mixtures with 100% absolute concentration at the upper calibration point
  - 4.3 Mixtures where the absolute concentration at the upper calibration point is less than 100%
    - 4.3.1 The Maxwell concentration /permittivity model
    - 4.3.2 The Series concentration/permittivity model
  - 4.4 Sample correction curves
5. Practical implementation of ECT sensor linearisation
6. Further notes on the linearisation process
  - 6.1 the concentration model.
  - 6.2 The C/K correction
  - 6.3 Overall effect of the correction factors

## **APPENDICES**

- Appendix 1 Implementing the sensor C/K correction
  - A1.1 Overview
  - A1.2. Generating the sensor C/K and coefficients files
  - A1.3. Implementation of sensor C/K correction in flowan
    - A1.3.1 Initialising Flowan
    - A1.3.2 Enabling the C/K correction:
  - A1.4. Use of test data file
  - A1.5. Demonstration of the permittivity/concentration model
- Appendix 2 The Series permittivity/concentration model
  - A2.1 Mathematical model
- Appendix 3 The Maxwell permittivity/concentration model
  - A.3.1 Mathematical model

- Appendix 4    Implementing the Series or Maxwell model corrections for mixtures where the  
                    packed density is less than 100%
- A4.1 Overview
  - A4.2 Modification details
  - A4.3 Series concentration/permittivity model correction
  - A4.4 Maxwell concentration/permittivity model correction
  - A4.5 Sample correction curves
- Appendix 5    QBasic program XNCOMP.BAS listing

## 1. OVERVIEW

An ECT system calculates the permittivity distribution of a mixture of dielectric materials inside a multi-electrode capacitance sensor from measurements of the capacitances between all possible pairs of a set of electrodes located uniformly around the circumference of the sensor.

A common measurement requirement when imaging a mixture of two dielectric materials using ECT is to know the concentration of one component of the mixture. For example, for a mixture of air and plastic beads, it might be useful to know what percentage of the mixture volume is occupied by the plastic beads. The mixture concentration is related to the permittivity distribution inside the sensor

If the relationship between the measured inter-electrode capacitances of the ECT sensor and the mixture concentration was linear, for the case where the sensor is filled with a uniform mixture, then the measured capacitances would be directly proportional to the mixture concentration. In practice, the capacitance/concentration relationship is non-linear for all practical ECT sensors and corrections must therefore be made for these non-linear effects if accurate concentration measurements are to be obtained.

It follows that, if an ECT system is to measure the concentration of a 2-phase mixture accurately, the relationship between the **mixture concentration** inside the sensor and the **measured capacitances** must be known precisely.

There are two main causes of non-linearity in an ECT sensor and these can be demonstrated by considering the effects which occur when the sensor is filled with a mixture of two dielectric materials having relative permittivities  $K_1$  and  $K_2$  respectively. We will define the material concentration to be  $X$ , where  $X$  is the fraction of the sensor volume occupied by the higher permittivity material ( $K_2$ ), and will also define the effective relative permittivity of this mixture to be  $K_E$ . (From now on we will use "permittivity" instead of "relative permittivity" for the sake of brevity.)

The first cause of non-linearity is the relationship between the **measured inter-electrode capacitances** and the **effective permittivity** of the mixture inside the sensor. We refer to this as the sensor C/K characteristic, which is largely determined by the geometry of individual ECT sensors. In general, ECT sensors with electrodes located outside the vessel wall will have significantly non-linear C/K characteristics, particularly for the capacitances between adjacent electrodes.

The second cause of ECT sensor non-linearity is the relationship between the **mixture concentration** and the **effective permittivity** inside the sensor. This relationship can be approximated by the use of one of three alternative physical concentration/permittivity models (**Parallel**, **Series** or **Maxwell**). This is a fundamental effect which is independent of the sensor geometry.

The theoretical basis of the sensor C/K characteristics and concentration/permittivity models and also the steps taken to linearise them are described in this application note.

## 2. SENSOR CAPACITANCE/PERMITTIVITY CHARACTERISTICS

### 2.1 ECT Sensor C/K characteristics

For most ECT sensors, the relationship between the permittivity  $K$  of the material inside the sensor and the measured inter-electrode capacitances  $C$  when the sensor is filled with a material of uniform permittivity is non-linear. This is particularly so for sensors where the electrodes are located outside the insulating sensor wall. Fortunately, the  $C/K$  characteristics for each electrode-pair can usually be measured relatively easily for individual ECT sensors and correction curves can be used to effectively re-linearise the sensor  $C/K$  relationships.

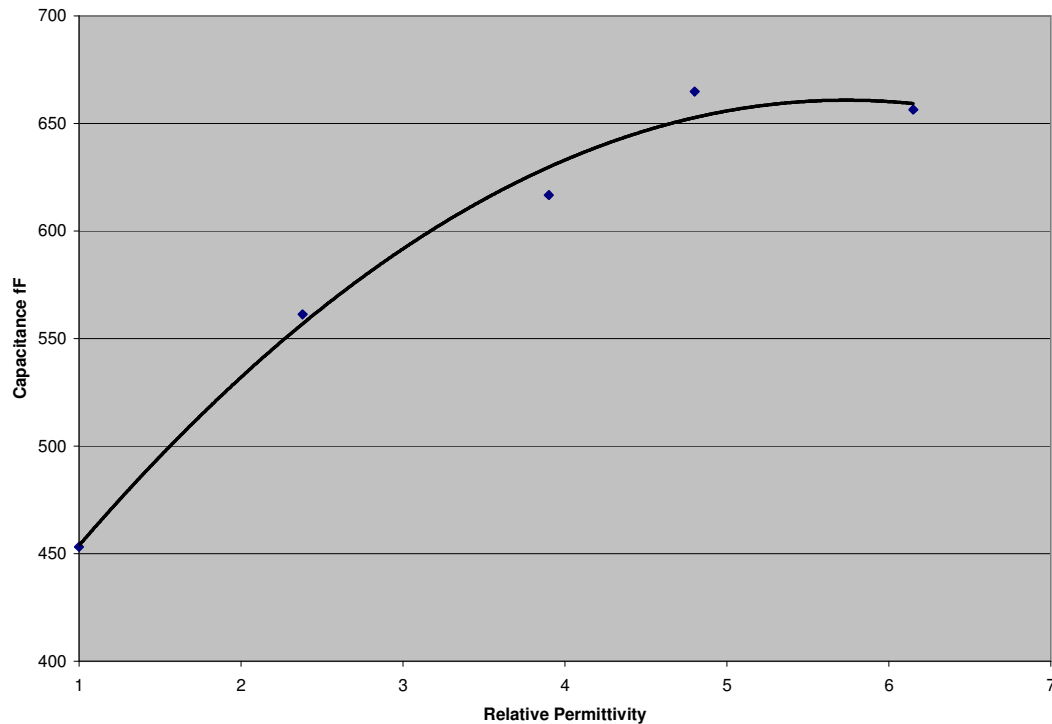


**Figure 2.1 Measured  $C_{12}$  Capacitance/Permittivity relationship**

Figure 2.1 above shows the measured capacitance/permittivity ( $C/K$ ) characteristic for a pair of adjacent electrodes (which display the most extreme non-linear characteristics) of a typical ECT sensor with electrodes located on the outside wall of a cylindrical polycarbonate tube. The capacitance values are plotted over the relative permittivity ( $K$ ) range from 1 to 6 and the  $C/K$  relationship can be seen to be very non-linear for the adjacent capacitance electrode-pair.

The curves for the other electrode-pairs become progressively more linear and in particular, the  $C/K$  characteristic for opposing electrode pairs is almost perfectly linear. This property of opposite electrodes is particularly useful, as it allows the permittivity of a uniform mixture to be measured directly when the mixture is located inside the sensor.

## 2.2 Measurement of sensor C/K characteristics

An ECT sensor is normally calibrated at two reference permittivity values and the measured capacitance and calculated pixel permittivity values are normalised to optimise the sensor operation over this range of permittivities.

The normalised capacitance/permittivity (C/K) characteristics of any ECT sensor can be measured for each electrode-pair over a range of material permittivities by filling the sensor with each different dielectric material in turn and measuring the set of inter-electrode capacitances.

In practice this can be done by calibrating the sensor in the usual way with each material (and air) and then using the PTL **Recal** software to generate the sensor C/K file as described in section 2.4 and Appendix 1.

Once these characteristic curves are known, the permittivity of any arbitrary material having a uniform permittivity can be deduced from the measured capacitances, as long as the sensor is completely filled with the unknown material.

The pink curve in figure 2.2 below shows a typical normalised capacitance/permittivity curve for a pair of adjacent electrodes, plotted over the sensor calibration range and compared with a true linear relationship (black line).

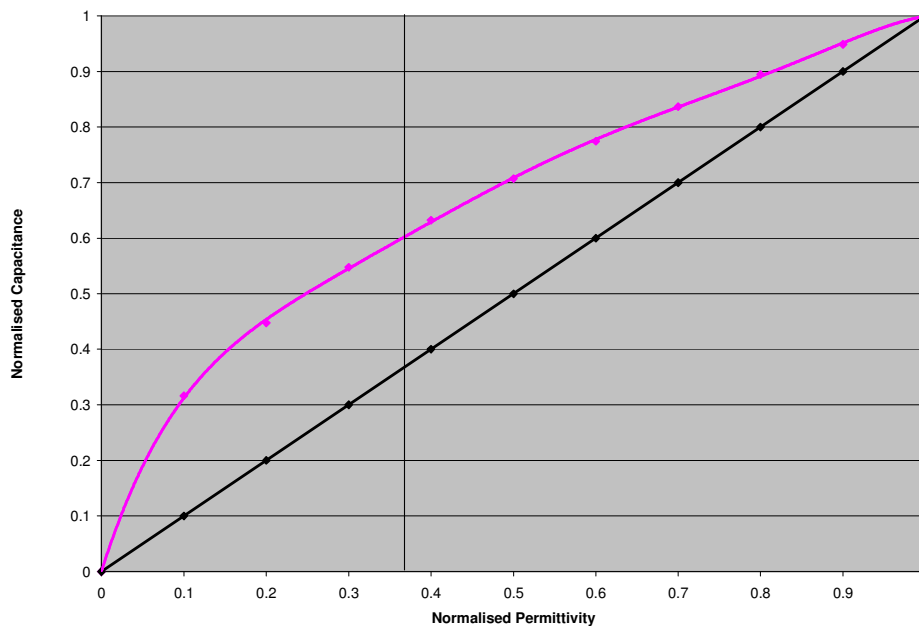


**Figure 2.2. Normalised C/K characteristics**

Note that for the adjacent capacitance pair, the capacitance increases more rapidly with the permittivity of the sensor contents than would occur if the relationship was linear. If left uncorrected, this characteristic will over-emphasise the contribution of the adjacent capacitance-pair reading to the calculation of the permittivity distribution inside the sensor and will tend to artificially enhance or over-emphasise the presence of any material located close to the sensor wall.



## 2.3 Correction for the sensor C/K characteristics

The permittivity distribution inside the sensor is calculated from the normalised measured inter-electrode capacitances, using a matrix operation which assumes a linear relationship between the sensor pixel permittivities and the measured capacitances.

In principle, the pixel permittivities could be calculated directly from the normalised capacitance measurements using the matrix transform and then corrected for the sensor C/K non-linearities. In practice, as the pixel permittivities are linearly related to the measured capacitances, it is simpler and more convenient to correct the measured capacitances before the pixel permittivities are calculated. This can be done by making the assumption (and major approximation) that the permittivity distribution inside the sensor is uniform.

The correction for the sensor C/K characteristics is therefore carried out as follows:

1. Normalise all of the measured sensor C/K curves for each inter-electrode pair, so that C and K have values of 0 and 1 at the lower and upper calibration points. Figure 2.2 shows a typical normalised C/K characteristic for a pair of adjacent electrodes in an ECT sensor with external electrodes.
2. For each inter-electrode capacitance pair, read off the normalised permittivity  $K_n$  which corresponds to the measured normalised capacitance  $C_n$  from the C/K curve for that electrode-pair. For example, in figure 2.2, if the measured normalised capacitance is 0.6, the normalised permittivity can be read from the pink curve as approximately 0.37.
3. Modify the normalised measured capacitance  $C_n$  by setting it to have the new normalised value  $C_n' = K_n$  (in the above case  $C_n$  changes from 0.6 to  $C_n' = 0.37$ ). Note that in the case of the characteristics shown in figure 2.2, the effect will be to decrease the measured capacitance value.
4. Repeat steps 3 and 4 for each of the capacitance-pair measurements which make up one frame of ECT data.
5. Reconstruct the pixel permittivity distribution using the modified set of normalised capacitances  $C_n'$ .

## 2.4 Practical Implementation of the sensor C/K correction.

In practice, the sensor C/K characteristics can be generated by calibrating the sensor using a range of dielectric materials. The PTL **Recal** software can then be used to generate the sensor C/K file. Full details of how this can be done are given in **Appendix 1**.

### 3. SENSOR CONCENTRATION/PERMITTIVITY CHARACTERISTICS

The second source of non-linearity occurs in the relationship between the mixture concentration  $X$  and the effective permittivity of the material inside the sensor. If the sensor is filled with a mixture of 2 dielectric materials, the effective permittivity of the material will increase with the concentration  $X$  of the higher permittivity material. However, the form of this relationship depends on the distribution of the 2 materials inside the sensor.

From an electrical viewpoint, there are two fundamentally different possible types of distributions of the materials within the mixture and a third type which is a combination of types 1 and 2. We refer to these as the Parallel, Series and Composite (Maxwell) concentration/permittivity models and these are described in the next few sections.

Further and more detailed information about these capacitance models is given in PTL Application Note 2 "Calculation of the volume ratio for ECT sensors".

#### 3.1 THE PARALLEL CAPACITANCE MODEL

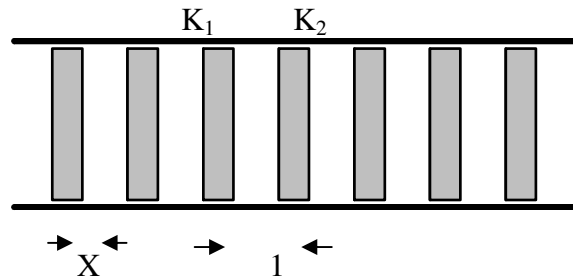


**Figure 3.1. Parallel capacitance model for circular ECT sensor**

Consider the entirely artificial case where thin discs of the two dielectric materials having permittivities  $K_1$  and  $K_2$  alternate along the axis of a cylindrical ECT sensor, as shown as a section along the sensor axis in figure 3.1. If the electric field lines inside the sensor are constrained so that they have no axial components, the discs will form elemental capacitances in parallel between pairs of opposing electrodes. In this case, the effective permittivity of the mixture  $K_E$  will increase linearly with the concentration ( $X$ ) of the higher ( $K_2$ ) permittivity material according to equation 3.1, which is known as the parallel capacitance permittivity/concentration model.

$$K_E = K_1.(1-X) + X.K_2 \quad (3.1)$$

The effective permittivity for a mixture of 2 materials having relative permittivities of 1 and 8, using the parallel model, is shown plotted (blue line) as a function of the concentration of the higher permittivity material in section 3.4 (figure 3.4) and can be seen to be linear. If the distribution of the materials inside the mixture can be represented by the Parallel model, the mixture concentration will equate directly to the measured permittivity and no further correction is required in this case. In practice the parallel model is not usually valid for most practical dielectric mixtures.

### 3.2 THE SERIES CAPACITANCE MODEL

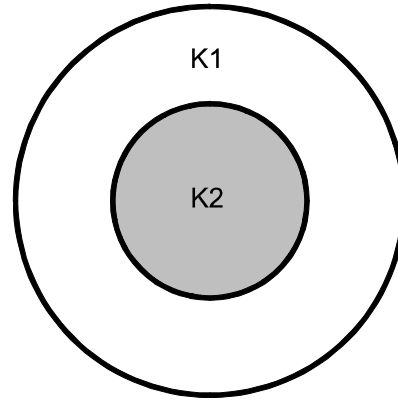


**Figure 3.2. Series capacitance model for circular ECT sensor**

Next consider the equally artificial case where the high permittivity material ( $K_2$ ) is a cylindrical rod at located at the centre of the sensor, which is otherwise filled with the lower permittivity material ( $K_1$ ) as shown in figure 3.2. In this case, the capacitance between pairs of opposing electrodes located on the sensor perimiter will be made up from a number of elemental capacitances in series.

The overall capacitance must be calculated using the reciprocal rule for adding series capacitances. For this situation, the effective permittivity  $K_E$  is given by equation 3.2. This is known as the series capacitance permittivity/concentration model. A more detailed discussion of the fundamentals of the series model is given in Appendix 2 and PTL Application Note AN2.

$$K_E = [K_1 \cdot K_2] / [K_1 \cdot X + K_2 \cdot (1 - X)] \quad (3.2)$$

The effective permittivity for a mixture of 2 materials having relative permittivities of 1 and 8 using the series model is shown plotted (pink line) as a function of the concentration ( $X$ ) of the higher permittivity material in figure 3.4.

Equation 3.2 can be easily inverted to give the concentration in terms of the effective permittivity (equation 3.3). Further details of the series model are given in Appendix 2.

$$X = K_2 \cdot (K_E - K_1) / [K_E \cdot (K_2 - K_1)] \quad (3.3)$$

Equation 3.3 is applicable when the mixture permittivity has the value  $K_2$  at the upper calibration point. If this is not the case, a further correction has to be applied. Full details of how the correction for the Series model can be applied to correct the concentration results for all mixtures is described in section 4.2 and also in Appendix 4.

Equation 3.3 can be further modified to allow the effective permittivity of the solid material ( $K_2$ ) to be calculated where direct measurement is not possible (eg for grain samples).

$$K_2 = X \cdot K_E \cdot K_1 / [K_1 - K_E \cdot (1 - X)] \quad (3.4)$$

### 3.3 THE MAXWELL MODEL

The Composite (or Maxwell) model, assumes a combination of parallel and series capacitance contributions to the capacitance measured between a pair of opposing electrodes.

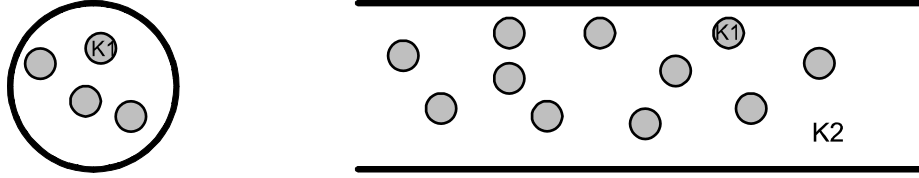


**Figure 3.3. Maxwell capacitance model for circular ECT sensor**

This model assumes that a number of uniform spheres of the higher permittivity material ( $K_2$ ) are suspended in a region otherwise occupied by the lower permittivity material ( $K_1$ ). In this case, the effective permittivity of the mixture ( $K_E$ ) is given by equation 3.5 below, which was originally derived by Maxwell in the 19th Century. Further details of this model are given in Appendix 3.

$$K_E = K_1 \cdot [2.K_1 + K_2 - 2.X.(K_1 - K_2)] / [2.K_1 + K_2 + X.(K_1 - K_2)] \quad (3.5)$$

This is known as the Maxwell permittivity/concentration model and has been plotted as the green curve in figure 3.4.

Equation can be easily inverted to give the concentration in terms of the effective permittivity (equation 3.6).

$$X = [(K_1 - K_E) \cdot (2K_1 + K_2)] / [(K_1 - K_2) \cdot (K_E + 2K_1)] \quad (3.6)$$

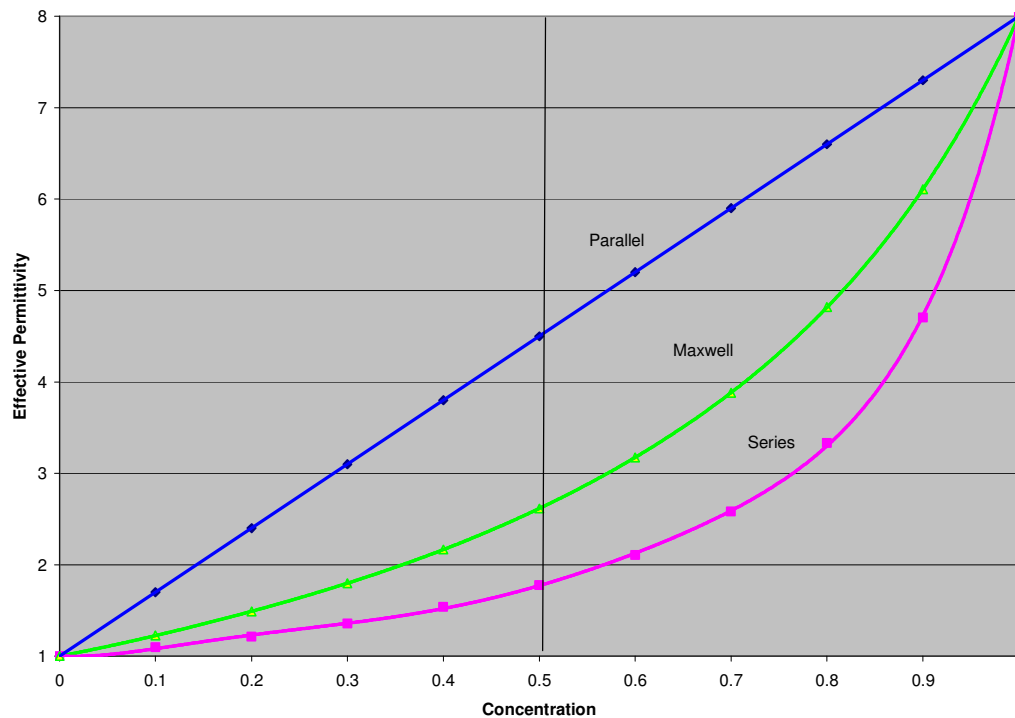
In practice, the Maxwell model has been found to approximate most closely to most realistic mixture of 2 dielectric materials and is the one which is most widely used in ECT to linearise the relationship between the effective permittivity and concentration of the mixture.

Equation 3.6 gives the mixture concentration when the mixture permittivity has the value  $K_2$  at the upper calibration point. If this is not the case, a further correction has to be applied. Full details of how the correction for the Maxwell model can be applied to correct the concentration results for all mixtures is described in section 4.2 and also in Appendix 4.

Equation 3.6 can be further modified to allow the effective permittivity of the solid material ( $K_2$ ) to be calculated where direct measurement is not possible (eg for grain samples).

$$K_2 = K_1 \cdot [X.(K_E + 2.K_1) - 2.(K_1 - K_E)] / [X.(K_E + 2.K_1) + (K_1 - K_E)] \quad (3.7)$$

### 3.4 CONCENTRATION MODEL CHARACTERISTICS



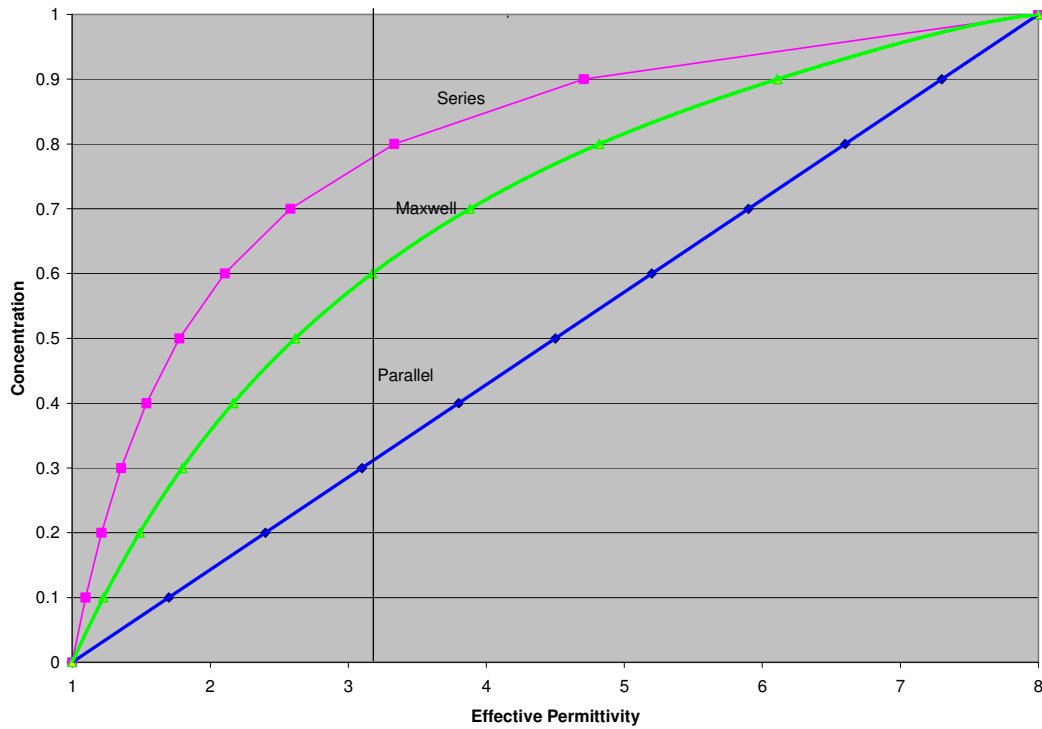
**Figure 3.4. Effective permittivity as a function of concentration for Parallel, Series and Maxwell models.**

Figure 3.4 confirms that the relationship between the concentration of the higher permittivity material and the effective permittivity of the mixture will be very non-linear for most real dielectric mixtures if the concentration follows either the Series or Maxwell models.

Specifically, the effective permittivity of the mixture can be seen to increase less rapidly than the concentration for these two models. As the measured capacitances respond directly to the effective permittivity inside the sensor, the ECT sensor capacitances will therefore tend to under-read as the mixture concentration inside the sensor increases.

This effect can be corrected by applying the inverse of these characteristics as a correction factor to the pixel permittivity values which are calculated from the sensor capacitances. These correction curves for the 3 concentration models are shown in figure 3.5.

In principle, the curves shown in figure 3.5 can be used to read off the concentration values from the effective permittivity values calculated from the measured inter-electrode capacitances (see section 2). In practice it is more convenient to apply the corrections directly to the measured sensor capacitances as described in section 4.



**Figure 3.5. Correction curves for Concentration models**

The effective mixture permittivity  $K_E$  at the upper calibration point can be deduced from the calibration file from the ratio of the capacitances of the diametrically-opposing sensor electrodes at the upper and lower calibration points. In this case, assuming the solid permittivity of the higher permittivity material ( $K_2$ ) is known accurately, the maximum packing density (absolute concentration) of the mixture can be read from the appropriate curve or calculated directly using either equation 3.3 or 3.6.

Alternatively, if the maximum packing density (absolute concentration) of the mixture is known accurately, the effective permittivity of the higher permittivity material ( $K_2$ ) can be read from the curves or calculated using either equation 3.4 or 3.7. This option is useful for materials (such as wheat grains) where it is not possible to measure a permittivity figure ( $K_2$ ) for the solid material directly.

The way in which the concentration correction is carried out in practice is described in the next section.

## 4. CORRECTING PIXEL CONCENTRATION USING CONCENTRATION MODELS

### 4.1 NORMALISATION OF MEASURED PARAMETERS

The algorithms used in PTL ECT systems convert the measured capacitances, calculated pixel permittivities and calculated mixture concentration to normalised values, where the normalised capacitance values, pixel permittivities and concentration are set to have values of 0 at the low calibration point and values of 1 (or 100% in the case of concentration) at the upper calibration point.

It is important to be clear about what is meant when referring to the mixture "concentration". To avoid confusion, the absolute mixture concentration (the fraction or percentage of the higher permittivity present in the total mixture volume) will be written as  $X_a$  and the normalised concentration will be written as  $X_n$  from now on.

### 4.2 MIXTURES WITH 100% ABSOLUTE CONCENTRATION AT THE UPPER CALIBRATION POINT

A mixture of two materials having (un-normalised) permittivities of  $K_1$  and  $K_2$ , will have an absolute concentration of 0% if there is no  $K_2$  material present and 100% if all of the mixture is the  $K_2$  material. In this type of mixture (which could, for example be an oil/gas mixture), a concentration of 100% (oil) is perfectly feasible at the upper calibration point.

In this case, the concentration/permittivity correction (eg equation 3.6 for the Maxwell model) can be applied directly over the sensor calibration range, as the permittivity figures for the two mixture components,  $K_1$  and  $K_2$  coincide with the beginning and end of the normalised permittivity range over which the sensor has been calibrated.

In Appendix 3, it is shown that the Maxwell model equation can be re-written to give the normalised mixture concentration  $X_N$  as a function of the normalised mixture permittivity  $K_{EN}$  as follows:

$$X_N = K_{EN} \cdot (2 + K) / (3 + K_{EN} \cdot (K - 1)) \quad (4.1)$$

where  $K$  is the ratio of the permittivities of the 2 materials. ie  $K = K_2/K_1$

Appendix 2 derives a similar normalised equation for the Series model:

$$X_N = K_{EN} \cdot K / [1 + K_{EN} \cdot (K - 1)] \quad (4.2)$$

For this type of mixture, either equation 4.1 or 4.2 can be applied directly to calculate the normalised concentration  $X_N$  from the normalised permittivity values  $K_{EN}$ , which are in turn calculated from the measured normalised capacitances.

### 4.3 MIXTURES WHERE THE ABSOLUTE CONCENTRATION AT THE UPPER CALIBRATION POINT IS LESS THAN 100%

If the low permittivity material is air ( $K_1 = 1$ ) and the high permittivity material ( $K_2$ ) is a solid material in bead form (eg glass beads), the maximum packing density of the beads will limit the absolute concentration of the mixture to approximately 60% at the upper calibration point. Although the permittivity of glass ( $K_2$ ) is around 6, the permittivity of a packed mixture of glass beads and air ( $K_3$ ) is around 3.2. Consequently, because the sensor is calibrated at the upper permittivity level when filled with a packed mixture of air and glass beads, the upper level calibration will be at a mixture permittivity of 3.2 and an absolute concentration of 60% (Maxwell curve).

The glass bead scenario is illustrated in figure 3.5, where a vertical line has been drawn on the figure, corresponding to an upper calibration point of  $K_3 = 3.2$  and an absolute concentration of 60%.

In this case, the ECT sensor will operate over the permittivity range from 1 to 3.2 and an absolute concentration range from 0 to 60%. However, the Maxwell or series correction equations operate over an absolute concentration range from 0 to 100% and the permittivity range from  $K_1$  to  $K_2$  (1 to 6 for air/glass). It is therefore necessary to modify equations 4.1 and 4.2 so that the correction is only carried out over the permittivity range from  $K_1$  to  $K_3$ .

#### 4.3.1 THE MAXWELL CONCENTRATION / PERMITTIVITY MODEL

In the case of the Maxwell model, this is achieved by modifying equation 4.1 as follows:

$$X_N \cdot (K_{EN}) = [K_{EN} \cdot (K_P/K) \cdot (2 + K)] / [(3 + K_{EN} \cdot (K_P/K) \cdot (K - 1))] \quad (4.3)$$

where  $K = K_2/K_1$ ,  $K_P = K_3/K_1$  and  $K_{EN}$  is the normalised permittivity.

This restricts the range of operation of the correction curve to the calibration range of the sensor. However, as the maximum possible mixture concentration (at  $K_3$ ) will be reduced to less than 100% by this operation, equation 4.3 must be re-normalised to give the correct normalised concentration (100%) at the upper calibration point. This can be done by dividing  $X_N$  by the concentration value at  $K_3$ , that is by:

$$X_N(1) = [1 \cdot (K_P/K) \cdot (2 + K)] / [(3 + 1 \cdot (K_P/K) \cdot (K - 1))] \quad (4.3)$$

So the normalised concentration  $X_N$  when the upper calibration point has a permittivity  $K_3$  which is less than  $K_2$ , is given by equation 4.4:

$$X_N = \frac{[K_{EN} \cdot (K_P/K) \cdot (2 + K)] / [(3 + K_{EN} \cdot (K_P/K) \cdot (K - 1))]}{[(K_P/K) \cdot (2 + K)] / [(3 + (K_P/K) \cdot (K - 1))]} \quad (4.4)$$

Note that if  $K_2 = K_3$ , equation 4.4 simplifies to equation 4.2.



### 4.3.2 THE SERIES CONCENTRATION / PERMITTIVITY MODEL

A similar process can be carried out for the Series model to give the concentration equation correction where the permittivity of the mixture at the upper calibration points is less than  $K_2$ . In this case, the re-normalised concentration equation becomes:

$$X_N = \frac{K_{EN} \cdot (K_P/K) \cdot K / [1 + K_{EN} \cdot (K_P/K) \cdot (K - 1)]}{(K_P/K) \cdot K / [1 + (K_P/K) \cdot (K - 1)]} \quad (4.5)$$

where  $K_P = K_3/K_1$

Note that if  $K_2 = K_3$ , equation 4.5 simplifies to equation 4.1.

### 4.4 SAMPLE CORRECTION CURVES

Equation 4.4 has been plotted as the green curve in figure 4.1 for a mixture of 2 materials having relative permittivities  $K_1 = 1$  and  $K_2 = 8$  and  $K_3 = 3$ . The form of the curve is similar to those plotted in figure 3.5 for the simpler case where  $K_2 = K_3$ . However, there are significant changes to the shape of the curve and its deviation from a linear relationship.

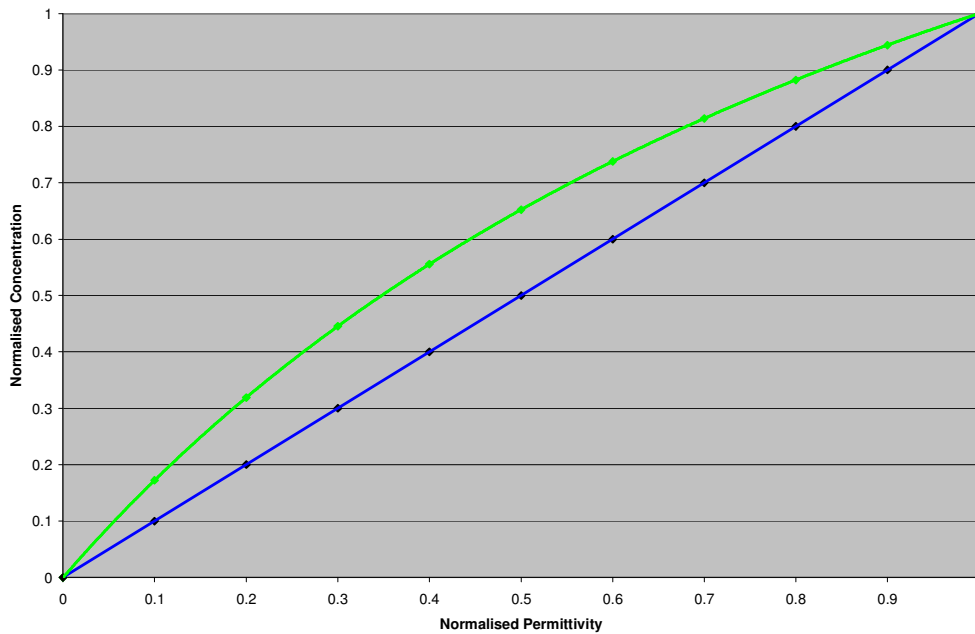


**Figure 4.1. Maxwell correction for a mixture where  $K_1=1$ ,  $K_2 = 8$  and  $K_3 = 3$ .**

In practice, because the matrix operation which calculates the pixel permittivities from the measured capacitances is a linear operation, equations 4.4 and 4.5 can be used as correction factors to the measured normalised capacitances. If this is done, the calculated normalised pixel permittivities will correspond directly to localised mixture concentration.

## 5. PRACTICAL IMPLEMENTATION OF ECT SENSOR LINEARISATION

The practical steps required to linearise the characteristics of an ECT sensor to correct for the C/K sensor characteristics and the sensor concentration/permittivity characteristics are as follows:

1. Measure the C/K characteristics of the sensor when filled with a range of materials having differing but known relative permittivities for each electrode-pair measurement. In practice, this can be carried out by calibrating the sensor with a range of materials using the standard PTL **ECT32** operating software.
2. Produce a sensor C/K file from this measured data and then convert this file into a sensor coefficients file. In practice the PTL **Recal** software can be used to convert a set of individual calibration files into both a **sensor C/K file** and also into a sensor coefficients file. Detailed information and instructions are given in **Appendix 1**.
3. Use the **sensor coefficients file** to modify the measured capacitances to correct for the sensor C/K non-linearities.
4. Re-normalise these modified capacitances.
5. Use the **Maxwell or Series model** correction to further modify the measured capacitances to correct for the sensor concentration/permittivity characteristics using equations 4.4 or 4.5 as appropriate.
6. Calculate the pixel concentration values from the modified capacitances,

## 6. FURTHER NOTES ON THE LINEARISATION PROCESS

### 6.1 The Concentration model.

The effect of applying either the **Maxwell** or **Series models** is to **increase** (boost) all of the normalised capacitances by the same amount (boost factor).

A simple QBasic program (**XNCOMP.BAS**) has been written to calculate the boost factors for these 2 models (compared with boost values of unity for the parallel model). It also calculates the **solid permittivity K2** from the upper calibration permittivity **K3** and the packing density. The program listing can be found in Appendix 5.

In the following text, **K1** and **K3** are the lower and upper calibration permittivities and **K2** is the **solid permittivity** of the higher permittivity material. Calculated boost factors for some practical mixtures are as follows:

For a PET/air mixture, ( $K_1 = 1$ ,  $K_2 = 3.3$ ,  $K_3 = 2.17$ ), the Maxwell model boost factor is  $\times 1.5$  at 1% concentration and the series model boost factor is 2.47. At 10% concentration, these figures fall to  $\times 1.43$  and 2.18 respectively.

For a flour/air mixture, ( $K_1 = 1$ ,  $K_2 = 8.66$ ,  $K_3 = 3.63$ ), the Maxwell model boost factor is  $\times 2.05$  at 1% concentration and the series model boost factor is 4.08. At 10% concentration, these figures fall to  $\times 1.87$  and 3.19 respectively.

For a wheat/air mixture, ( $K_1 = 1$ ,  $K_2 = 45.4$ ,  $K_3 = 5.67$ ), the Maxwell model boost factor is  $\times 2.8$  at 1% concentration and the series model boost factor is 6.2. At 10% concentration, these figures fall to  $\times 2.4$  and 4.2 respectively.

XNCOMP also calculates the boost factor normalised to the 1% value for all concentration levels. The variation from unity gives some idea of how much the concentration/permittivity curve is bent by this correction.

The model curvature is most extreme for the series model.

## **6.2 C/K Correction**

The effect of applying the sensor C/K correction is to reduce (attenuate) the normalised capacitances, but by varying amounts depending on the capacitance-pair. The attenuation is largest for the adjacent-pair capacitances and smallest for the opposite-pair capacitances. The attenuation factor has a maximum value at the lowest permittivity values and reduces with increasing permittivity.

The effect is particularly noticeable where the sensor contains material close to the walls of the sensor as an uncorrected sensor will appear to have excessive sensitivity close to the sensor wall.

## **6.3 Overall effect of the correction factors**

The Concentration/permittivity and Capacitance/permittivity correction factors work in opposing directions to increase/reduce the measured capacitances respectively. However, the overall effect is complex because of the different ways in which the two models modify the measured capacitances.

## APPENDIX 1

### IMPLEMENTING THE SENSOR C/K CORRECTION

#### A1.1 OVERVIEW

The PTL **Recal** software is first used to generate a set of sensor C/K curves for each electrode pair (sensor file) and these curves are then approximated as a set of second order (quadratic) polynomials. The polynomial coefficients are then stored in a second (coefficients) file which is read by the PTL **Flowan** software and used to correct the capacitance measurements. The detailed method for implementing this correction is described in the following paragraphs.

#### A1.2. GENERATING THE SENSOR C/K AND COEFFICIENTS FILES

The **sensor C/K file** and the related **coefficients file** are generated from a number of **individual sensor calibration files** measured with the sensor filled with a range of materials having differing permittivities, as described in the following sections.

The process for generating the sensor capacitance/permittivity file is to build up points (permittivities) in the file by adding them one at a time from either the high or low permittivity calibration points from a specified calibration file (in any order). This is carried out by inputting data into the **sensor file generation group** of boxes in the lower part of the **Recal** window (shown in figure A1.1 below) as follows:

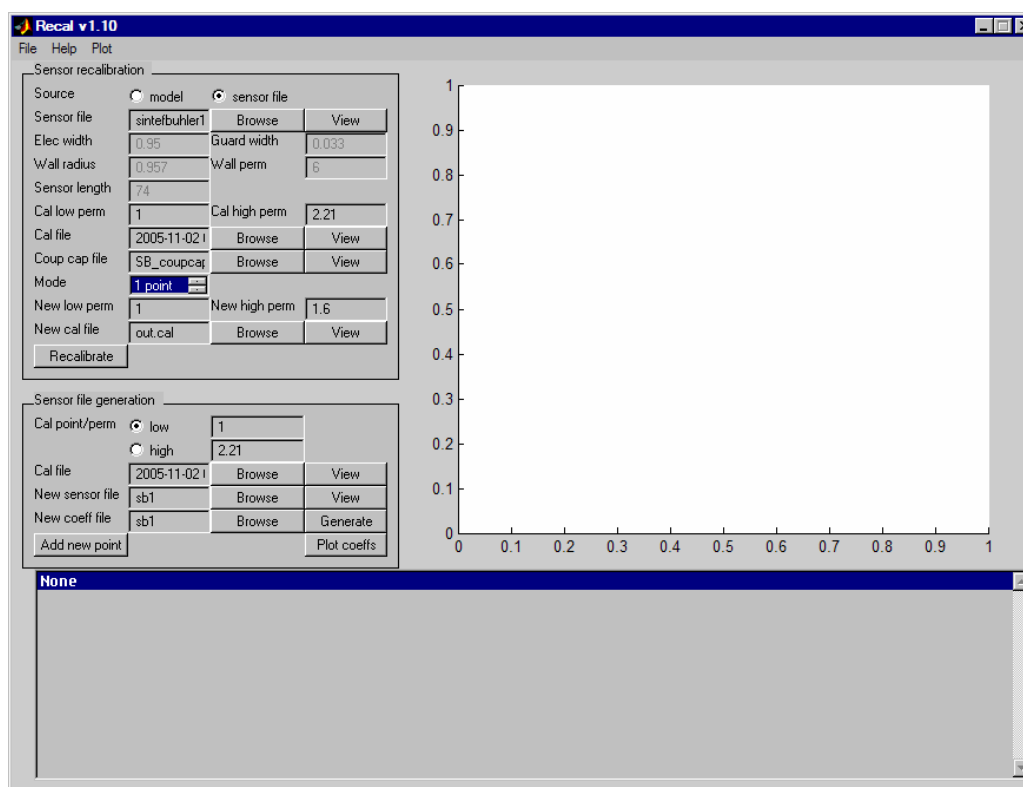
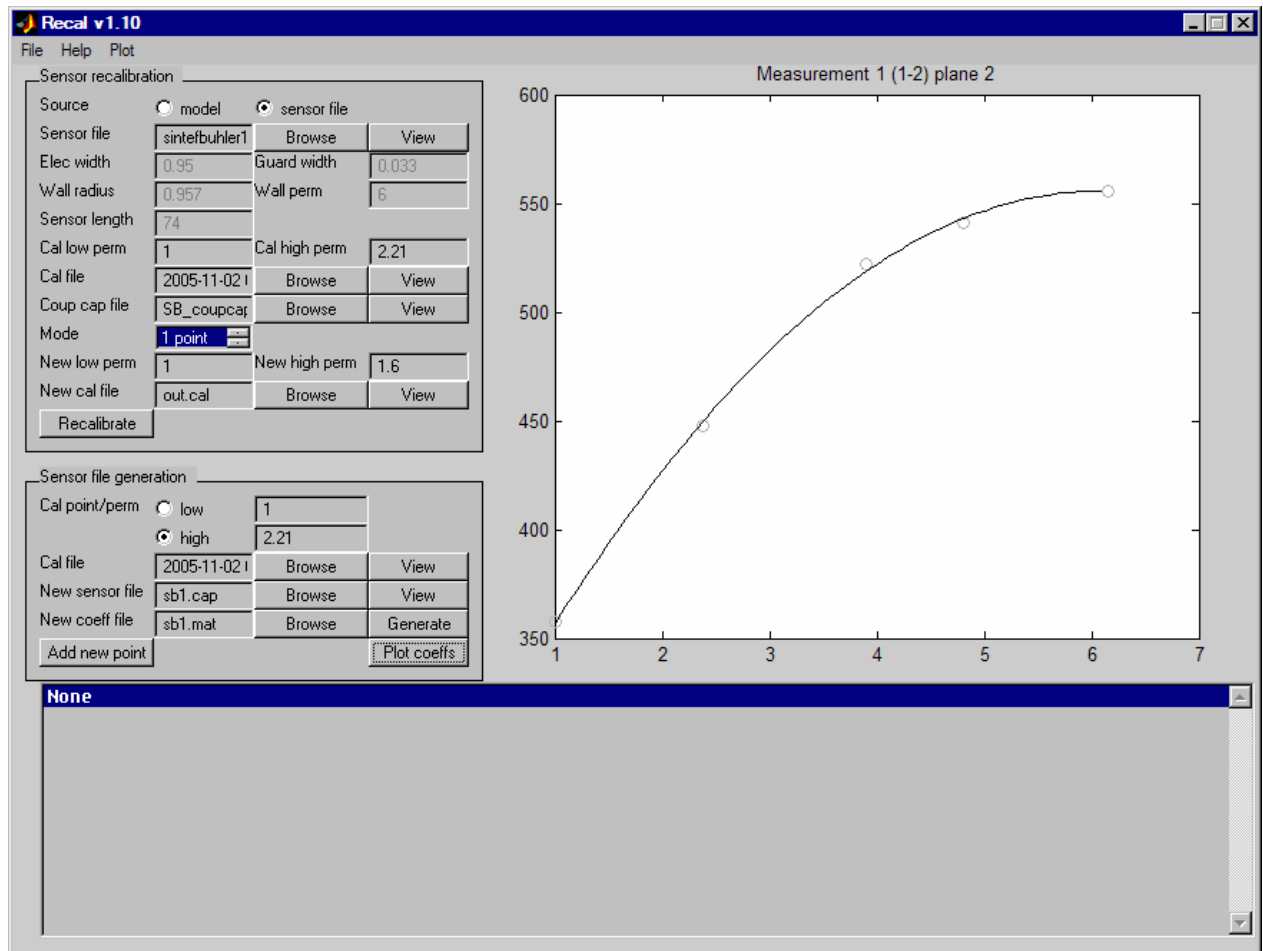


Figure A1.1. Recal window

1. In the **Sensor Recalibration** section, use the **Browse** button to locate the Coupling capacitance file (Coup cap file) for the ECT system in use.
2. In the **Sensor File generation** section, use the **Browse** button to locate the **calibration file** from which the **low permittivity** capacitance/permittivity calibration data is to be extracted.

3. Select the **low calibration point** option in the **Cal point/perm** area of the **sensor file generation** section and enter the relative permittivity of the low permittivity calibration point at which the cal file to be input (see below) was generated (= 1 for air). It is important that the specified permittivity is accurate for each set of input calibration data.
4. Once the required input **calibration file** has been selected, the **high permittivity** figure for the file will be calculated automatically and entered in the **Cal high perm** box. This figure is calculated from the **ratio of the capacitances of opposing electrode-pairs** at the **high** and **low permittivity points**, assuming that the low permittivity has the value 1. However, it should be noted that for sensors of increasing wall thickness, this derived value becomes increasing inaccurate and will tend to underestimate the mixture permittivity.
5. Enter the name of the **sensor permittivity file** which is to hold the capacitance/permittivity data for the sensor in the **New sensor file** box.
6. Click on **Add new point**. This button will add a new data point at the **low permittivity calibration point** to the **New sensor file**.
7. Set the **Cal point/perm** to select the **high** calibration point and again click on **Add new point**. This will add the **high permittivity calibration data** from the calibration file to the **sensor file**.
8. Use the **Browse** button to locate another calibration file containing data from a calibration at a different high permittivity value.
9. Repeat steps 7 and 8 for as many calibration files as data is available to build up the sensor permittivity file.
10. The sensor file can be viewed in numerical format at any stage by clicking on the **New sensor file View** button.
10. Once all the points have been added, generate the **Coefficients file** by clicking on the **Generate** button.
11. To view the **sensor** and coefficients files in graphical format, click on the **Plot coeffs** button. The **capacitance/permittivity** characteristics for individual electrode-pairs will be plotted as shown in figure A1.2.



**Figure A1.2. Recal window showing C/K curves for electrode-pair 1-2**

In figure A1.2, the discrete points are the experimental values for the specified electrode-pair extracted from the calibration files. The continuous curves are the equivalent approximations generated using a second order polynomial whose coefficients are stored in the coefficients file.

The characteristics for the other electrode-pairs can be viewed by clicking on the **Plot menu** and selecting the required **electrode-pair** from the **drop-down list**. The **selected electrode-pair** is listed at the **top of the Recal window**.

## A1.3. IMPLEMENTATION OF SENSOR C/K CORRECTION IN FLOWAN

### A1.3.1 Initialising Flowan

#### Start Flowan

Load the **capacitance data** and **configuration** files as normal.

Set the **reconstruction parameters** in the **Reconstructions Settings** window as normal.

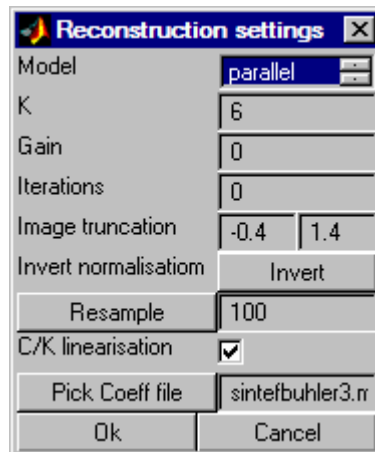


Figure A1.3 Reconstruction settings window

### A1.3.2 Enabling the C/K correction:

1. Click on the **Pick Coeff file** button and use it to **Browse** to and select the **sensor coefficients file** which was previously generated for the sensor using the **Recal** software.
2. Select (check) the **C/K linearisation** option.
3. Click on the **OK** button.

The measured capacitance data will now be processed by **Flowan** to include the sensor C/K non linearity correction.

## A1.4. USE OF TEST DATA FILE

A special capacitance data file (**cktest.bcp**) has been synthesised so that the effects of the C/K (and also the K/Concentration) corrections can be demonstrated. This file contains normalised capacitances which all increase linearly from values of zero at  $t = 0$  to 1 at  $t = 10$  seconds, and is located in the **Flowan/datafiles/examples** folder.

The use of this file can be demonstrated using a sample sensor permittivity coefficients file (**cktestcoef.mat**, which is also located in the **Examples** folder) as described below:

1. Start **Flowan** and load the capacitance data file **cktest.bcp** and also the configuration file **refconfig.ini.**, which are both located in the **Flowan/datafiles/examples** folder.
2. In the **Reconstruction settings** window, set the **Model** option to **Parallel** and untick the **C/K linearisation** option.
3. The **concentration data** should be displayed as shown in figure A1.4, which shows the concentration increasing linearly for both measurement planes. This demonstrates the use of simple linear model for the C/K and Cap/permittivity relationships.

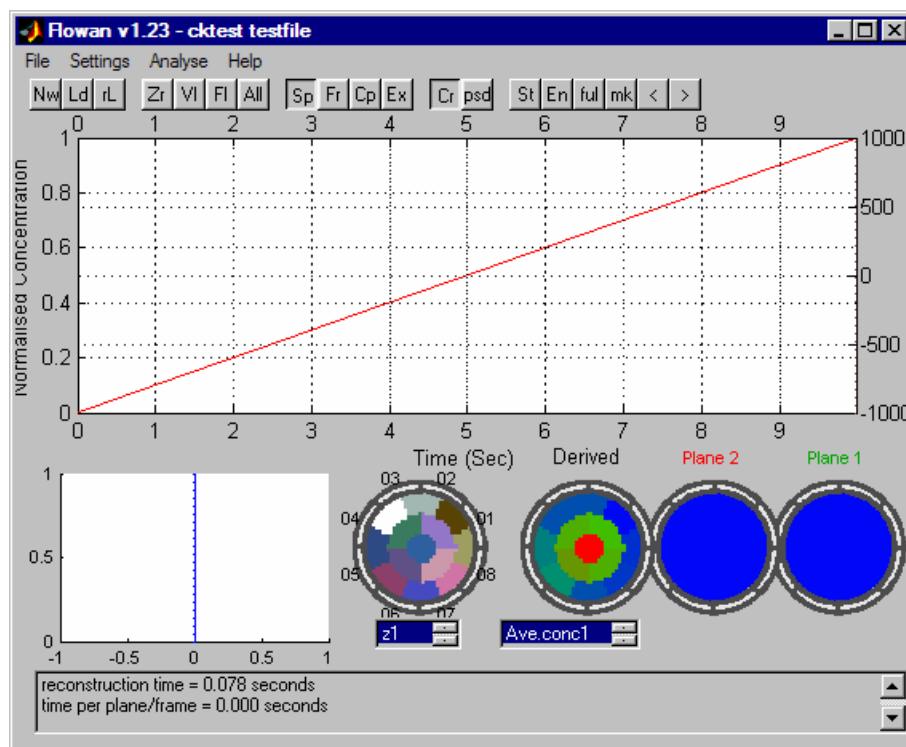


**Figure A1.4. Flowan window for cktest data in parallel mode with no c/k correction.  
(linear model)**



Now click on the **Pick Coef file** button and browse and select the **cktestcoef.mat** file.

Select (check) the **C/K option** and click the OK button. A modified concentration graph will appear and the curve for the **central zone** is shown in figure A1.5. The curves for other zones can be seen by clicking on the appropriate zone. Note that the curves differ for each zone.

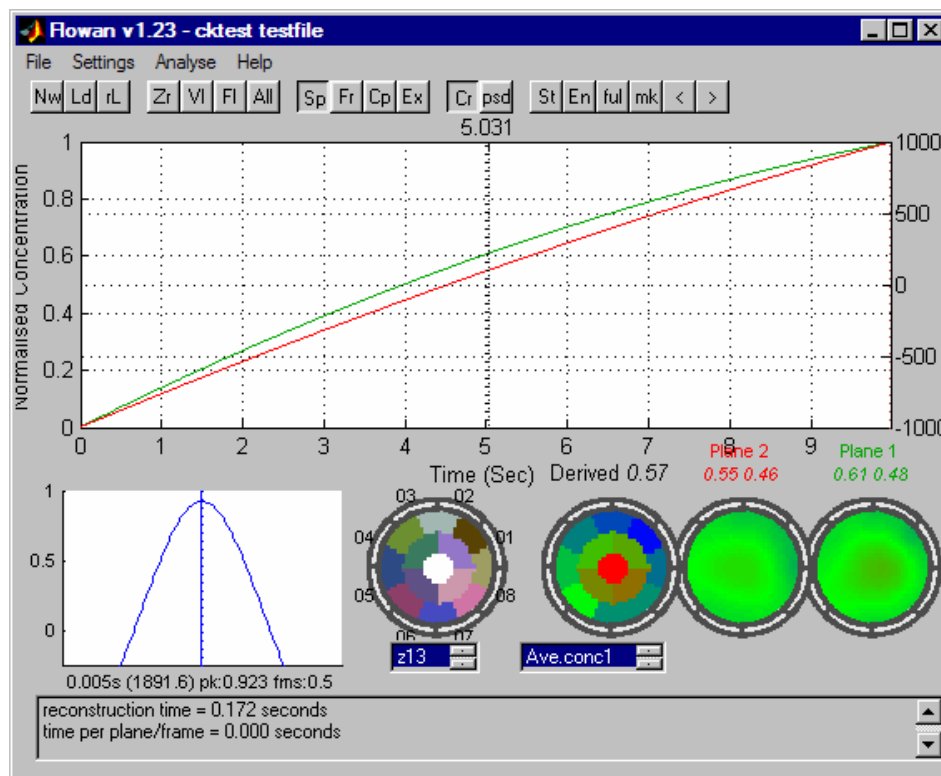


**Figure A1.5. Flowan window for cktest data in parallel mode with c/k correction.**

This demonstrates the use of a real sensor C/K model.

## A1.5. DEMONSTRATION OF PERMITTIVITY/CONCENTRATION MODEL

Unselect the **C/K linearisation** option in the **Reconstruction** window.

Select the **Series** model and click on **OK**. The **Flowan** window will now display the concentration curve corrected by the **series permittivity/concentration model** as shown in figure A1.6. Note that the correction is identical for all of the zones.

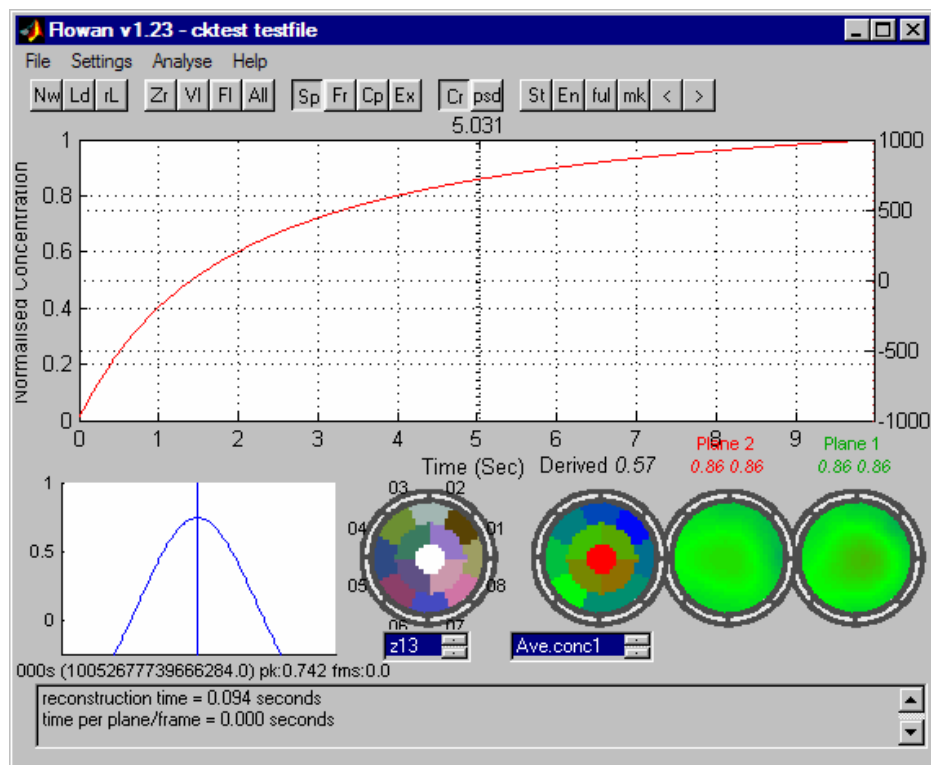


**Figure A1.6. Flowan window for cktest data in series mode with no c/k correction.**

The effect of using the **Maxwell** concentration model can be similarly demonstrated by selecting this model instead of the series model.

## APPENDIX 2

### THE SERIES PERMITTIVITY/CONCENTRATION MODEL

#### A2.1 MATHEMATICAL MODEL

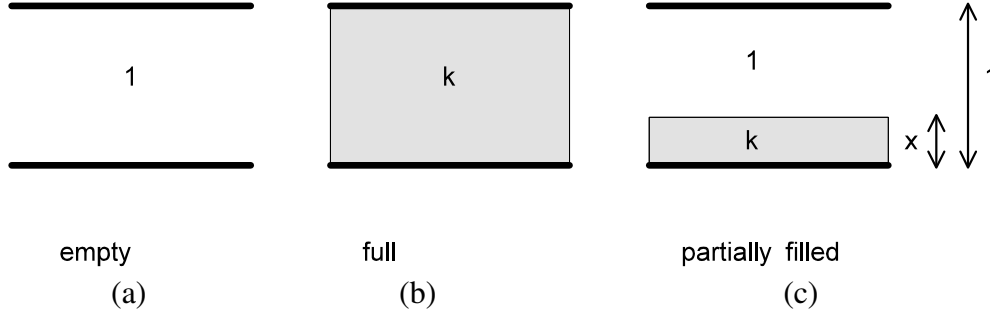


**Figure A2.1 Capacitance cell containing horizontally-stratified material**

The figures in A2.1 show a simple capacitance cell formed from a pair of pair of horizontal electrodes. The figures show the cell (a) empty (containing air), (b) filled with a dielectric material of relative permittivity  $k$  and (c) partially filled with a horizontal division between the dielectric material and air.

Where the dielectric materials exist as alternating layers of material as shown in figure A2.1(c), the overall capacitance can no longer be calculated by simply adding up the individual capacitance components.

The model which fits this situation is the series capacitance model, where we assume that the effective permittivity of a mixture of two materials can be found by assuming that the two materials act as two capacitors connected in series. (This model applies where neither material exists as continuous bands between the sensor electrodes). The first capacitor consists of a unit cell containing the higher permittivity material  $K_2$  and the second capacitor consists of a similar cell containing the lower permittivity material  $K_1$ . The cell capacitances are weighted by their permittivity values and concentrations, so that the effective permittivity of the mixture ( $K_E$ ) is obtained using the reciprocal law for two capacitors in series, ie:

$$1/C = 1/C_{K1} + 1/C_{K2} \quad (A2.1)$$

These capacitances are proportional to the permittivity and inversely proportional to the concentration. Hence:

$$1 / K_E = (1 - X) / K_1 + (X / K_2) \quad (A2.2)$$

which simplifies to:

$$K_E = (K_1 \cdot K_2) / (K_2 + X \cdot (K_1 - K_2)) \quad (A2.3)$$

We can define a normalised permittivity  $K_{EN}$  as follows:

$$K_{EN} = (K_E - K_1) / (K_2 - K_1) \quad (A2.4)$$

Substituting equation A2.3 in A2.4 we obtain:

$$K_{EN} = (K_1 \cdot K_2) / (K_2 + X \cdot (K_1 - K_2)) - K_1 / (K_2 - K_1) \quad (A2.4)$$

$$\text{which simplifies to: } K_{EN} = K_1 \cdot X / ((K_2 \cdot (1 - X) + K_1 \cdot X)) \quad (A2.5)$$

Let  $K_1/K_2 = K$

$$\text{then } K_{EN} = X / ((K \cdot (1 - X) + X)) \quad (A2.5)$$

It is a simple task to invert this equation to obtain the volume ratio  $X$  as a function of the normalised pixel permittivity values  $K_{EN}$ :

$$X = K_{EN} \cdot K / [1 + K_{EN} \cdot (K - 1)] \quad (A2.6)$$

It is clear from this equation, that the volume ratio  $X$  is no longer equal to the values of normalised pixel permittivities  $K_{EN}$ .

Equation A2.6 shows that to obtain the correct values of volume ratio when applying the series capacitance model, the pixel values obtained by linear back-projection must be modified by multiplying them by a correction factor CF where:

$$CF = K / (1 + K_{EN} \cdot (1 - K)) \quad (A2.7)$$

Equations A2.6 and A2.7 are applicable when the mixture permittivity has the value  $K_2$  at the upper calibration point. If this is not the case, a further correction has to be applied as described in Appendix 4.

## APPENDIX 3

### THE MAXWELL PERMITTIVITY/CONCENTRATION MODEL

#### A3.1 MATHEMATICAL MODEL

The Maxwell model states that the effective permittivity  $K_E$  of a mixture of two dielectric material having permittivities  $K_1$  and  $K_2$  is given by equation A2.1 below:

$$K_E = K_1 \cdot [2 \cdot K_1 + K_2 - 2 \cdot X \cdot (K_1 - K_2)] / [2 \cdot K_1 + K_2 + X \cdot (K_1 - K_2)] \quad (A3.1)$$

where  $X$  is the fraction (concentration) of the sensor volume occupied by the higher permittivity material.

Let  $K = K_2/K_1$ . Then equation A3.1 can be re-written as:

$$K_E = K_1 \cdot [2 + K - 2 \cdot X \cdot (1 - K)] / [2 + K + X \cdot (1 - K)] \quad (A3.2)$$

We can define a normalised permittivity  $K_{EN}$  as follows:

$$K_{EN} = (K_E - K_1) / (K_2 - K_1) \quad (A3.3)$$

Substituting equation A2.2 in A2.3 we obtain:

$$K_{EN} = K_1 \cdot \{ [2 + K - 2 \cdot X \cdot (1 - K)] / [2 + K + X \cdot (1 - K)] - K_1 \} / (K_2 - K_1) \quad (A3.4)$$

$$= [(2+K) - 2 \cdot X \cdot (1-K) - (2+K) - X \cdot (1-K)] / [(K-1) \cdot (2+K+X \cdot (1-K))] \quad (A3.5)$$

which simplifies to:

$$K_{EN} = 3 \cdot X / [2 + K + X \cdot (1 - K)] \quad (A3.6)$$

Equation A3.6 gives the normalised permittivity of a mixture of 2 dielectric materials of permittivities  $K_1$  and  $K_2$ , where the concentration of the the  $K_2$  material is  $X$ .

This equation can be readily inverted to give the concentration ( $X$ ) of a mixture of 2 dielectric materials in terms of the normalised measured permittivity ( $K_{EN}$ ), with the result:

$$X = K_{EN} \cdot (2 + K) / [3 + K_{EN} \cdot (K - 1)] \quad (A3.7)$$

Equation A3.7 is applicable when the mixture permittivity has the value  $K_2$  at the upper calibration point. If this is not the case, a further correction has to be applied as described in Appendix 4.

## APPENDIX 4

### IMPLEMENTING THE SERIES OR MAXWELL MODEL CORRECTIONS FOR MIXTURES WHERE THE PACKED DENSITY IS LESS THAN 100%

#### A4.1 OVERVIEW

The Series or Maxwell model corrections applies over the full range of possible permittivities  $K$ , that is from  $K_1$  to  $K_2$ , where  $K_1$  is the value for the lower permittivity material and  $K_2$  is the value for the higher permittivity material. However, for many real mixtures, the calibration range for the sensor will normally be over a more restricted range of permittivities, because the higher calibration permittivity value will be that for a mixture of the upper and lower permittivity materials. For example, if the lower permittivity material is air ( $K_1=1$ ) and the higher permittivity material is in the form of polypropylene beads, ( $K_2= 3$ ), then the effective permittivity at the upper calibration point will be around 1.7 because of the packing density (around 60%) of a mixture of spherical polypropylene beads and air. It follows that the ECT sensor will operate over the lower part only of the Concentration correction curve. The way allowances are made for this situation are described in the following paragraphs.

#### A4.2 MODIFICATION DETAILS

Equations A2.6 and A3.7 allow the normalised pixel permittivity values calculated from the measured capacitances to be converted into concentration values. However, they are only applicable if the sensor operates over the full permittivity range from  $K_1$  to  $K_2$ .

In cases where the upper calibration mixture permittivity ( $K_3$ ) is less than  $K_2$ , the following modifications must be made to equations A2.6 and A3.7:

1. The values of  $K_{EN}$  must be modified to have the value  $K_{ENN}$ , where:

$$K_{ENN} = K_{EN} \cdot K_3 / K_2 \quad (A4.1)$$

This limits the range of normalised mixture permittivities to less than the full range from 0 to 1, reflecting the fact that the sensor is calibrated over a range of permittivities ( $K_1$  to  $K_3$ ), which is less than the full range assumed by the Series or Maxwell corrections ( $K_1$  to  $K_2$ ).

2. Because of the restricted range of normalised permittivities, the maximum concentration and permittivity (which were both previously normalised to have values between 0 and 1) will no longer have upper values of 1. It is therefore necessary to renormalise both of these quantities to have maximum values of 1.

The modified versions of equations A2.6 and A3.7, for use when the upper permittivity calibration is carried out with a mixture permittivity which is less than that of the higher (solid) permittivity material are given in the following 2 sections.

### A4.3 SERIES CONCENTRATION/PERMITTIVITY MODEL CORRECTION

Where the upper calibration point has a permittivity  $K_3$ , which is less than  $K_2$ , the re-normalised concentration equation becomes:

$$(A4.2) \quad X_N = \frac{K_{EN} \cdot (K_P/K) \cdot K}{[1 + K_{EN} \cdot (K_P/K) \cdot (K - 1)]}$$
$$(K_P/K) \cdot K / [1 + (K_P/K) \cdot (K - 1)]$$

where  $K_P = K_3/K_1$

### A4.4 MAXWELL CONCENTRATION/PERMITTIVITY MODEL CORRECTION

$$X_N = \frac{[K_{EN} \cdot (K_P/K) \cdot (2 + K)]}{[(3 + K_{EN} \cdot (K_P/K) \cdot (K - 1))]} \quad (A4.3)$$
$$[(K_P/K) \cdot (2 + K)] / [(3 + (K_P/K) \cdot (K - 1))]$$

where  $K_P = K_3/K_1$

In practice these correction factors can be applied to the normalised measured capacitances directly before the pixel permittivities are calculated.

Some sample correction curves are shown in figure A4 .1.

## A4.5 SAMPLE CORRECTION CURVES

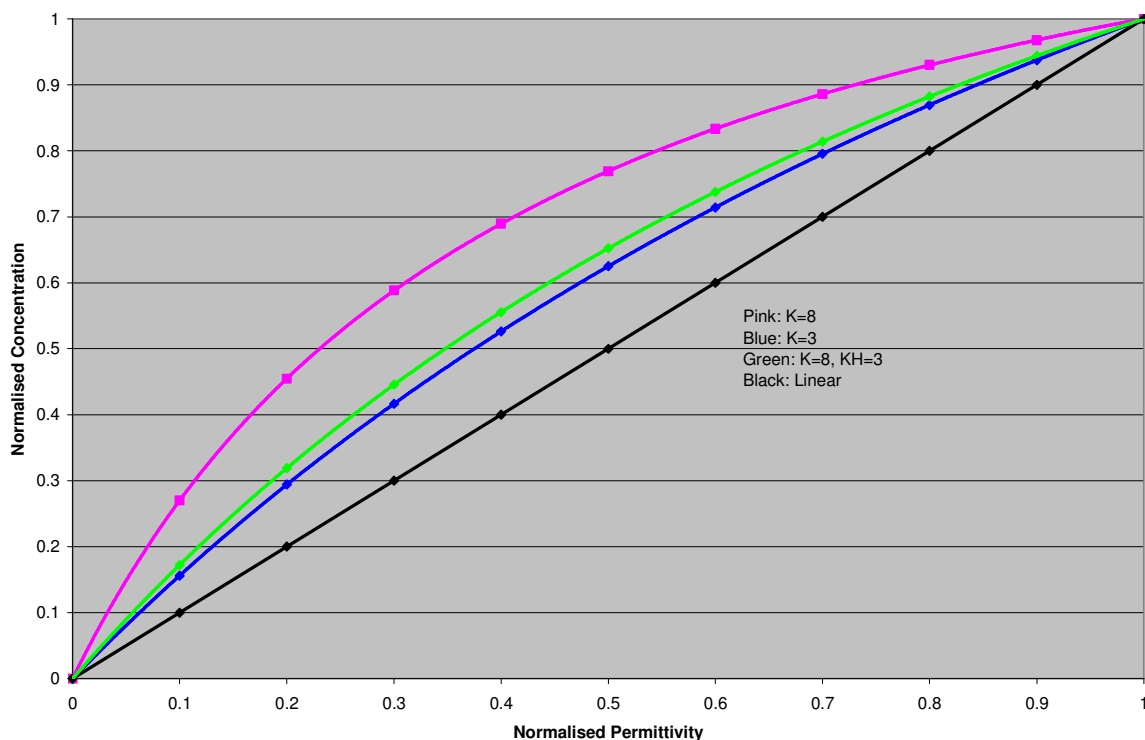


**Figure A4.1 Concentration/permittivity correction plots (Maxwell model)**

The Pink and blue correction curves have been plotted for the simple case where the ratio of the upper and lower permittivities are 8 and 3 respectively with an assumed packing density of 100% at the upper calibration point.

For comparison, the green correction curve has been plotted for a pair of materials where the ratio of the upper and lower permittivities is 8 but where a reduced packing density at the upper calibration point gives an effective permittivity of 3.

In this case, the effective correction required is larger than that for the simpler case of a permittivity ratio of 3 with an assumed 100% packing density at the upper calibration point.



## APPENDIX 5

### QBASIC PROGRAM XNCOMP.BAS LISTING

```
REM    PROGRAM XNCOMP
REM    CALCULATES THE CONCENTRATION BOOST FACTORS FOR THE SERIES
REM    AND MAXWELL MODELS COMPARED WITH THE PARALLEL MODEL
CLS
K1 = 1
K2 = 8.66
K3 = 3.63
K = K2 / K1
KP = K3 / K1
XP = .65

PRINT "PROGRAM XNCOMP"
PRINT "K1 = "; K1, "K2 = "; K2, "K3 = "; K3, "XP = "; XP
LPRINT "PROGRAM XNCOMP"
LPRINT "K1 = "; K1, "K2 = "; K2, "K3 = "; K3, "XP = "; XP

REM MAXWELL CALCULATION OF K2 FROM CONCENTRATION AND K3
K2MNUM = XP * (K3 + 2 * K1) - 2 * (K1 - K3)
K2MDEN = XP * (K3 + 2 * K1) + (K1 - K3)
K2M = K1 * K2MNUM / K2MDEN

REM MAXWELL CALCULATION OF K2 FROM CONCENTRATION AND K3
K2SNUM = XP * K3
K2SDEN = K1 - K3 * (1 - XP)
K2S = K1 * K2SNUM / K2SDEN

PRINT "K2 MAXWELL = "; K2M, "K2 SERIES = "; K2S
LPRINT "K2 MAXWELL = "; K2M, "K2 SERIES = "; K2S

PRINT "XP      "; "XM      "; "XS      "; "XM/XP      "; "XMPN      ";
"XS/XP      "; "XSPN      "
LPRINT "XP      "; "XM      "; "XS      "; "XM/XP      "; "XMPN      ";
"XS/XP      "; "XSPN      "

FOR N = 1 TO 20
KEN = N / 100

REM PARALLEL MODEL
XP = KEN

REM SERIES MODEL
NUMS = (KEN * (KP / K) * K) / (1 + KEN * (KP / K) * (K - 1))
DENS = ((KP / K) * K) / (1 + (KP / K) * (K - 1))
XS = NUMS / DENS

REM MAXWELL MODEL
NUMM = KEN * ((KP / K) * (2 + K)) / ((3 + KEN * (KP / K) * (K - 1)))
DENM = ((KP / K) * (2 + K)) / ((3 + (KP / K) * (K - 1)))
XM = NUMM / DENM

XMP = XM / XP
XSP = XS / XP

IF N = 1 THEN
XMP0 = XMP
XSP0 = XSP
ELSE
END IF
```

```

XMPN = XMP / XMP0
XSPN = XSP / XSP0

```

```

PRINT USING "#.####" "; XP; XM; XS; XMP; XMPN; XSP; XSPN
LPRINT USING "#.####" "; XP; XM; XS; XMP; XMPN; XSP; XSPN
NEXT N

```

A typical program output listing is shown below.

Note that:

XP is the mixture concentration

XM is the boosted Maxwell model capacitance value and XS is the equivalent value for the Series model.

XMPN is the Maxwell boost factor normalised to the value at 0.01 concentration and XSPN is the equivalent value for the series model.

```

PROGRAM XNCOMP
K1 = 1          K2 = 8.66      K3 = 3.63      XP = .65
K2 MAXWELL = 8.663917      K2 SERIES = -8.722732
XP      XM      XS      XM/XP      XMPN      XS/XP      XSPN
0.0100  0.0205  0.0408  2.0484  1.0000  4.0798  1.0000
0.0200  0.0405  0.0791  2.0269  0.9895  3.9567  0.9698
0.0300  0.0602  0.1152  2.0059  0.9793  3.8409  0.9414
0.0400  0.0794  0.1493  1.9853  0.9692  3.7316  0.9146
0.0500  0.0983  0.1814  1.9651  0.9594  3.6283  0.8893
0.0600  0.1167  0.2118  1.9454  0.9497  3.5307  0.8654
0.0700  0.1348  0.2407  1.9260  0.9403  3.4381  0.8427
0.0800  0.1526  0.2680  1.9070  0.9310  3.3503  0.8212
0.0900  0.1700  0.2940  1.8884  0.9219  3.2668  0.8007
0.1000  0.1870  0.3187  1.8701  0.9130  3.1874  0.7813
0.1100  0.2037  0.3423  1.8522  0.9042  3.1118  0.7627
0.1200  0.2202  0.3648  1.8346  0.8957  3.0397  0.7450
0.1300  0.2363  0.3862  1.8174  0.8873  2.9708  0.7282
0.1400  0.2521  0.4067  1.8005  0.8790  2.9050  0.7120
0.1500  0.2676  0.4263  1.7839  0.8709  2.8420  0.6966
0.1600  0.2828  0.4451  1.7676  0.8629  2.7818  0.6818
0.1700  0.2978  0.4631  1.7516  0.8551  2.7240  0.6677
0.1800  0.3125  0.4803  1.7359  0.8474  2.6685  0.6541
0.1900  0.3269  0.4969  1.7204  0.8399  2.6153  0.6410
0.2000  0.3411  0.5128  1.7053  0.8325  2.5642  0.6285

```

**Figure A5.1 Output listing for program XBCOMP.BAS**

